Measurement of *WW/WZ -> lvqq'* production with the hadronically decaying boson reconstructed as one or two jets in *pp* collisions at $\sqrt{s}$=8 TeV with ATLAS, and constraints on anomalous gauge couplings

M. Aaboud et al. (ATLAS Collaboration)

2017

Eur. Phys. J. C (2017) 77:563
DOI 10.1140/epjc/s10052-017-5084-2

THE EUROPEAN PHYSICAL JOURNAL C

Regular Article - Experimental Physics

Measurement of $WW/WZ \to \ell\nu qq'$ production with the hadronically decaying boson reconstructed as one or two jets in pp collisions at $\sqrt{s} = 8$ TeV with ATLAS, and constraints on anomalous gauge couplings

ATLAS Collaboration[⋆]

CERN, 1211 Geneva 23, Switzerland

Received: 7 June 2017 / Accepted: 18 July 2017 / Published online: 20 August 2017

Abstract This paper presents a study of the production of WW or WZ boson pairs, with one W boson decaying to $e\nu$ or $\mu\nu$ and one W or Z boson decaying hadronically. The analysis uses 20.2 fb^{-1} of $\sqrt{s} = 8$ TeV pp collision data, collected by the ATLAS detector at the Large Hadron Collider. Cross-sections for WW/WZ production are measured in high-p_{T} fiducial regions defined close to the experimental event selection. The cross-section is measured for the case where the hadronically decaying boson is reconstructed as two resolved jets, and the case where it is reconstructed as a single jet. The transverse momentum distribution of the hadronically decaying boson is used to search for new physics. Observations are consistent with the Standard Model predictions, and 95% confidence intervals are calculated for parameters describing anomalous triple gauge-boson couplings.

Contents

⋆ e-mail: atlas.publications@cern.ch

1 Introduction

Measurements of the production of two massive vector gauge bosons (hereafter, "diboson" production) represent an important test of the Standard Model (SM) of particle physics. Diboson measurements are powerful probes of the electroweak theory of the SM, in particular the structure of the triple gauge-boson couplings (TGCs) [1,2]. In addition, precise diboson measurements are a valuable test of higher-order calculations in quantum chromodynamics (QCD).

Measurements of WW and WZ production in the leptonic channels $\ell\nu\ell\nu$ and $\ell\nu\ell\ell$ ($\ell = e, \mu$) have been performed by the ATLAS and CMS collaborations in pp collisions at $\sqrt{s} = 8$ TeV and $\sqrt{s} = 13$ TeV [3–9], and by the Tevatron experiments in $p\bar{p}$ collisions [10–13]. Measurements in the semileptonic channel $WV \to \ell\nu qq'$ ($V = W, Z$) have been performed by ATLAS [14] and CMS [15] at $\sqrt{s} = 7$ TeV, and by the Tevatron experiments in $p\bar{p}$ collisions [16,17]. The semileptonic channel offers features complementary to the leptonic channels. On the one hand, the presence of jets and the large background from W + jets and $t\bar{t}$ production limit the experimental precision. On the other hand, the semileptonic channel has an approximately six times higher branching fraction than the fully leptonic channels. Also, for WW, the original diboson kinematics can be better reconstructed in an $\ell\nu qq'$ final state than in an $\ell\nu\ell\nu$ final state, since the latter has two invisible particles, rather than only one in $\ell\nu qq'$. Both of these advantages are particularly beneficial for searching for beyond-the-Standard-Model (BSM) enhancements of diboson production due to heavy new parti-

cles, which could modify the diboson spectrum at high transverse momentum (p_{T}) of the bosons [18].

It is possible to reconstruct the $V \to qq'$ decay as two small-radius jets ("small-R" jets, denoted by j) or as a single large-radius jet ("large-R" jet, denoted by J). Reconstructing the $V \to qq'$ decay as a large-R jet enables an increased reconstruction efficiency at high $p_{\mathrm{T}}(V)$, thus improving the sensitivity to BSM signals. In addition, by applying grooming [19] techniques such as trimming [20] to the large-R jets, it is possible to better distinguish events containing $V \to qq'$ decays from background events [21].

In this paper, measurements of $WV \to \ell\nu qq'$ fiducial cross-sections are presented in phase spaces containing a $V \to qq'$ candidate with high p_{T}. Two fiducial cross-sections are measured, in phase spaces chosen to closely match the two experimental selections used in this paper. The first event selection, denoted $WV \to \ell\nu$jj, reconstructs the $V \to qq'$ decay as two small-R jets, while the second one, denoted $WV \to \ell\nu$J, reconstructs the $V \to qq'$ as a single large-R jet. Previous cross-section measurements of $WV \to \ell\nu qq'$ have not exploited large-R jets.

A search for anomalous triple gauge-boson couplings (aTGCs) is also presented in this paper, using both the $WV \to \ell\nu$jj and $WV \to \ell\nu$J channels. Previous searches for charged aTGC contributions to $WV \to \ell\nu qq'$ production have been conducted by the ATLAS Collaboration [14] using 7 TeV pp collisions, by the CMS Collaboration [15,22] using 7 and 8 TeV pp collisions, and by the D0 [23] and CDF [24] collaborations using $p\bar{p}$ collisions. Most published aTGC searches in the $WV \to \ell\nu qq'$ channel have reconstructed the $V \to qq'$ as two small-R jets, with the exception of Ref. [22], which reconstructed the $V \to qq'$ as a single large-R jet.

2 Analysis overview

As mentioned above, measurements of $WV \to \ell\nu qq'$ production are performed using either two small-R jets or a single large-R jet to reconstruct the hadronically decaying V boson. For both channels, the leptonically decaying W boson is reconstructed by requiring the presence of a lepton (electron or muon) and missing transverse momentum.

After applying stringent event selection requirements, the signal-to-background ratio remains quite low at 5–10%, because of the large W + jets background. In order to distinguish the SM WV signal from the background, the dijet mass distribution (in the $WV \to \ell\nu$jj channel) or the mass distribution of the large-R jet (in the $WV \to \ell\nu$J channel) is used as a discriminating variable. The signal events peak near the W/Z mass in these distributions, while the shape of the dominant W + jets background is smoothly falling. In both channels, the signal is extracted from a fit to the discriminating variable. Wide fitting ranges are used, in order to allow the backgrounds to be constrained by the data.

A fiducial cross-section is measured separately in the $WV \to \ell\nu$jj and the $WV \to \ell\nu$J channel; the fiducial phase spaces for the measurements are defined to be close to the experimental event selections. The fiducial cross-section in each channel is extracted from the previously mentioned fits. The events in the two channels partially overlap, because there are some events for which the $V \to qq'$ decay can be reconstructed both as two small-R jets and as one large-R jet. In order to simplify the interpretation of the results and allow easier comparison with theoretical predictions, the overlap events are not removed, and both measurements are presented separately. No combination of the $WV \to \ell\nu$jj and $WV \to \ell\nu$J cross-section measurements is performed. The electron and muon channels are combined when performing the measurements, since little improvement in sensitivity is expected from separating by lepton flavour. Event kinematics and the signal-to-background ratio are similar in the electron and muon channels, and the dominant sources of uncertainty are unrelated to lepton flavour.

A search for aTGC contributions is also performed in the $WV \to \ell\nu$jj and $WV \to \ell\nu$J channels. The event selection is the same as for the cross-section measurements, except that a tighter requirement is made on the dijet mass or on the mass of the large-R jet. The search is performed by fitting the p_{T} distribution of the dijet system ($WV \to \ell\nu$jj channel) or of the large-R jet ($WV \to \ell\nu$J channel). These distributions are sensitive to aTGCs, which are expected to lead to deviations from the SM prediction at high p_{T}.

3 ATLAS detector

The ATLAS detector [25], which surrounds one of the interaction points of the Large Hadron Collider (LHC) [26], is built of several subdetectors. The first subdetector layer consists of the inner detector (ID), which provides charged-particle tracking for $|\eta| < 2.5$.[1] The ID is further subdivided into (ordered from innermost to outermost) a pixel detector, a silicon-microstrip tracker, and a transition radiation tracker. Surrounding the ID there is a superconducting solenoid that provides a 2 T magnetic field. Outside of the solenoid, there is an electromagnetic (EM) calorimeter based on liquid-argon technology, which provides coverage up to $|\eta| = 3.2$. Additionally, a scintillator-tile

[1] ATLAS uses a right-handed coordinate system with its origin at the nominal interaction point (IP) in the centre of the detector and the z-axis along the beam pipe. The x-axis points from the IP to the centre of the LHC ring, and the y-axis points upward. Cylindrical coordinates (r, ϕ) are used in the transverse plane, ϕ being the azimuthal angle around the z-axis. The pseudorapidity is defined in terms of the polar angle θ as $\eta = -\ln\tan(\theta/2)$.

calorimeter provides hadronic energy measurements in the range $|\eta|<1.7$, and liquid-argon-based endcap and forward calorimeters extend the EM and hadronic measurements up to $|\eta| = 4.9$. A muon spectrometer, consisting of tracking and triggering detectors and three toroidal magnets, surrounds the calorimeters; it provides muon tracking and identification up to $|\eta| = 2.7$ and triggering capability up to $|\eta| = 2.4$.

A three-level trigger system is used to select the most interesting events for data storage [27]. An initial hardware-based trigger stage is followed by two software-based triggers, which reduce the final event rate to about 400 Hz.

4 Data and Monte Carlo samples

This analysis is based on an integrated luminosity of 20.2 ± 0.4 fb^{-1} of 8 TeV pp collisions recorded by the ATLAS detector in 2012. Events are required to pass one of several single-lepton triggers. The triggers require either an isolated electron or muon with $p_{\mathrm{T}} > 24$ GeV, or an electron (muon) having $p_{\mathrm{T}} > 60$ (36) GeV without an isolation requirement.

The nominal signal Monte Carlo (MC) samples consist of $qq' \to WV$ events generated at next-to-leading order (NLO) in QCD using MC@NLO v4.07 [28] interfaced with HERWIG v6.520 [29] and JIMMY v4.31 [30] for the simulation of parton showering, hadronization, and the underlying event. The CT10 parton distribution function (PDF) set [31] and parameter values from the AUET2 tune [32] are used for these samples. The W and Z bosons are generated on-shell by MC@NLO and decayed subsequently by HERWIG. The same MC configuration is also used to model aTGC contributions to WV production, using an event reweighting feature built into MC@NLO.

In order to study systematic uncertainties, alternative $qq' \to WV$ samples are generated at NLO in QCD with POWHEG-BOX [33–35] using the CT10 PDF set. The parton showering and hadronization is modelled with PYTHIA 8.175 [36] using the AU2 tune [37]. Off-shell W and Z/γ^* decays are included; the Z/γ^* decays have a requirement of $m_{qq'} > 20$ GeV and $m_{\ell\ell} > 20$ GeV.

Another set of alternative $qq' \to WV$ samples are generated with SHERPA v1.4.1 [38–41]. These samples are generated at leading order (LO) in QCD, but include up to three additional partons in the matrix element. Off-shell W and Z/γ^* decays are included; the Z/γ^* decays have a requirement of $m_{qq'} > 4$ GeV and $m_{\ell\ell} > 4$ GeV.

Contributions from $gg \to H \to WW^*$ are only at the 1% level after applying the full event selection and are thus neglected. Signal MC samples for non-resonant $gg \to WW$ production are not used in the analysis, but the contribution from this process is estimated as described in Sect. 10, and included in the final cross-section predictions.

The W + jets and Z + jets backgrounds (collectively referred to as V + jets) are modelled at LO in QCD with SHERPA v1.4.1, with up to four additional final-state partons. The CT10 PDF set is used for these samples, and they are normalized using inclusive cross-sections that are next-to-next-to-leading order (NNLO) in QCD, obtained using FEWZ [42]. For studies of systematic uncertainties, alternative W + jets samples are generated with ALPGEN [43] interfaced with PYTHIA 6.426 [44], modelling the process at LO in QCD with up to five final-state partons. These additional samples use the Perugia 2011C tune [45] and the CTEQ6L1 PDF set [46].

The MC samples for the $t\bar{t}$ and single-top-quark (t-channel, s-channel, and Wt) processes (collectively referred to as top-quark processes) are generated with POWHEG-BOX [47–49] interfaced with PYTHIA 6.426 [44] (or PYTHIA 6.427 for the t-channel single-top-quark process). All of these samples use the CT10 PDF set for the matrix element, the CTEQ6L1 PDF set for the parton shower, and the Perugia 2011C tune.

The ZZ background process is modelled with POWHEG interfaced with PYTHIA 8. The sample is normalized using the NLO prediction from MCFM [50,51].

The MC samples are passed through a GEANT4-based [52] simulation of the ATLAS detector [53]. For some of the MC samples, a fast simulation is used that makes use of a parameterization of the showers in the calorimeter. The hard-scattering processes in the MC samples are overlaid with simulated minimum-bias events in order to model additional collisions in the same or neighbouring bunch crossings ("pile-up"). The MC samples are reweighted so that their pile-up profile matches that observed in the data.

5 Event reconstruction

This analysis considers events with exactly one lepton (electron or muon), missing transverse momentum, and either two small-R jets or one large-R jet.

In each event, primary vertices are reconstructed, which must be formed from at least three tracks with $p_{\mathrm{T}} > 400$ MeV. In case an event has multiple primary vertices (due to pile-up), the primary vertex with the highest $\sum p_{\mathrm{T}}^2$ of the associated tracks is defined as the hard-scatter vertex.

Electron candidates are formed from energy clusters in the EM calorimeter matched to ID tracks. They are required to have $p_{\mathrm{T}} > 30$ GeV and $|\eta| < 2.47$. Candidates in the transition region between the barrel and endcaps of the EM calorimeter, $1.37 < |\eta| < 1.52$, are excluded. In order to ensure that the electron candidates are consistent with having been produced at the hard-scatter vertex, the transverse impact parameter d_0 and longitudinal impact parameter z_0 are required to satisfy $|d_0|/\sigma_{d_0} < 5$ and $|z_0 \sin\theta| < 0.5$ mm,

respectively, where σ_{d_0} is the uncertainty in the measured d_0. Both d_0 and z_0 are measured with respect to the hard-scatter vertex. Electron candidates must also satisfy the "tight" cut-based identification criteria from Ref. [54], based on track parameters and on the shower shapes in the calorimeter. Candidates must also pass isolation requirements based on calorimeter and track measurements. The calorimeter isolation requires $R^{\text{iso}}_{\text{cal}} < 0.14$, where $R^{\text{iso}}_{\text{cal}}$ is defined as the scalar transverse energy sum of the calorimeter energy deposits within a $\Delta R \equiv \sqrt{(\Delta\eta)^2 + (\Delta\phi)^2} = 0.3$ cone centred on the electron candidate (excluding transverse energy from the candidate itself), divided by the p_{T} of the electron candidate. Similarly, the track isolation requires $R^{\text{iso}}_{\text{ID}} < 0.07$, where $R^{\text{iso}}_{\text{ID}}$ is the scalar sum of the p_{T} of the tracks within a $\Delta R = 0.3$ cone centred on the electron candidate (excluding the p_{T} of the candidate's track itself), divided by the electron candidate's p_{T}.

Muon candidates are formed from the combination of a track in the muon spectrometer and one in the ID. They are required to have $p_{\text{T}} > 30$ GeV and $|\eta| < 2.4$. Their impact parameters must satisfy $|d_0|/\sigma_{d_0} < 3$ and $|z_0 \sin\theta| < 0.5$ mm. The candidates must also satisfy the isolation criteria $R^{\text{iso}}_{\text{cal}} < 0.07$ and $R^{\text{iso}}_{\text{ID}} < 0.07$, where $R^{\text{iso}}_{\text{cal}}$ and $R^{\text{iso}}_{\text{ID}}$ are defined analogously to the electron case.

Small-R jets are reconstructed from topological energy clusters [55] in the calorimeter using the anti-k_t algorithm [56] with radius parameter $R = 0.4$. The jet energies are calibrated as described in Ref. [57] and are corrected for pile-up. They are required to have $p_{\text{T}} > 25$ GeV and $|\eta| < 2.5$ for the $WV \to \ell\nu\text{jj}$ channel. Small-R jets with $|\eta| < 4.5$ are used in the $WV \to \ell\nu\text{J}$ channel as part of a jet veto (see Sect. 6). In order to remove jets originating from pile-up, small-R jets having $p_{\text{T}} < 50$ GeV and $|\eta| < 2.4$ are required to have an absolute value of the "jet vertex fraction" variable (JVF) [58] greater than 0.5.

In the $WV \to \ell\nu\text{J}$ channel, large-R jets are reconstructed using the anti-k_t algorithm with radius parameter $R = 1.0$, and are trimmed [20] using a subjet radius of 0.2 and a momentum-fraction parameter $f_{\text{cut}} = 0.05$; the trimming procedure discards soft subjets from the large-R jets and reduces their sensitivity to pile-up [21]. They are required to have $p_{\text{T}} > 200$ GeV and $|\eta| < 2.0$. The energies of the small-R and large-R jets and the masses of the large-R jets are calibrated using p_{T}- and η-dependent scale factors [57,59].

If an electron and a muon candidate share the same ID track, the electron candidate is rejected. If a small-R jet is within $\Delta R = 0.2$ of a selected electron candidate, the jet is rejected; if the jet is within $0.2 < \Delta R < 0.4$ of a selected electron, the electron candidate is rejected. Muon candidates are rejected if they are within $\Delta R = 0.4$ of a small-R jet. Finally, large-R jets are rejected if they are within $\Delta R = 1.0$ of a selected lepton candidate. In the object selection stage, small-R jets and large-R jets are allowed to overlap; however, in the event selection stage a ΔR requirement is applied between the small-R and large-R jets, as explained in Sect. 6.

The missing transverse momentum $\vec{E}^{\text{miss}}_{\text{T}}$ is computed as the negative vector sum of the transverse momentum of all the detected objects in the event, including reconstructed jets, photons, electrons, and muons. An additional "soft term" is included that accounts for the p_{T} of clusters in the calorimeter which are not associated with any specific reconstructed object [60]. The magnitude of $\vec{E}^{\text{miss}}_{\text{T}}$ is denoted $E^{\text{miss}}_{\text{T}}$.

6 Event selection

Two independent sets of event selection criteria are developed that target different event topologies: the $WV \to \ell\nu\text{jj}$ selection, described in Sect. 6.1, and the $WV \to \ell\nu\text{J}$ selection, described in Sect. 6.2. The $WV \to \ell\nu\text{J}$ channel and $WV \to \ell\nu\text{jj}$ channel differ significantly from one another in their kinematics, expected signal yields, and signal-to-background ratios. Therefore, the event selection criteria are optimized separately for the two channels.

For both the $WV \to \ell\nu\text{jj}$ and $WV \to \ell\nu\text{J}$ selections, all events are required to contain at least one primary vertex. Events must have exactly one good electron or muon candidate. Events are vetoed if they contain any additional lepton candidates that have $p_{\text{T}} > 15$ GeV and satisfy a looser set of selection criteria.

6.1 $WV \to \ell\nu\text{jj}$ channel

Events must have $E^{\text{miss}}_{\text{T}} > 40$ GeV and a transverse mass[2] $m_{\text{T}} > 40$ GeV. Events must contain exactly two small-R jets. The requirement of exactly two jets substantially reduces the background from top-quark decays. The pseudorapidity separation of the selected jets is required to satisfy $\Delta\eta(\text{j},\text{j}) < 1.5$, in order to improve the signal-to-background ratio.

In order to reduce the multijet background not removed by the $E^{\text{miss}}_{\text{T}} > 40$ GeV requirement, an azimuthal-angle difference between the $E^{\text{miss}}_{\text{T}}$ direction and the direction of the leading-p_{T} jet of $|\Delta\phi(\text{j}_1, E^{\text{miss}}_{\text{T}})| > 0.8$ is required. Also, both the $V \to qq'$ and $W \to \ell\nu$ candidates must pass requirements on their transverse momenta: $p_{\text{T}}(\text{jj}) > 100$ GeV and $p_{\text{T}}(W \to \ell\nu) > 100$ GeV, where $p_{\text{T}}(W \to \ell\nu) \equiv |\vec{E}^{\text{miss}}_{\text{T}} + \vec{p}_{\text{T}}(\ell)|$. These p_{T} requirements enhance the separation between the signal and background distributions in the dijet mass.

As described in Sect. 8, the signal is extracted using a maximum-likelihood (ML) fit to the dijet mass (m_{jj}) distribu-

[2] The transverse mass is defined as $m_{\text{T}} \equiv \sqrt{(E^{\text{miss}}_{\text{T}} + p_{\text{T}}(\ell))^2 - |\vec{E}^{\text{miss}}_{\text{T}} + \vec{p}_{\text{T}}(\ell)|^2}$, where $p_{\text{T}}(\ell)$ is the transverse momentum of the lepton candidate.

tion. In the dijet mass calculation, the mass of each individual jet is set to zero, which makes the variable easier to model in the MC simulation. Since the signal is extracted from a fit to m_{jj}, only a loose requirement is made on this variable: 40 GeV $< m_{jj} <$ 200 GeV.

6.2 $WV \to \ell\nu$J channel

Events must contain exactly one large-R jet with $p_T >$ 200 GeV and $|\eta| < 2.0$. The backgrounds from top-quark decays are suppressed by rejecting events containing any small-R jets with $p_T > 25$ GeV and $|\eta| < 4.5$ that are separated from the large-R jet by $\Delta R(j, J) > 1.0$. In order to suppress the multijet background, a requirement of $E_T^{miss} > 50$ GeV is applied. The trimmed mass of the large-R jet, m_J, must be 50 GeV $< m_J <$ 170 GeV, and the signal is measured from the ML fit to m_J.

Since the $WV \to \ell\nu$jj and $WV \to \ell\nu$J event selections are done independently, some events pass both selections. About 10% of the signal MC events that pass the $WV \to \ell\nu$jj selection also pass the $WV \to \ell\nu$J selection, while about 50% of the signal MC events that pass the $WV \to \ell\nu$J selection also pass the $WV \to \ell\nu$jj selection.

7 Background estimation

The methods for estimating the expected background yields and kinematic distributions are described in this section. The estimates from this section are used as inputs to the ML fit in which the signal is measured while the backgrounds are allowed to vary within their systematic uncertainties. In that ML fit, the V + jets normalization is allowed to vary without constraint, so the estimates given in this section are pre-fit estimates.

Most of the backgrounds (W + jets, Z + jets, $t\bar{t}$, single top-quark, and ZZ) are estimated using MC simulation, with data-driven corrections applied in some cases, as described later in this section. By far the largest background in the analysis is from W + jets, followed by top-quark production. Despite the latter background's subdominant contribution, it plays an important role because it contains contributions from real $W \to qq'$ decays, which make it more difficult to distinguish from the signal. About 80% of the top-quark background is due to $t\bar{t}$ production, and the remainder comes from single-top-quark production.

Multijet processes form another source of background. Multijet events can pass the event selection if they contain non-prompt leptons (produced from semileptonic decays of c- and b-hadrons) or "fake" leptons (resulting from misidentified jets). The multijet backgrounds are estimated using data-driven techniques, as described in Sects. 7.1 and 7.2.

7.1 $WV \to \ell\nu$jj channel

The V + jets background prediction is MC-based, but data-driven corrections are applied to the MC prediction in order to improve the description of the jet kinematics. A V + jets control region (CR) is defined identically to the signal region, except that the region 65 GeV $< m_{jj} <$ 95 GeV is vetoed, in order to remove most of the signal events. One-dimensional reweighting functions of the variables $p_T(j_1)$ and $\Delta\phi(jj)$ are derived from this V + jets CR. These reweighting functions have approximately 10% effects on the shapes of the $p_T(j_1)$ and $\Delta\phi(jj)$ distributions. Data–MC comparisons in the V + jets CR are shown in Fig. 1, before and after application of the reweighting functions. All further results in this paper are shown with these two reweighting functions applied to the V + jets MC samples. The same reweighting functions are used for both the W + jets and Z + jets processes. It was checked that the reweighting functions obtained from the low-m_{jj} and high-m_{jj} portions of the V + jets control region are compatible.

The top-quark background is modelled with MC simulation, and is cross-checked in a validation region containing three small-R jets, one of which is b-tagged using the MV1 algorithm [61,62]. Good agreement is observed between the data and the MC simulation, so no corrections are applied to the prediction. The background from ZZ events is also modelled with MC simulation.

The data-driven multijet background estimate makes use of a multijet CR. The multijet CR is formed by selecting events in data that pass the same selection requirements as for the signal region, except that the lepton quality criteria are modified in order to produce a CR enriched in non-prompt and fake leptons. Lepton candidates satisfying these modified criteria are called "anti-identified" lepton candidates. Anti-identified muon candidates must have a non-negligible impact parameter, $|d_0|/\sigma_{d_0} > 4$, and satisfy looser isolation criteria than the signal muon candidates. Anti-identified electrons must fail the "tight" but satisfy the "medium" cut-based identification criteria from Ref. [54], and are also required to contain a hit in the innermost layer of the pixel detector. In addition, the isolation criteria are modified for anti-identified electron candidates, in order to enrich the sample in non-prompt and fake electrons.

The shapes of the kinematic distributions [such as m_{jj}, E_T^{miss}, and $p_T(jj)$] of the multijet background are estimated from events in the multijet CR, after subtracting the MC predictions of the non-multijet contributions to the CR. These non-multijet contributions are about 20% (50%) of the total in the electron (muon) channel. The overall multijet background event yield is estimated from a fit to the E_T^{miss} distribution of events that pass the full signal region selection, except that the requirements on E_T^{miss} and $\Delta\phi(j_1, E_T^{miss})$ (and also $\Delta\eta(j, j)$ and m_T for the muon channel) are removed in order

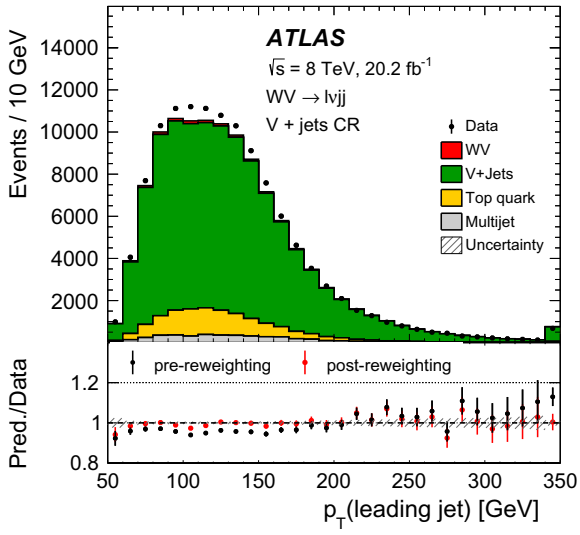

Fig. 1 Comparisons between the data and the prediction in the $V+$jets control region of the $WV \to \ell\nu$jj channel. The *top panel* shows the data and prediction before applying the $p_{\mathrm{T}}(\mathrm{j}_1)$ and $\Delta\phi(\mathrm{j}_1, \mathrm{j}_2)$ kinematic reweighting to the $V+$jets predictions. The distributions shown are **a** p_{T} of the leading jet and **b** $\Delta\phi$ between the leading jet and subleading jet. Overflow is included in the last bin of the $p_{\mathrm{T}}(\mathrm{j}_1)$ plot. The *bottom panel* shows the ratio of the SM prediction to the data before and after applying the kinematic reweighting to the $V+$jets prediction. The *hatched bands* indicate the statistical uncertainty in the predictions

to enhance the number of multijet events. This selection is referred to as the *extended* signal region. In this $E_{\mathrm{T}}^{\mathrm{miss}}$ fit, the multijet $E_{\mathrm{T}}^{\mathrm{miss}}$ shape is estimated from an extended multijet CR, defined analogously to the extended signal region, but requiring the lepton to pass the anti-identified-lepton selection. The $E_{\mathrm{T}}^{\mathrm{miss}}$ shapes of the other backgrounds are estimated using MC samples. The multijet event yield obtained from this fit is then extrapolated to the signal region, using the ratio of events in the multijet CR and the extended multijet CR, corrected for non-multijet contributions. The multijet background estimates are performed separately for the electron and muon channels. Only about 5% of the total multijet background is in the muon channel.

The expected signal and background yields in the $WV \to \ell\nu$jj signal region are given in Table 1, and compared to the number of events observed in data. The predictions for the m_{jj} distribution shapes of the signal and backgrounds are shown in Fig. 2a.

7.2 $WV \to \ell\nu$J channel

In the $WV \to \ell\nu$J channel, the $W+$jets, $Z+$jets, and top-quark backgrounds are estimated using MC samples. The MC predictions for the two largest backgrounds ($W+$jets and top-quark production) are corrected by scale factors obtained from dedicated control regions.

The top-quark control region (top CR) is formed by events satisfying the signal region selection, except that the presence of at least one small-R b-tagged jet with $p_{\mathrm{T}} > 25$ GeV and $\Delta R(\mathrm{j}, \mathrm{J}) > 1.0$ is required instead of applying the nominal veto on small-R jets. The jets are b-tagged using the MV1 algorithm [61,62], using a working point with a b-tagging efficiency of about 70% and a gluon/light-quark jet rejection

Table 1 Expected number of signal and background events in the $WV \to \ell\nu$jj and $WV \to \ell\nu$J signal regions, prior to performing the m_{jj} and m_{J} fits. The quoted uncertainties only include detector-related uncertainties and statistical uncertainties of the MC samples and control regions. The number of events observed in data is also shown. The signal predictions only correspond to qq'-initiated WV production

	$WV \to \ell\nu$jj	$WV \to \ell\nu$J
Signal		
WW	2860 ± 110	542 ± 61
WZ	730 ± 30	128 ± 15
Total expected signal	3590 ± 140	670 ± 75
Background		
$W+$jets	$136{,}000 \pm 8600$	10500 ± 1300
$Z+$jets	2750 ± 340	245 ± 32
$t\bar{t}$	$12{,}980 \pm 520$	1130 ± 150
Single top-quark	3620 ± 150	249 ± 35
Multijet	3689 ± 60	313 ± 18
ZZ	14 ± 1	–
Total expected background	$159{,}000 \pm 8600$	$12{,}400 \pm 1500$
Total SM expected	$162{,}600 \pm 8700$	$13{,}100 \pm 1600$
Observed	164,502	12,999
S/B ($65\ \mathrm{GeV} < m_{\mathrm{jj}} < 95\ \mathrm{GeV}$)	5.5%	10.1%
$S/\sqrt{B}$ ($65\ \mathrm{GeV} < m_{\mathrm{jj}} < 95\ \mathrm{GeV}$)	11.1	7.1

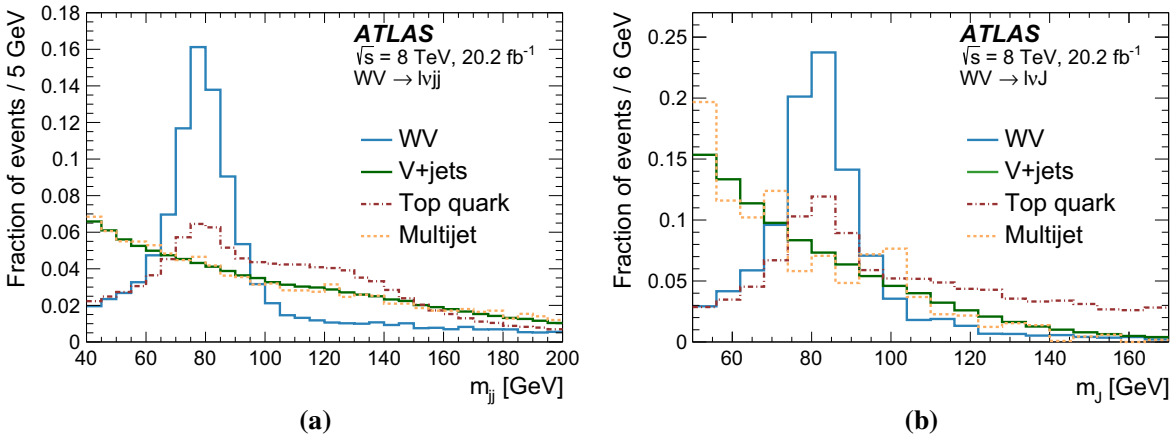

Fig. 2 The shapes of **a** the predicted m_{jj} distributions in the $WV \to \ell\nu\mathrm{jj}$ signal region and **b** the predicted m_{J} distributions in the $WV \to \ell\nu\mathrm{J}$ signal region, for the signal (peaked near 80 GeV) and various background processes. The distributions are normalized to unity

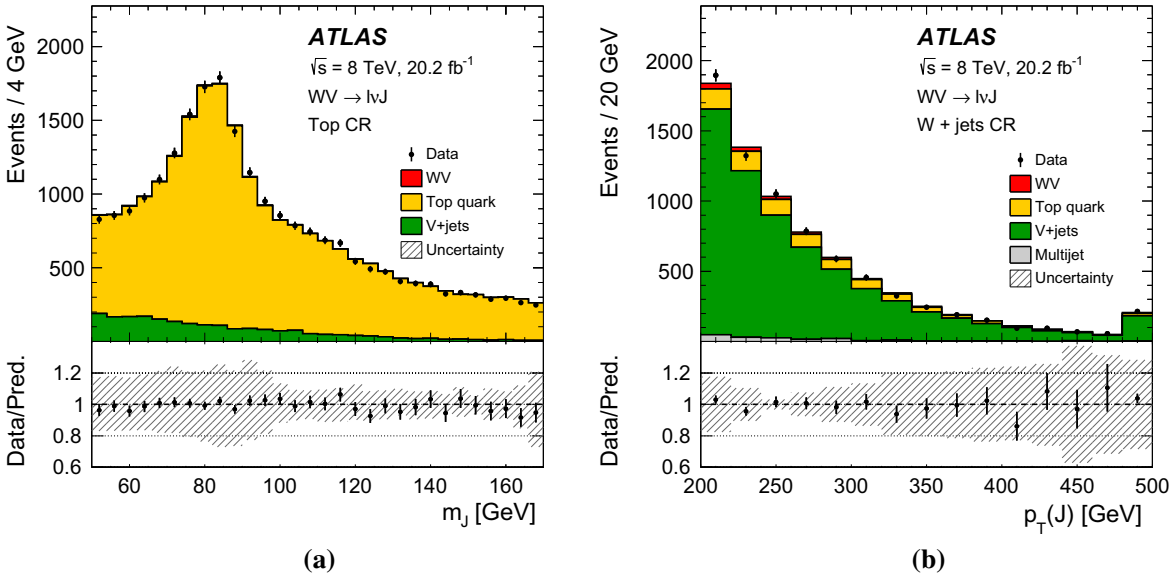

Fig. 3 Comparison between data and prediction in the $WV \to \ell\nu\mathrm{J}$ channel for **a** m_{J} in the top CR, and **b** $p_{\mathrm{T}}(\mathrm{J})$ in the W + jets CR. A scale factor is applied to the top-quark background prediction in the top CR and the W + jets CR, and a scale factor is applied to the W + jets background prediction (which is part of the "V + jets" histogram) in the W + jets CR. The *hatched bands* indicate the systematic uncertainty of the prediction. For the V + jets component, only shape systematic uncertainties are included in the bands

factor of over 100 in $t\bar{t}$ events. About 90% of the events in this top CR originate from top-quark backgrounds. There is a deficit in data in the top CR relative to the MC prediction, which is attributed to a mismodelling of the top-quark backgrounds. A global scale factor of 0.87 for the top-quark backgrounds is obtained from this CR, after subtracting the prediction for non-top-quark backgrounds. The data in the top CR is shown in Fig. 3a, compared to the SM prediction after application of the top-quark scale factor. This scale factor is applied to the top-quark background predictions in the signal region.

The control region for the W + jets background (W + jets CR) is obtained by applying the standard signal region selection, but adding the requirement that $m_{\mathrm{J}} < 65$ GeV or $m_{\mathrm{J}} > 95$ GeV. This additional m_{J} requirement removes almost all of the WV signal events and also a large fraction of the top-quark events. About 85% of the events in this CR originate from W + jets backgrounds. The top-quark background prediction in the W + jets CR is scaled by the top-quark scale factor obtained above. A data deficit is observed in the W + jets CR relative to the prediction. A global scale factor of 0.84 is obtained for the W + jets background, after subtracting the expected contributions from the other signal/background processes. A comparison between the data and the prediction in the W + jets CR is shown in Fig. 3b, after application of the W + jets scale factor. The W + jets scale factor is applied to the W + jets prediction in the signal region.

The method for estimating the multijet background is similar to that used in the $WV \to \ell\nu$jj channel. As in the $WV \to \ell\nu$jj channel, a multijet CR is defined by requiring an "anti-identified" lepton candidate. The shapes of the kinematic distributions are estimated from this CR using the same method as in the $WV \to \ell\nu$jj channel. The non-multijet background contributions to the CR are about 6% of the total. The multijet event yield is estimated from a fit to the $E_{\mathrm{T}}^{\mathrm{miss}}$ distribution, as in the $WV \to \ell\nu$jj channel, but the only requirement that is removed for the definition of the extended signal region/multijet CR is the $E_{\mathrm{T}}^{\mathrm{miss}} > 50$ GeV requirement. The multijet background is found to be negligible for the muon channel, so only the contribution in the electron channel is considered for the final results.

The numbers of expected and observed events in the $WV \to \ell\nu$J signal region are summarized in Table 1. The previously mentioned top-quark and W+jets scale factors are applied to the predictions. The contribution from ZZ events is expected to be very small in the $WV \to \ell\nu$J channel, so it is neglected. The nominal predictions for the m_{J} distribution shapes of the signal and backgrounds are shown in Fig. 2b.

8 Cross-section extraction

The fiducial cross-section σ_{fid} for $WV \to \ell\nu qq'$ production is measured independently for the $WV \to \ell\nu$jj and $WV \to \ell\nu$J phase spaces, in both cases using the formula:

$$\sigma_{\mathrm{fid}} = \frac{N^{WV}}{\mathcal{L} \cdot D_{\mathrm{fid}}},$$

where N^{WV} is the measured signal yield, $\mathcal{L}$ is the integrated luminosity, and D_{fid} is a factor that corrects for experimental acceptance and efficiencies. Since this analysis measures N^{WV} as the sum of the WW and WZ processes, which can each have different acceptances and efficiencies, D_{fid} is given by:

$$D_{\mathrm{fid}} = f_{\mathrm{fid}}^{WW} \cdot C^{WW} + \left(1 - f_{\mathrm{fid}}^{WW}\right) \cdot C^{WZ},$$

where the C^{WV} are reconstruction correction factors and the variable f_{fid}^{WW} is the predicted ratio of the WW fiducial cross-section to the $WW + WZ$ fiducial cross-section. The C^{WV} and f_{fid}^{WW} values are estimated from MC simulation. The C^{WV} factors are defined as the predicted number of WV signal events passing the reconstruction-level event selection divided by the number of WV events in the fiducial phase space defined with generator-level particles. The C^{WV} factors account for reconstruction inefficiencies, resolution effects, and for contributions to the signal region from WV events that do not decay to $\ell\nu qq'$ (such as $WV \to \tau\nu qq'$ or $WW \to \ell\nu\ell\nu$); the latter are included in the C^{WV} numerator and not in the denominator. The cross-section σ_{fid} is measured for the sum of the electron and muon channels, so D_{fid} is computed as a weighted average over the electron and muon channels. The fiducial cross-section measurement therefore assumes that the signal MC simulation correctly predicts the ratio of WW to WZ and of electrons to muons. The value of D_{fid} is 0.83 ± 0.05 in the $WV \to \ell\nu$jj channel and 0.60 ± 0.08 in the $WV \to \ell\nu$J channel, including systematic uncertainties (see Sect. 9).

The fiducial phase spaces for the $WV \to \ell\nu$jj and $WV \to \ell\nu$J channels are defined in Sects. 8.1 and 8.2, respectively. These fiducial phase spaces partially overlap. In order to cope with the small signal-to-background ratios in this analysis (5–10%), the cross-section σ_{fid} is extracted using a binned ML fit to the m_{jj} distribution (in the $WV \to \ell\nu$jj analysis) or the m_{J} distribution (in the $WV \to \ell\nu$J analysis). The ML fits are performed on the sum of the electron and muon channels. It was cross-checked that the electron and muon channels are compatible, in both the $WV \to \ell\nu$jj and $WV \to \ell\nu$J channels.

In the ML fits, the value of σ_{fid} and the V+jets background yield are both free to vary without constraint. Systematic uncertainties in the signal and backgrounds are incorporated in the fit by including nuisance parameters that are allowed to vary within prior constraints. The nuisance parameters allow the luminosity, D_{fid}, the non-V + jets background yields, and the m_{jj} and m_{J} shapes of the signal and background distributions to vary within their systematic uncertainties. The correlations between the uncertainty in D_{fid} and the uncertainty in the signal $m_{\mathrm{jj}}/m_{\mathrm{J}}$ shapes are accounted for in the fit. The sources of systematic uncertainty and the methods to assess these uncertainties are described in detail in Sect. 9.

8.1 $WV \to \ell\nu$jj fiducial phase space

The $WV \to \ell\nu$jj fiducial phase space is defined to closely match the experimental event selection. The phase-space definition requires a WV pair with the bosons decaying as $V \to qq'$ and $W \to \ell\nu$, where $\ell = e, \mu$. Events containing other kinds of WV decay channels (such as $WW \to \ell\nu\ell\nu$ events or $WV \to \tau\nu qq'$ with the τ decaying to $\ell + X$), are not included in the fiducial phase-space definition. Such WV events can still pass the experimental event selection (where they are included in the signal category), and they are accounted for in the D_{fid} definition.

Leptons selected in the fiducial region must have $p_{\mathrm{T}}(\ell) > 30$ GeV and $|\eta(\ell)| < 2.47$. The four-momentum of the lepton is modified by adding to it the four-momenta of all the photons within $\Delta R = 0.1$, excluding photons produced by hadron decays. Particle-level anti-k_t $R = 0.4$ jets are constructed using as constituents all stable particles, excluding muons and neutrinos. Stable particles are defined as those having a mean lifetime of $\tau > 30$ ps. The particle-level jets must have $p_{\mathrm{T}} > 25$ GeV and $|\eta| < 2.5$. Jets within $\Delta R = 0.2$

Table 2 Summary of the fiducial phase-space definitions. All the specified selection criteria are applied at the particle level as specified in the text. The notations "j" and "J" refer to $R = 0.4$ and $R = 1.0$ jets, respectively, as explained in the text

	$WV \to \ell\nu$jj	$WV \to \ell\nu$J
Lepton	$N_\ell = 1$ with $p_{\mathrm{T}} > 30$ GeV and $\lvert\eta\rvert < 2.47$, $\Delta R(\ell, \mathrm{j}) > 0.4$	
$W \to \ell\nu$	$p_{\mathrm{T}}(\ell\nu) > 100$ GeV	–
	$m_{\mathrm{T}} > 40$ GeV	–
$E_{\mathrm{T}}^{\mathrm{miss}}$	$E_{\mathrm{T}}^{\mathrm{miss}} > 40$ GeV	$E_{\mathrm{T}}^{\mathrm{miss}} > 50$ GeV
Jet	$N_{\mathrm{j}} = 2$ with $p_{\mathrm{T}} > 25$ GeV, $\lvert\eta\rvert < 2.5$,	$N_{\mathrm{J}} = 1$ with $p_{\mathrm{T}} > 200$ GeV, $\lvert\eta\rvert < 2.0$,
	$\Delta R(\mathrm{j}, e) > 0.2$	$\Delta R(\mathrm{J}, \ell) > 1.0$
		No small-R jets with $p_{\mathrm{T}} > 25$ GeV, $\lvert\eta\rvert < 4.5$, $\Delta R(\mathrm{j}, \mathrm{J}) > 1.0$, $\Delta R(\mathrm{j}, e) > 0.2$
	$40 < m_{\mathrm{jj}} < 200$ GeV	$50 < m_{\mathrm{J}} < 170$ GeV
	$p_{\mathrm{T}}(\mathrm{jj}) > 100$ GeV	–
	$\Delta\eta(\mathrm{j}, \mathrm{j}) < 1.5$	–
Global	$\Delta\phi(\mathrm{j}_1, E_{\mathrm{T}}^{\mathrm{miss}}) > 0.8$	–

of a selected electron are rejected, and then leptons within $\Delta R = 0.4$ of a remaining jet are rejected. The true $E_{\mathrm{T}}^{\mathrm{miss}}$ in the event is defined as the magnitude of the vector p_{T} sum of all the neutrinos.

The event must have exactly one lepton and two $R = 0.4$ jets matching the above definitions. The remaining requirements for the fiducial phase space are summarized in Table 2, and are analogous to the experimental event selection, but are defined using the lepton, $E_{\mathrm{T}}^{\mathrm{miss}}$, and particle-level jets described in this section.

8.2 $WV \to \ell\nu$J fiducial phase space

As in the $WV \to \ell\nu$jj channel, the fiducial phase-space definition requires a WV pair with $V \to qq'$ and $W \to \ell\nu$. Leptons, $E_{\mathrm{T}}^{\mathrm{miss}}$, and particle-level $R = 0.4$ jets are defined in the same way as in the $WV \to \ell\nu$jj channel, except that two sets of leptons and small-R jets are considered: *central* leptons (small-R jets) are required to have $\lvert\eta\rvert < 2.47$ ($\lvert\eta\rvert < 2.5$), and *extended* leptons and small-R jets are required to have $\lvert\eta\rvert < 4.5$. Particle-level large-R jets are defined by applying the anti-k_t algorithm with radius parameter $R = 1.0$ to all stable particles, excluding muons and neutrinos. No trimming is applied to these jets. The large-R jets are required to have $p_{\mathrm{T}} > 200$ GeV and $\lvert\eta\rvert < 2.0$. Central (extended) small-R jets that are within $\Delta R = 0.2$ of a central (extended) electron are rejected. Then, central leptons are rejected if they are within $\Delta R = 0.4$ of a remaining central small-R jet. Large-R jets are rejected if they are within $\Delta R = 1.0$ of any remaining central leptons. Events are required to contain exactly one central lepton and one large-R jet with the above definitions, and events are discarded if they contain any extended small-R jets with $\Delta R(\mathrm{j}, \mathrm{J}) > 1.0$. The event must also have $E_{\mathrm{T}}^{\mathrm{miss}} > 50$ GeV, and the large-R jet must have a mass greater than 50 GeV. The fiducial phase-space definition is summarized in Table 2.

9 Systematic uncertainties

Systematic uncertainties in the measured σ_{fid} can be due to uncertainties in $\mathcal{L}$, D_{fid}, and/or N^{WV}. Uncertainties in the measured N^{WV} can in turn be due to uncertainties in the background yields or in the shapes of the kinematic distributions ($m_{\mathrm{jj}}, m_{\mathrm{J}}$) of the signal and backgrounds (hereafter called "shape uncertainties"). The dominant systematic uncertainties in the σ_{fid} measurement are those affecting the measured N^{WV}.

A wide variety of detector-related experimental uncertainties are considered, which affect D_{fid}, the predicted background yields, and the signal and background shapes. The most important of these uncertainties are those related to the jet reconstruction. Uncertainties in the small-R jet energy scale and resolution are accounted for [57,63]. In the $WV \to \ell\nu$J channel, uncertainties in the large-R jet energy and jet mass scales are also taken into account. The scale uncertainties of the large-R jets are estimated using a double-ratio method that compares calorimeter- and track-jets in data and MC simulation [21]. The energy and mass resolution uncertainties of large-R jets are estimated by smearing the jet energies/masses so as to degrade the resolutions by 20%; this approach is based on prior studies of large-R jets [64,65]. The systematic uncertainty due to the JVF requirement is also included [66]. In addition to the jet-related uncertainties, there are also systematic uncertainties in the electron and muon reconstruction (including triggering, object reconstruction, identification, and the energy scale and resolution) [54,67–70]. The effects of the jet and lepton uncertainties are propagated to the $E_{\mathrm{T}}^{\mathrm{miss}}$ calculation, and an additional systematic uncertainty in the soft terms entering the $E_{\mathrm{T}}^{\mathrm{miss}}$ calculation is also included [60].

In the cross-section fits, the V + jets yield is taken to be a free parameter, while several uncertainties in the modelling of its shape are accounted for (in addition to the shape uncertainties from the previously mentioned detector effects). Systematic uncertainties in the V + jets shape are estimated by varying the MC event generator used (SHERPA compared to ALPGEN+PYTHIA). The differences between the predictions of the two generators are taken as additional systematic uncertainties. Additional uncertainties in the V + jets shape are estimated by varying the renormalization and factorization scales by factors of 2 and 0.5, and by varying the scale used

in SHERPA for matching the matrix elements to the parton showers [39] from its nominal value of 20 GeV to alternative values of 15 GeV and 30 GeV. In the $WV \to \ell\nu$jj channel, the uncertainty in the shapes of the $V+$jets predictions due to the two kinematic reweighting functions (see Sect. 7.1) is estimated by including the full difference between applying and not applying each reweighting function as additional systematic uncertainties. In the $WV \to \ell\nu$jj channel, an uncertainty of 10% in the $(W+\text{jets})/(Z+\text{jets})$ cross-section ratio is also included; this uncertainty is ignored in the $WV \to \ell\nu$J channel as it has a negligible effect.

For the $t\bar{t}$ background, uncertainties due to the matrix-element event generator, parton shower/hadronization model, and amount of initial- and final-state radiation are all included. The theoretical uncertainties in the top-quark background cross-sections are also taken into account. In the $WV \to \ell\nu$J channel, instead of using the theoretical cross-section uncertainty, the top-quark background is assigned a normalization uncertainty of 14% to account for the uncertainty in the data-driven scale factor. Systematic uncertainties in the multijet background estimate are also included, which affect both its normalization and its shape. These uncertainties are derived from studies of variations of the data-driven estimate, such as changing the control region definitions and varying the non-multijet background subtraction. The uncertainty in the multijet yield amounts to 30% (100%) for the electron (muon) channel in the $WV \to \ell\nu$jj channel. In the $WV \to \ell\nu$J channel, an uncertainty of 50% is assigned to the multijet yield in the electron channel, while the multijet background is neglected in the muon channel. A 30% uncertainty is assigned to the ZZ event yield in the $WV \to \ell\nu$jj channel, to account for uncertainties in the ZZ cross-section and the extrapolation to the fiducial phase space.

Additionally, the uncertainty in the modelling of pile-up interactions is accounted for [71]. The uncertainty in the integrated luminosity is also included, computed as described in Ref. [72]. The statistical uncertainty of the MC samples is taken into account, which affects each bin in the ML fits in an uncorrelated way.

Uncertainties in the signal shapes and in the D_{fid} parameter due to variations of the signal model are computed by varying the renormalization and factorization scales by factors of 2 and 0.5, and by comparing the nominal MC@NLO signal samples to alternative samples generated with SHERPA and POWHEG +PYTHIA 8. The effect on D_{fid} from the uncertainties in the CT10 PDF set is also taken into account; the PDF uncertainty has a negligible impact on the signal shapes.

The measured σ_{fid} values are compared to theoretical predictions from MC@NLO. The uncertainty in the theoretical σ_{fid} prediction is calculated including the uncertainties due to renormalization and factorization scales. Since the fiducial phase spaces contain a veto on additional jets, the Stewart–Tackmann procedure [73] is used to estimate the scale uncertainties. These uncertainties are also propagated to the theoretical f_{fid}^{WW} value which enters into the D_{fid} calculation, although the effect of this on the measured σ_{fid} is very small ($\sim$0.1%). PDF-induced uncertainties in the theoretical prediction are also taken into account.

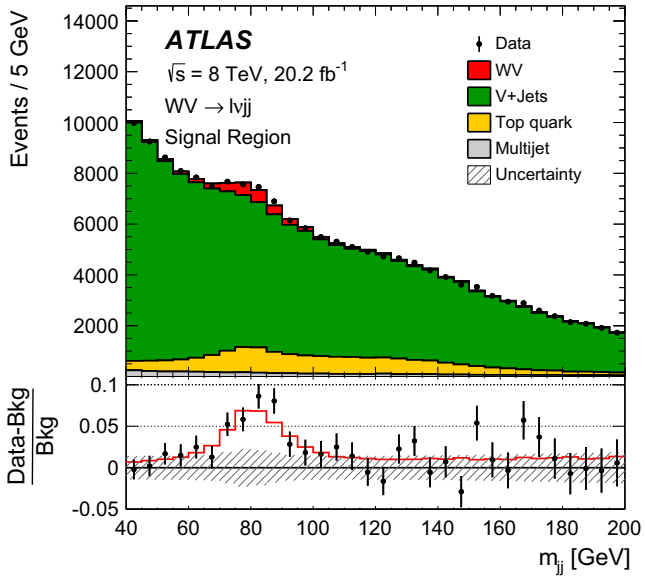

Fig. 4 The observed m_{jj} distribution in the $WV \to \ell\nu$jj signal region, overlaid with the post-fit background and signal estimates. The *hatched band* indicates the total uncertainty of the fit result

10 Cross-section results

The result of the ML fit to the m_{jj} distribution for the $WV \to \ell\nu$jj channel is shown in Fig. 4. The fit is performed on the sum of events in the electron and muon channels. The observed significance is 4.5σ, including statistical and systematic uncertainties,[3] while the expected significance, calculated using the Asimov data set [74], is 5.2σ. The fitted $V+$jets background normalization is 1.02 ± 0.01 times its pre-fit value, while the fitted top-quark background normalization is 0.96 ± 0.10 times its pre-fit value.

The fiducial cross-section for the signal process is extracted from the fit as described in Sect. 8, and the result is

$$\sigma_{\text{fid}}(WV \to \ell\nu\text{jj, observed}) = 209 \pm 28(\text{stat}) \pm 45(\text{syst})\ \text{fb}.$$

The impacts of the various systematic uncertainties on the cross-section measurement are shown in Table 3. The measurement can be compared to the theoretical prediction of

$$\sigma_{\text{fid}}(WV \to \ell\nu\text{jj, theory}) = 225 \pm 13\ \text{fb}.$$

[3] The significance is calculated based on the profile-likelihood ratio of the background-only and signal-and-background hypotheses. This ratio is converted to a significance using the asymptotic approximation [74].

Table 3 Breakdown of the uncertainties in the measured fiducial cross-section in the $WV \to \ell\nu$jj channel. Uncertainties smaller than 1% are omitted from the table

Source of uncertainty	Relative uncertainty for σ_{fid} (%)
Top-quark background modelling	13
Signal modelling	12
V + jets modelling	4
Multijet background modelling	1
Small-R jet energy/resolution	9
Other experimental (leptons, pile-up)	4
Luminosity	2
MC statistics	9
Data statistics	14

Table 4 Breakdown of the uncertainties in the measured fiducial cross-section in the $WV \to \ell\nu$J channel. Uncertainties smaller than 1% are omitted from the table

Source of uncertainty	Relative uncertainty for σ_{fid} (%)
V + jets modelling	60
Top-quark background modelling	32
Signal modelling	15
Multijet background modelling	13
Large-R jet energy/resolution	45
Small-R jet energy/resolution	16
Other experimental (leptons, pile-up)	3
Luminosity	2
MC statistics	19
Data statistics	33

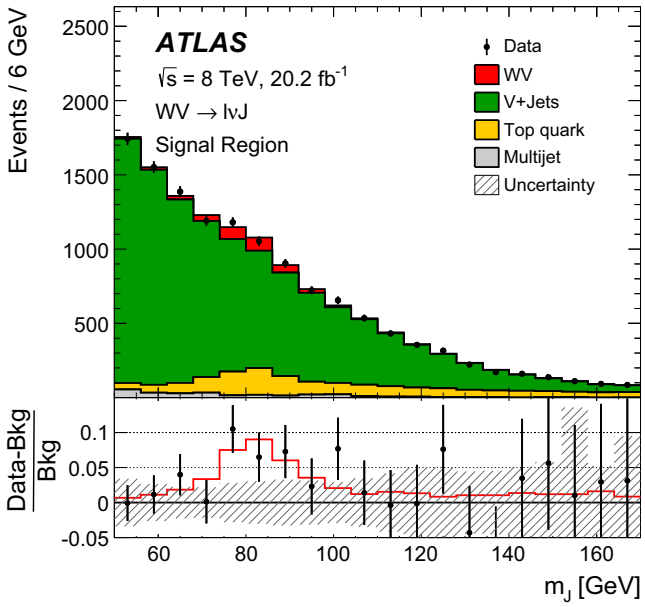

Fig. 5 The observed m_{J} distribution in the $WV \to \ell\nu$J signal region, overlaid with the post-fit background and signal estimates. The *hatched band* indicates the total uncertainty of the fit result

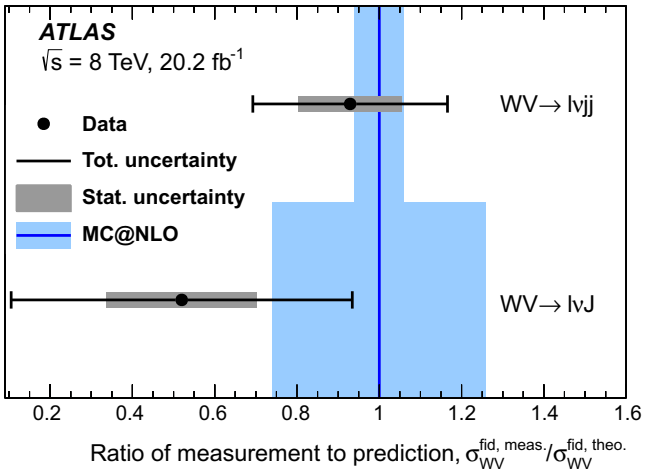

Fig. 6 The ratios of the measured fiducial cross-sections to the cross-sections predicted by MC@NLO, for the $WV \to \ell\nu$jj and $WV \to \ell\nu$J phase spaces. The $WV \to \ell\nu$jj and $WV \to \ell\nu$J phase spaces partially overlap

The theoretical prediction is obtained using MC@NLO for the $qq' \to WV$ prediction. The $gg \to WW$ prediction is also included, and is calculated using the total NLO $gg \to WW$ cross-section prediction [75] multiplied by the $qq' \to WW$ acceptance from MC@NLO. The $gg \to WW$ contribution increases the fiducial cross-section prediction by 4% in both the $WV \to \ell\nu$jj and $WV \to \ell\nu$J channels. Given the relatively small $gg \to WW$ contribution, the possible differences in acceptance between the $gg \to WW$ and $qq' \to WW$ processes are neglected. The uncertainty in the MC@NLO prediction is described in Sect. 9.

The result of the m_{J} fit for the $WV \to \ell\nu$J channel is shown in Fig. 5. Although the signal-to-background ratio is better in this case than in the $WV \to \ell\nu$jj channel, the total number of signal events is much smaller. The observed significance of the result is 1.3σ (including statistical and systematic uncertainties), compared to an expected significance of 2.5σ. The fitted V + jets (top-quark) background normalization is 1.01 ± 0.04 (1.06 ± 0.20) times its pre-fit value.

The extracted fiducial cross-section for the signal process is

$$\sigma_{\text{fid}}(WV \to \ell\nu\text{J, observed}) = 30 \pm 11(\text{stat}) \pm 22(\text{syst})\ \text{fb},$$

which is compatible with the theoretical prediction of

$$\sigma_{\text{fid}}(WV \to \ell\nu\text{J, theory}) = 58 \pm 15\ \text{fb}.$$

The breakdown of the uncertainties contributing to the fiducial cross-section measurement is shown in Table 4.

The cross-section measurements are summarized in Fig. 6. As mentioned in Sect. 8, the two cross-section measurements

are performed in partially overlapping phase spaces. The uncertainty in the theory prediction is significantly larger in the $WV \to \ell\nu$J channel than in the $WV \to \ell\nu$jj channel. The theoretical uncertainty in the $WV \to \ell\nu$J channel is dominated by the scale uncertainties, which are particularly large because of the aggressive jet veto in this channel (only about 30% of signal MC events pass the jet veto in the $WV \to \ell\nu$J channel, compared to about 80% in the $WV \to \ell\nu$jj channel).

11 Constraints on anomalous gauge couplings

In many extensions of the SM, diboson production can be modified, such as through new resonances that couple to bosons. If the scale of new physics is sufficiently high, new resonances may not be visible in the current data; however, diboson production could still be affected below the new-physics scale, in the form of modified couplings. One common framework for parameterizing new physics in diboson production is an effective Lagrangian [1] of the form:

$$\mathcal{L}^{WWX} \propto \Big[(1+\Delta g_1^X)(W^+_{\mu\nu}W^{-\mu} - W^{+\mu}W^-_{\mu\nu})X^\nu + (1+\Delta\kappa_X)W^+_\mu W^-_\nu X^{\mu\nu} + \frac{\lambda_X}{m_W^2}W^{+\nu}_\mu W^{-\rho}_\nu X^\mu_\rho\Big],$$

where $X = Z$ or γ, $W^\pm_{\mu\nu} = \partial_\mu W^\pm_\nu - \partial_\nu W^\pm_\mu$, and $X_{\mu\nu} = \partial_\mu X_\nu - \partial_\nu X_\mu$. The six parameters λ_X, $\Delta\kappa_X$, and Δg_1^X (hereafter called "aTGC parameters") are all zero in the SM. The parameter Δg_1^γ is zero because of EM gauge invariance, leaving five free aTGC parameters, which describe deviations of the triple gauge-boson couplings from their SM predictions. It is common to apply the so-called *LEP constraint* [76], which imposes $SU(2) \times U(1)$ gauge invariance, and which reduces the number of independent aTGC parameters to three, by introducing the following constraints: $\lambda_\gamma = \lambda_Z$ and $\Delta g_1^Z = \Delta\kappa_Z + \Delta\kappa_\gamma \tan^2\theta_W$, where θ_W is the weak mixing angle. Since aTGC parameters lead to violation of unitarity at high energies, form factors are often applied to them in order to ensure unitarity:

$$\alpha \to \frac{\alpha}{\left(1+\frac{\hat{s}}{\Lambda^2_{\mathrm{FF}}}\right)^2},$$

where α is one of the aTGC parameters, $\hat{s}$ is the square of the diboson invariant mass, and Λ_{FF} is the form factor's energy scale.

An alternative framework for describing modifications of diboson production is an effective field theory (EFT) [77,78] that is assumed to be valid below an energy scale Λ, and which introduces three CP-conserving dimension-six operators:

$$\mathcal{O}_W = (D_\mu\Phi)^\dagger W^{\mu\nu}(D_\nu\Phi),$$
$$\mathcal{O}_B = (D_\mu\Phi)^\dagger B^{\mu\nu}(D_\nu\Phi),$$
$$\mathcal{O}_{WWW} = Tr[W_{\mu\nu}W^{\nu\rho}W^\mu_\rho].$$

Here, Φ is the Higgs doublet field, D_μ is the covariant derivative, and $W^{\mu\nu}$ and $B^{\mu\nu}$ are the field strength tensors of the W and B gauge boson fields. The coefficients of these operators (EFT parameters), c_W/Λ^2, c_B/Λ^2, and c_{WWW}/Λ^2, are zero in the SM and can be related to the LEP-constraint aTGC parameters as follows:

$$\frac{c_W}{\Lambda^2} = \frac{2}{m_Z^2}\Delta g_1^Z,$$
$$\frac{c_B}{\Lambda^2} = \frac{2}{m_W^2}\Delta\kappa_\gamma - \frac{2}{m_Z^2}\Delta g_1^Z,$$
$$\frac{c_{WWW}}{\Lambda^2} = \frac{2}{3g^2m_W^2}\lambda.$$

This relation only holds if no form factor is applied to the aTGCs. The effect of aTGC/EFT parameters on the $H \to WW$ process is neglected.

The aTGC and EFT parameters both tend to increase the diboson cross-section at high $p_{\mathrm{T}}(V)$ and high invariant mass of the diboson system. Both the $WV \to \ell\nu$jj channel and the $WV \to \ell\nu$J channel can be used to search for these BSM enhancements. The $WV \to \ell\nu$J channel, although currently less sensitive as a SM WV measurement, is expected to provide a higher sensitivity to the aTGC/EFT models, because of the better efficiency at high $p_{\mathrm{T}}(V)$. On the other hand, the $WV \to \ell\nu$jj channel, where the SM WV measurement is clearly established, is useful as a complementary search channel that probes a different energy range.

In this analysis, the new-physics search uses signal regions with exactly the same event selection as the cross-section measurements, except that the m_{jj} requirement is tightened to 65 GeV $< m_{\mathrm{jj}} <$ 95 GeV in the $WV \to \ell\nu$jj channel and the m_{J} requirement is tightened to 65 GeV $< m_{\mathrm{J}} <$ 95 GeV in the $WV \to \ell\nu$J channel. These tighter requirements lead to an increase in the signal-to-background ratio. In the $WV \to \ell\nu$jj channel, events which fail the m_{jj} requirement (i.e. 40 GeV $< m_{\mathrm{jj}} <$ 65 GeV or 95 GeV $< m_{\mathrm{jj}} <$ 200 GeV) are put into a *sideband* control region. The ZZ background is neglected in the new-physics search, due to its very small expected contribution.

The search makes use of the p_{T}(jj) ($WV \to \ell\nu$jj channel) or p_{T}(J) ($WV \to \ell\nu$J channel) distribution. Hereafter, $p_{\mathrm{T}}(V_{\mathrm{rec}})$ is used to refer to both p_{T}(jj) and p_{T}(J). The $p_{\mathrm{T}}(V_{\mathrm{rec}})$ distributions of the events in the signal regions are shown in Fig. 7. This figure also shows the expected enhancement at high $p_{\mathrm{T}}(V_{\mathrm{rec}})$ in the presence of different EFT parameter values. As can be seen from the figure, no significant deviation from the SM prediction is observed; there-

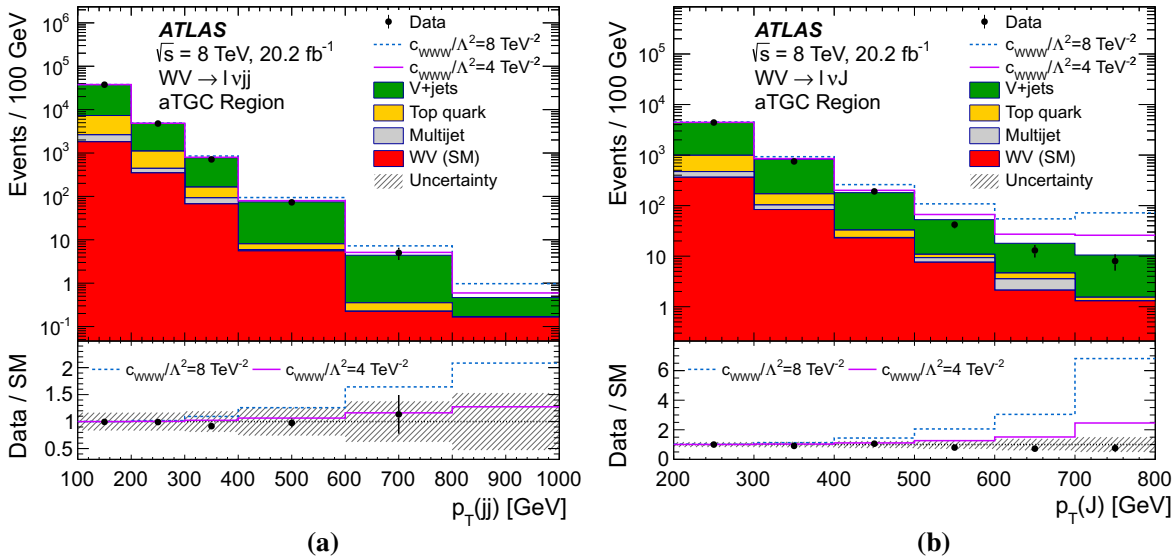

Fig. 7 The observed **a** p_{T}(jj) distribution in the $WV \to \ell\nu$jj aTGC signal region, and **b** p_{T}(J) distribution in the $WV \to \ell\nu$J aTGC signal region, overlaid with the background and signal prediction. The expected BSM enhancements due to anomalous values of the EFT parameter c_{WWW}/Λ^2 are also shown, for $c_{WWW}/\Lambda^2 = 4$ TeV^{-2} and $c_{WWW}/\Lambda^2 = 8$ TeV^{-2}. The *hatched bands* indicate the systematic uncertainty in the SM prediction. The *histograms* are displayed with the binning that is used for the computation of the confidence intervals for the aTGC and EFT parameters. The last bin includes overflow

Table 5 The observed and expected 95% confidence intervals for the aTGC parameters without the LEP constraint. The confidence intervals are computed separately for the $WV \to \ell\nu$jj and $WV \to \ell\nu$J channels, and are calculated both for $\Lambda_{\mathrm{FF}} = 5$ TeV and $\Lambda_{\mathrm{FF}} = \infty$ (i.e. no form factor). The confidence intervals for each parameter are calculated while fixing the other parameters to zero

Form factor	Parameter	$WV \to \ell\nu$jj		$WV \to \ell\nu$J	
		Observed	Expected	Observed	Expected
$\Lambda_{\mathrm{FF}} = \infty$	Δg_1^Z	[−0.039, 0.059]	[−0.050, 0.066]	[−0.033, 0.036]	[−0.039, 0.042]
	$\Delta\kappa_Z$	[−0.045, 0.063]	[−0.060, 0.076]	[−0.028, 0.030]	[−0.033, 0.035]
	λ_Z	[−0.024, 0.024]	[−0.029, 0.029]	[−0.015, 0.015]	[−0.017, 0.017]
	$\Delta\kappa_\gamma$	[−0.099, 0.14]	[−0.13, 0.17]	[−0.058, 0.063]	[−0.067, 0.073]
	λ_γ	[−0.084, 0.084]	[−0.10, 0.10]	[−0.042, 0.041]	[−0.049, 0.049]
$\Lambda_{\mathrm{FF}} = 5$ TeV	Δg_1^Z	[−0.042, 0.064]	[−0.055, 0.073]	[−0.044, 0.048]	[−0.051, 0.054]
	$\Delta\kappa_Z$	[−0.047, 0.068]	[−0.064, 0.083]	[−0.037, 0.040]	[−0.043, 0.047]
	λ_Z	[−0.026, 0.026]	[−0.032, 0.032]	[−0.020, 0.019]	[−0.023, 0.022]
	$\Delta\kappa_\gamma$	[−0.10, 0.15]	[−0.14, 0.18]	[−0.077, 0.084]	[−0.089, 0.097]
	λ_γ	[−0.089, 0.089]	[−0.11, 0.11]	[−0.056, 0.056]	[−0.065, 0.065]

fore, 95% confidence intervals are computed for the aTGC and EFT parameters.

The confidence intervals are computed from binned ML fits to the $p_{\mathrm{T}}(V_{\mathrm{rec}})$ distributions. The intervals are calculated using a frequentist Feldman–Cousins approach [79]. In the $WV \to \ell\nu$jj channel, simultaneous fits to the $p_{\mathrm{T}}(V_{\mathrm{rec}})$ distributions in the signal region and sideband CR are used, while in the $WV \to \ell\nu$J channel, only the $p_{\mathrm{T}}(V_{\mathrm{rec}})$ distribution in the signal region is used. Since the $WV \to \ell\nu$J and $WV \to \ell\nu$jj selections overlap, the confidence intervals are calculated separately for the $WV \to \ell\nu$J and $WV \to \ell\nu$jj selections. In the fits, the SM WV and background predictions are allowed to vary within their uncertainties. The measured cross sections of Sect. 10 are consistent with theoretical SM WV predictions, but have large associated uncertainties; for this reason the theoretical prediction is used here. The systematic uncertainties in the normalizations and $p_{\mathrm{T}}(V_{\mathrm{rec}})$ shapes of the signal and backgrounds are accounted for through nuisance parameters. The systematic uncertainties that have the largest impact on the results are the jet-related uncertainties (in both channels) and the uncertainty from the limited size of the MC samples (in the $WV \to \ell\nu$jj channel).

The observed 95% confidence intervals for the aTGC parameters are shown in Table 5, without applying the LEP

Table 6 The observed and expected 95% confidence intervals for the aTGC parameters in the LEP-constraint scenario with $\Lambda_{\mathrm{FF}} = \infty$, computed separately for the $WV \to \ell\nu\mathrm{jj}$ and $WV \to \ell\nu\mathrm{J}$ channels. The confidence intervals for each parameter are calculated while fixing the other parameters to zero

Parameter	$WV \to \ell\nu\mathrm{jj}$		$WV \to \ell\nu\mathrm{J}$	
	Observed	Expected	Observed	Expected
Δg_1^Z	$[-0.027, 0.045]$	$[-0.036, 0.051]$	$[-0.021, 0.024]$	$[-0.024, 0.027]$
$\Delta\kappa_\gamma$	$[-0.11, 0.13]$	$[-0.15, 0.16]$	$[-0.061, 0.064]$	$[-0.071, 0.075]$
$\lambda_Z = \lambda_\gamma$	$[-0.022, 0.022]$	$[-0.027, 0.026]$	$[-0.013, 0.013]$	$[-0.015, 0.015]$

Table 7 The observed and expected 95% confidence intervals for the EFT parameters. The parameters are given in units of TeV^{-2}. The confidence intervals for each parameter are calculated while fixing the other parameters to zero

Parameter	$WV \to \ell\nu\mathrm{jj}$		$WV \to \ell\nu\mathrm{J}$	
	Observed (TeV^{-2})	Expected (TeV^{-2})	Observed (TeV^{-2})	Expected (TeV^{-2})
c_{WWW}/Λ^2	$[-5.3, 5.3]$	$[-6.4, 6.3]$	$[-3.1, 3.1]$	$[-3.6, 3.6]$
c_B/Λ^2	$[-36, 43]$	$[-45, 51]$	$[-19, 20]$	$[-22, 23]$
c_W/Λ^2	$[-6.4, 11]$	$[-8.7, 13]$	$[-5.1, 5.8]$	$[-6.0, 6.7]$

constraint. The confidence intervals for a given aTGC parameter are computed while fixing the other aTGC parameters to zero. The confidence intervals are shown separately for the $WV \to \ell\nu\mathrm{jj}$ and $WV \to \ell\nu\mathrm{J}$ selections, and the expected confidence intervals under the SM hypothesis are also shown for comparison. Confidence intervals for the aTGC parameters are shown for $\Lambda_{\mathrm{FF}} = 5$ TeV and for the case of no form factor (equivalent to $\Lambda_{\mathrm{FF}} = \infty$). The value of $\Lambda_{\mathrm{FF}} = 5$ TeV is chosen in order to ensure unitarity over the range of aTGC parameter values to which this analysis is sensitive [80].

The $WV \to \ell\nu\mathrm{J}$ selection has significantly better sensitivity to the aTGC parameters. No combination of the $WV \to \ell\nu\mathrm{jj}$ and $WV \to \ell\nu\mathrm{J}$ constraints is performed, since it is expected that the $WV \to \ell\nu\mathrm{J}$ channel would dominate the combination. The sensitivity to the aTGC parameters in the $WV \to \ell\nu\mathrm{J}$ channel mainly comes from the $p_{\mathrm{T}}(V_{\mathrm{rec}}) >$ 600 GeV bins, whereas the sensitivity in the $WV \to \ell\nu\mathrm{jj}$ channel mainly comes from the 300–600 GeV bins. Since the $WV \to \ell\nu\mathrm{jj}$ channel probes a lower $p_{\mathrm{T}}(V_{\mathrm{rec}})$ range, its sensitivity is less degraded by the form factors (which have a larger effect at higher p_{T}) than the $WV \to \ell\nu\mathrm{J}$ channel.

In addition, the observed and expected confidence intervals for the aTGC parameters in the LEP-constraint scenario are given in Table 6 for $\Lambda_{\mathrm{FF}} = \infty$.

The observed and expected confidence intervals for the EFT parameters are shown in Table 7, separately for the $WV \to \ell\nu\mathrm{jj}$ and $WV \to \ell\nu\mathrm{J}$ selections. Confidence regions for combinations of two EFT parameters are shown in Fig. 8; for each combination the third EFT parameter is held fixed to zero. Although the constraints from the $WV \to \ell\nu\mathrm{jj}$ channel are less stringent than those from the $WV \to \ell\nu\mathrm{J}$ channel, they probe a complementary phase space. The sensitivity of the $WV \to \ell\nu\mathrm{J}$ channel is similar to the most sensitive previous analyses to publish constraints on these parameters [3,5,6,22]. The $WV \to \ell\nu\mathrm{J}$ channel probes a similar phase space to Ref. [22]; these analyses benefit from their ability to reconstruct high-p_{T} $V \to qq'$ decays.

12 Conclusion

The production of $WV \to \ell\nu qq'$, with V being a W or Z boson, is measured using 20.2 fb^{-1} of pp collisions at 8 TeV at the LHC with the ATLAS detector. The measurements focus on WV production where the bosons have large transverse momentum. Fiducial cross-sections for the $WV \to \ell\nu qq'$ process are measured in two different, but partially overlapping, phase spaces.

The first phase space, denoted $WV \to \ell\nu\mathrm{jj}$, targets a hadronically decaying V boson whose decay products can be distinguished as two $R = 0.4$ jets. In this phase space, the $WV \to \ell\nu qq'$ process is measured with a significance of 4.5σ, and the fiducial cross-section is measured to be $209 \pm 28(\mathrm{stat}) \pm 45(\mathrm{syst})$ fb, in agreement with the MC@NLO prediction of 225 ± 13 fb.

The second phase space, denoted $WV \to \ell\nu\mathrm{J}$, contains a single $R = 1.0$ jet consistent with the collimated decay products of a high-p_{T} V boson. The WV process is measured with a significance of 1.3σ in this phase space. The fiducial cross-section for this phase space is measured to be $30 \pm 11(\mathrm{stat}) \pm 22(\mathrm{syst})$ fb, consistent with the MC@NLO prediction of 58 ± 15 fb.

The events are also used to search for new physics modifying triple gauge-boson vertices, which could lead to enhance-

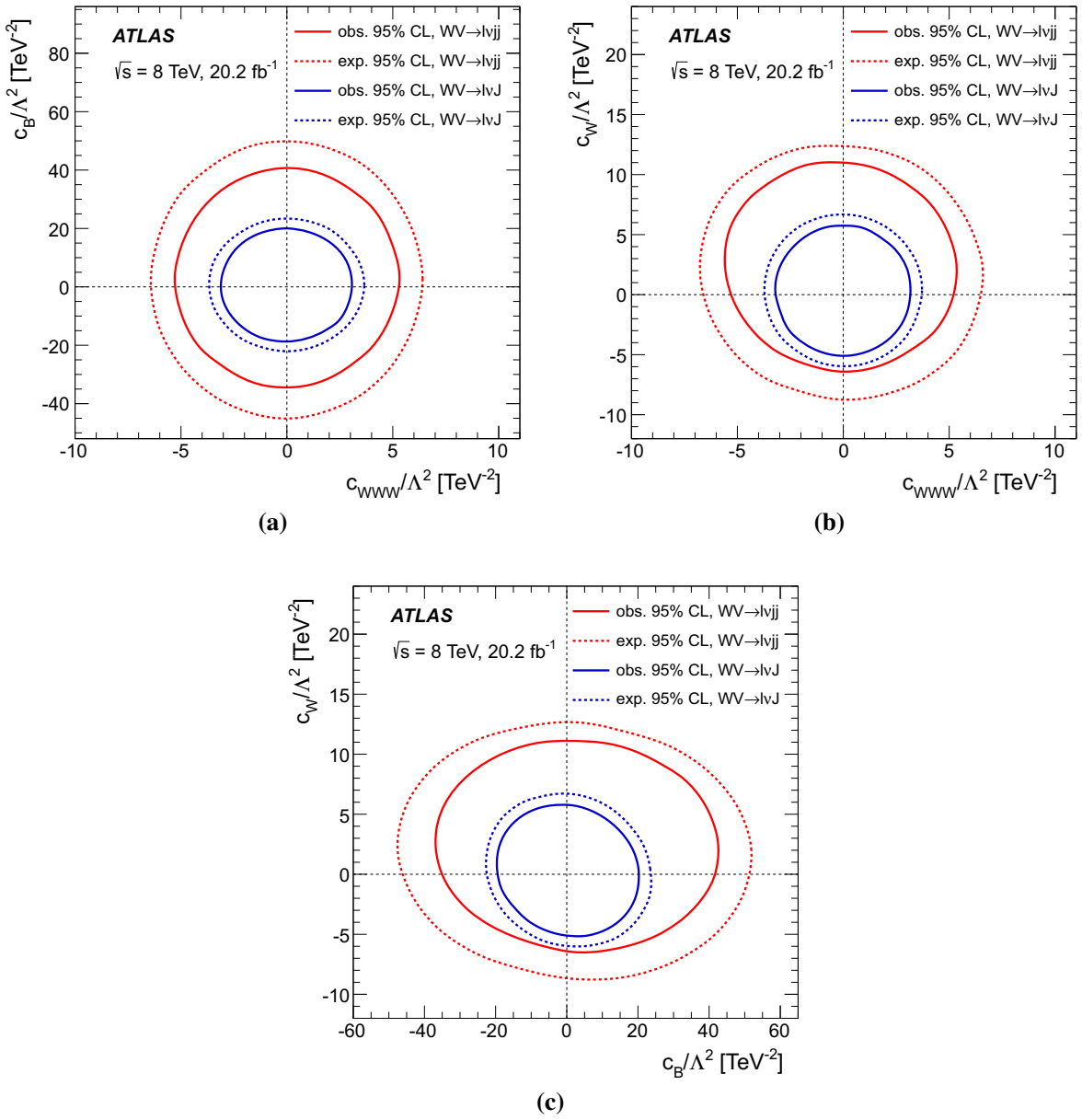

Fig. 8 The 95% confidence-level regions for combinations of two EFT parameters. **a** c_{WWW}/Λ^2 and c_B/Λ^2, **b** c_{WWW}/Λ^2 and c_W/Λ^2, **c** c_B/Λ^2 and c_W/Λ^2. The expected and observed confidence regions are shown for the $WV \to \ell\nu$jj channel (*outer contours*) and the $WV \to \ell\nu$J channel (*inner contours*). When computing the confidence regions for two parameters, the third EFT parameter is held fixed to zero

ments of the cross-section at high p_{T} of the bosons. No evidence is found for new physics, and 95% confidence intervals are computed for anomalous coupling parameters. The constraints on new physics are also interpreted in terms of an effective field theory. The $WV \to \ell\nu$J channel is found to be significantly more sensitive to the new-physics parameters than the $WV \to \ell\nu$jj channel, which demonstrates the power of large-radius jet substructure techniques. The constraints from this analysis on the new physics parameters are comparable to the previous most stringent constraints from other diboson analyses.

Acknowledgements We thank CERN for the very successful operation of the LHC, as well as the support staff from our institutions without whom ATLAS could not be operated efficiently. We acknowledge the support of ANPCyT, Argentina; YerPhI, Armenia; ARC, Australia; BMWFW and FWF, Austria; ANAS, Azerbaijan; SSTC, Belarus; CNPq and FAPESP, Brazil; NSERC, NRC and CFI, Canada; CERN; CONICYT, Chile; CAS, MOST and NSFC, China; COLCIENCIAS, Colombia; MSMT CR, MPO CR and VSC CR, Czech Republic; DNRF and DNSRC, Denmark; IN2P3-CNRS, CEA-DSM/IRFU, France; SRNSF, Georgia; BMBF, HGF, and MPG, Germany; GSRT, Greece; RGC, Hong Kong SAR, China; ISF, I-CORE and Benoziyo Center, Israel; INFN, Italy; MEXT and JSPS, Japan; CNRST, Morocco; NWO, Netherlands; RCN, Norway; MNiSW and NCN, Poland; FCT, Portugal; MNE/IFA, Romania; MES of Russia and NRC KI, Russian

Federation; JINR; MESTD, Serbia; MSSR, Slovakia; ARRS and MIZŠ, Slovenia; DST/NRF, South Africa; MINECO, Spain; SRC and Wallenberg Foundation, Sweden; SERI, SNSF and Cantons of Bern and Geneva, Switzerland; MOST, Taiwan; TAEK, Turkey; STFC, United Kingdom; DOE and NSF, United States of America. In addition, individual groups and members have received support from BCKDF, the Canada Council, CANARIE, CRC, Compute Canada, FQRNT, and the Ontario Innovation Trust, Canada; EPLANET, ERC, ERDF, FP7, Horizon 2020 and Marie Skłodowska-Curie Actions, European Union; Investissements d'Avenir Labex and Idex, ANR, Région Auvergne and Fondation Partager le Savoir, France; DFG and AvH Foundation, Germany; Herakleitos, Thales and Aristeia programmes co-financed by EU-ESF and the Greek NSRF; BSF, GIF and Minerva, Israel; BRF, Norway; CERCA Programme Generalitat de Catalunya, Generalitat Valenciana, Spain; the Royal Society and Leverhulme Trust, United Kingdom. The crucial computing support from all WLCG partners is acknowledged gratefully, in particular from CERN, the ATLAS Tier-1 facilities at TRIUMF (Canada), NDGF (Denmark, Norway, Sweden), CC-IN2P3 (France), KIT/GridKA (Germany), INFN-CNAF (Italy), NL-T1 (Netherlands), PIC (Spain), ASGC (Taiwan), RAL (UK) and BNL (USA), the Tier-2 facilities worldwide and large non-WLCG resource providers. Major contributors of computing resources are listed in Ref. [81].

References

1. K. Hagiwara, R. Peccei, D. Zeppenfeld, K. Hikasa, Probing the weak boson sector in $e^+e^- \to W^+W^-$. Nucl. Phys. B **282**, 253 (1987). doi:10.1016/0550-3213(87)90685-7
2. A. Butter et al., The Gauge-Higgs legacy of the LHC run I. JHEP **07**, 152 (2016). doi:10.1007/JHEP07(2016)152. arXiv:1604.03105 [hep-ph]
3. ATLAS Collaboration, Measurement of total and differential W^+W^- production cross sections in proton-proton collisions at $\sqrt{s} = 8$ TeV with the ATLAS detector and limits on anomalous triple-gauge-boson couplings. JHEP **09**, 029 (2016). doi:10.1007/JHEP09(2016)029. arXiv:1603.01702 [hep-ex]
4. ATLAS Collaboration, Measurement of the W^+W^- production cross section in pp collisions at a centre-of-mass energy of $\sqrt{s}$ = 13 TeV with the ATLAS experiment (2017). arXiv:1702.04519 [hep-ex]
5. CMS Collaboration, Measurement of the W^+W^- cross section in pp collisions at $\sqrt{s} = 8$ TeV and limits on anomalous gauge couplings. Eur. Phys. J. C **76**, 401 (2016). doi:10.1140/epjc/s10052-016-4219-1. arXiv:1507.03268 [hep-ex]
6. ATLAS Collaboration, Measurements of $W^\pm Z$ production cross sections in pp collisions at $\sqrt{s} = 8$ TeV with the ATLAS detector and limits on anomalous gauge boson self-couplings. Phys. Rev. D **93**, 092004 (2016). doi:10.1103/PhysRevD.93.092004. arXiv:1603.02151 [hep-ex]
7. ATLAS Collaboration, Measurement of the $W^\pm Z$ boson pair-production cross section in pp collisions at $\sqrt{s} = 13$ TeV with the ATLAS detector. Phys. Lett. B **762**, 1 (2016). doi:10.1016/j.physletb.2016.08.052. arXiv:1606.04017 [hep-ex]
8. CMS Collaboration, Measurement of the WZ production cross section in pp collisions at $\sqrt{s}$ = 7 and 8 TeV and search for anomalous triple gauge couplings at $\sqrt{s}$ = 8 TeV. Eur. Phys. J. C **77**, 236 (2017). doi:10.1140/epjc/s10052-017-4730-z. arXiv:1609.05721 [hep-ex]
9. CMS Collaboration, Measurement of the WZ production cross section in pp collisions at $\sqrt{s}$ = = 13 TeV. Phys. Lett. B **766**, 268 (2017). doi:10.1016/j.physletb.2017.01.011. arXiv:1607.06943 [hep-ex]
10. D0 Collaboration, V.M. Abazov et al., Measurement of the WW production cross section with dilepton final states in $p\bar{p}$ collisions at $\sqrt{s} = 1.96$ TeV and limits on anomalous trilinear gauge couplings. Phys. Rev. Lett. **103**, 191801 (2009). doi:10.1103/PhysRevLett.103.191801. arXiv:0904.0673 [hep-ex]
11. CDF Collaboration, T. Aaltonen et al., Measurement of the W^+W^- production cross section and search for anomalous $WW\gamma$ and WWZ couplings in $p\bar{p}$ collisions at $\sqrt{s} = 1.96$ TeV. Phys. Rev. Lett. 104, 201801 (2010). doi:10.1103/PhysRevLett.104.201801. arXiv:0912.4500 [hep-ex]. Erratum. Phys. Rev. Lett. **105**, 019905 (2010). doi:10.1103/PhysRevLett.105.019905
12. CDF Collaboration, T. Aaltonen et al., Measurement of the WZ cross section and triple gauge couplings in $p\bar{p}$ collisions at $\sqrt{s} =$ 1.96 TeV. Phys. Rev. D **86**, 031104 (2012). doi:10.1103/PhysRevD.86.031104. arXiv:1202.6629 [hep-ex]
13. D0 Collaboration, V.M. Abazov et al., A measurement of the WZ and ZZ production cross sections using leptonic final states in $8.6 fb^{-1}$ of $p\bar{p}$ collisions. Phys. Rev. D **85**, 112005 (2012). doi:10.1103/PhysRevD.85.112005. arXiv:1201.5652 [hep-ex]
14. ATLAS Collaboration, Measurement of the $WW + WZ$ cross section and limits on anomalous triple gauge couplings using final states with one lepton, missing transverse momentum, and two jets with the ATLAS detector at $\sqrt{s} = 7$ TeV. JHEP **01**, 049 (2015). doi:10.1007/JHEP01(2015)049. arXiv:1410.7238 [hep-ex]
15. CMS Collaboration, Measurement of the sum of WW and WZ production with W+dijet events in pp collisions at $\sqrt{s} = 7$ TeV. Eur. Phys. J. C **73**, 2283 (2013). doi:10.1140/epjc/s10052-013-2283-3. arXiv:1210.7544 [hep-ex]
16. D0 Collaboration, V.M. Abazov et al., Measurements of WW and WZ production in W + jets final states in $p\bar{p}$ collisions. Phys. Rev. Lett. **108**, 181803 (2012). doi:10.1103/PhysRevLett.108.181803. arXiv:1112.0536 [hep-ex]
17. CDF Collaboration, T.A. Aaltonen et al., Measurement of the WW and WZ production cross section using final states with a charged lepton and heavy-flavor jets in the full CDF run II data set. Phys. Rev. D **94**, 032008 (2016). doi:10.1103/PhysRevD.94.032008. arXiv:1606.06823 [hep-ex]
18. A. Falkowski, M. Gonzalez-Alonso, A. Greljo, D. Marzocca, M. Son, Anomalous triple gauge couplings in the effective field theory approach at the LHC. JHEP **02**, 115 (2017). doi:10.1007/JHEP02(2017)115. arXiv:1609.06312 [hep-ph]
19. A. Altheimer et al., Boosted objects and jet substructure at the LHC. Eur. Phys. J. C **74**, 2792 (2014). doi:10.1140/epjc/s10052-014-2792-8. arXiv:1311.2708 [hep-ex]
20. D. Krohn, J. Thaler, L.-T. Wang, Jet trimming. JHEP **02**, 084 (2010). doi:10.1007/JHEP02(2010)084. arXiv:0912.1342 [hep-ph]
21. ATLAS Collaboration, Identification of boosted, hadronically decaying W bosons and comparisons with ATLAS data taken at $\sqrt{s} = 8$ TeV. Eur. Phys. J. C **76**, 154 (2016). doi:10.1140/epjc/s10052-016-3978-z. arXiv:1510.05821 [hep-ex]
22. CMS Collaboration, Search for anomalous couplings in boosted $WW/WZ \to \ell\nu q\bar{q}$ production in proton-proton collisions at $\sqrt{s} = 8$ TeV. Phys. Lett. B **772**, 21 (2017). doi:10.1016/j.physletb.2017.06.009. arXiv:1703.06095 [hep-ex]
23. D0 Collaboration, V.M. Abazov et al., Limits on anomalous trilinear gauge boson couplings from WW, WZ and $W\gamma$ production in $p\bar{p}$ collisions at $\sqrt{s} = 1.96$ TeV. Phys. Lett. B **718**, 451 (2012). doi:10.1016/j.physletb.2012.10.062. arXiv:1208.5458 [hep-ex]

24. CDF Collaboration, T. Aaltonen et al., Limits on anomalous triple gauge couplings in $p\bar{p}$ collisions at $\sqrt{s}$ = 1.96 TeV. Phys. Rev. D **76**, 111103 (2007). doi:10.1103/PhysRevD.76.111103. arXiv:0705.2247 [hep-ex]
25. ATLAS Collaboration, The ATLAS experiment at the CERN large hadron collider. JINST **3**, S08003 (2008). doi:10.1088/1748-0221/3/08/S08003
26. L. Evans, P. Bryant, LHC Machine, JINST **3**, S08001 (2008). doi:10.1088/1748-0221/3/08/S08001
27. ATLAS Collaboration, Performance of the ATLAS trigger system in 2010. Eur. Phys. J. C **72**, 1849 (2012). doi:10.1140/epjc/s10052-011-1849-1. arXiv:1110.1530 [hep-ex]
28. S. Frixione, B.R. Webber, Matching NLO QCD computations and parton shower simulations. JHEP **06**, 029 (2002). doi:10.1088/1126-6708/2002/06/029. arXiv:hep-ph/0204244
29. G. Corcella et al., HERWIG 6: an event generator for hadron emission reactions with interfering gluons (including supersymmetric processes). JHEP **01**, 010 (2001). doi:10.1088/1126-6708/2001/01/010. arXiv:hep-ph/0011363
30. J. Butterworth, J.R. Forshaw, M. Seymour, Multiparton interactions in photoproduction at HERA. Z. Phys. C **72**, 637 (1996). doi:10.1007/s002880050286. arXiv:hep-ph/9601371
31. H.-L. Lai et al., New parton distributions for collider physics. Phys. Rev. D **82**, 074024 (2010). doi:10.1103/PhysRevD.82.074024. arXiv:1007.2241 [hep-ph]
32. ATLAS Collaboration, New ATLAS event generator tunes to 2010 data. ATL-PHYS-PUB-2011-008 (2011) https://cds.cern.ch/record/1345343
33. P. Nason, A New method for combining NLO QCD with shower Monte Carlo algorithms. JHEP **11**, 040 (2004). doi:10.1088/1126-6708/2004/11/040. arXiv:hep-ph/0409146
34. S. Frixione, P. Nason, C. Oleari, Matching NLO QCD computations with parton shower simulations: the POWHEG method. JHEP **11**, 070 (2007). doi:10.1088/1126-6708/2007/11/070. arXiv:0709.2092
35. S. Alioli, P. Nason, C. Oleari, E. Re, A general framework for implementing NLO calculations in shower Monte Carlo programs: the POWHEG BOX. JHEP **06**, 043 (2010). doi:10.1007/JHEP06(2010)043. arXiv:1002.2581 [hep-ph]
36. T. Sjöstrand, S. Mrenna, P.Z. Skands, A brief introduction to PYTHIA 8.1. Comput. Phys. Commun. **178**, 852 (2008). doi:10.1016/j.cpc.2008.01.036. arXiv:0710.3820 [hep-ph]
37. ATLAS Collaboration, Summary of ATLAS Pythia 8 tunes. ATL-PHYS-PUB-2012-003 (2012). https://cds.cern.ch/record/1474107
38. T. Gleisberg, S. Höche, F. Krauss, M. Schönherr, S. Schumann et al., Event generation with SHERPA 1.1. JHEP **02**, 007 (2009). doi:10.1088/1126-6708/2009/02/007. arXiv:0811.4622 [hep-ph]
39. S. Höche, F. Krauss, S. Schumann, F. Siegert, QCD matrix elements and truncated showers. JHEP **05**, 053 (2009). doi:10.1088/1126-6708/2009/05/053. arXiv:0903.1219 [hep-ph]
40. T. Gleisberg, S. Höche, Comix, a new matrix element generator. JHEP **12**, 039 (2008). doi:10.1088/1126-6708/2008/12/039. arXiv:0808.3674 [hep-ph]
41. S. Schumann, F. Krauss, A parton shower algorithm based on Catani-Seymour dipole factorisation. JHEP **03**, 038 (2008). doi:10.1088/1126-6708/2008/03/038. arXiv:0709.1027 [hep-ph]
42. C. Anastasiou, L.J. Dixon, K. Melnikov, F. Petriello, High precision QCD at hadron colliders: electroweak gauge boson rapidity distributions at NNLO. Phys. Rev. D **69**, 094008 (2004). doi:10.1103/PhysRevD.69.094008. arXiv:hep-ph/0312266
43. M.L. Mangano et al., ALPGEN, a generator for hard multiparton processes in hadronic collisions. JHEP **07**, 001 (2003). doi:10.1088/1126-6708/2003/07/001. arXiv:hep-ph/0206293
44. T. Sjöstrand, S. Mrenna, P.Z. Skands, PYTHIA 6.4 physics and manual. JHEP **05**, 026 (2006). doi:10.1088/1126-6708/2006/05/026. arXiv:hep-ph/0603175
45. P.Z. Skands, Tuning Monte Carlo generators: the Perugia tunes. Phys. Rev. D **82**, 074018 (2010). doi:10.1103/PhysRevD.82.074018. arXiv:1005.3457 [hep-ph]
46. J. Pumplin, D. Stump, J. Huston, H. Lai, P.M. Nadolsky et al., New generation of parton distributions with uncertainties from global QCD analysis. JHEP **07**, 012 (2002). doi:10.1088/1126-6708/2002/07/012. arXiv:hep-ph/0201195
47. S. Frixione, P. Nason, G. Ridolfi, A positive-weight next-to-leading-order Monte Carlo for heavy flavour hadroproduction. JHEP **09**, 126 (2007). doi:10.1088/1126-6708/2007/09/126. arXiv:0707.3088 [hep-ph]
48. S. Alioli, P. Nason, C. Oleari, E. Re, NLO single-top production matched with shower in POWHEG: s- and t-channel contributions. JHEP **09**, 111 (2009). doi:10.1088/1126-6708/2009/09/111. arXiv:0907.4076 [hep-ph]. Erratum: JHEP **02**, 011 (2010). doi:10.1007/JHEP02(2010)011
49. E. Re, Single-top Wt-channel production matched with parton showers using the POWHEG method. Eur. Phys. J. C **71**, 1547 (2011). doi:10.1140/epjc/s10052-011-1547-z. arXiv:1009.2450 [hep-ph]
50. J.M. Campbell, R.K. Ellis, MCFM for the Tevatron and the LHC. Nucl. Phys. Proc. Suppl. **205–206**, 10 (2010). doi:10.1016/j.nuclphysbps.2010.08.011. arXiv:1007.3492 [hep-ph]
51. J.M. Campbell, R.K. Ellis, Update on vector boson pair production at hadron colliders. Phys. Rev. D **60**, 113006 (1999). doi:10.1103/PhysRevD.60.113006. arXiv:hep-ph/9905386
52. S. Agostinelli et al., GEANT4: a simulation toolkit. Nucl. Instrum. Methods A **506**, 250 (2003). doi:10.1016/S0168-9002(03)01368-8
53. ATLAS Collaboration, The ATLAS simulation infrastructure. Eur. Phys. J. C **70**, 823 (2010). doi:10.1140/epjc/s10052-010-1429-9. arXiv:1005.4568 [hep-ex]
54. ATLAS Collaboration, Electron efficiency measurements with the ATLAS detector using 2012 LHC proton-proton collision data. Eur. Phys. J. C **77**, 195 (2017). doi:10.1140/epjc/s10052-017-4756-2. arXiv:1612.01456 [hep-ex]
55. W. Lampl et al., Calorimeter clustering algorithms: description and performance. ATL-LARG-PUB-2008-002 (2008). https://cds.cern.ch/record/1099735
56. M. Cacciari, G.P. Salam, G. Soyez, The anti-k_t jet clustering algorithm. JHEP **04**, 063 (2008). doi:10.1088/1126-6708/2008/04/063. arXiv:0802.1189 [hep-ph]
57. ATLAS Collaboration, Jet energy measurement and its systematic uncertainty in proton-proton collisions at $\sqrt{s} = 7$ TeV with the ATLAS detector. Eur. Phys. J. C **75**, 17 (2015). doi:10.1140/epjc/s10052-014-3190-y. arXiv:1406.0076 [hep-ex]
58. ATLAS Collaboration, Performance of pile-up mitigation techniques for jets in pp collisions at $\sqrt{s} = 8$ TeV using the ATLAS detector. Eur. Phys. J. C **76**, 581 (2016). doi:10.1140/epjc/s10052-016-4395-z. arXiv:1510.03823 [hep-ex]
59. ATLAS Collaboration, Performance of jet substructure techniques for large-R jets in proton-proton collisions at $\sqrt{s} = 7$ TeV using the ATLAS detector. JHEP **09**, 076 (2013). doi:10.1007/JHEP09(2013)076. arXiv:1306.4945 [hep-ex]
60. ATLAS Collaboration, Performance of algorithms that reconstruct missing transverse momentum in $\sqrt{s} = 8$ TeV proton-proton collisions in the ATLAS detector. Eur. Phys. J. C **77**, 241 (2017). doi:10.1140/epjc/s10052-017-4780-2. arXiv:1609.09324 [hep-ex]
61. ATLAS Collaboration, Calibration of the performance of b-tagging for c and light-flavour jets in the 2012 ATLAS data. ATLAS-CONF-2014-046 (2014). https://cds.cern.ch/record/1741020
62. ATLAS Collaboration, Performance of b-jet identification in the ATLAS experiment. JINST **11**, P04008 (2016). doi:10.1088/1748-0221/11/04/P04008. arXiv:1512.01094 [hep-ex]

63. ATLAS Collaboration, Jet energy resolution in proton-proton collisions at $\sqrt{s} = 7$ TeV recorded in 2010 with the ATLAS detector. Eur. Phys. J. C **73**, 2306 (2013). doi:10.1140/epjc/s10052-013-2306-0. arXiv:1210.6210 [hep-ex]
64. ATLAS Collaboration, Jet mass and substructure of inclusive jets in $\sqrt{s} = 7$ TeV pp collisions with the ATLAS experiment. JHEP **05**, 128, (2012). doi:10.1007/JHEP05(2012)128. arXiv:1203.4606 [hep-ex]
65. ATLAS Collaboration, Search for a high-mass Higgs boson decaying to a W boson pair in pp collisions at $\sqrt{s} = 8$ TeV with the ATLAS detector. JHEP **01**, 032 (2016). doi:10.1007/JHEP01(2016)032. arXiv:1509.00389 [hep-ex]
66. ATLAS Collaboration, Pile-up subtraction and suppression for jets in ATLAS. ATLAS-CONF-2013-083 (2013). https://cds.cern.ch/record/1570994
67. ATLAS Collaboration, Measurement of the muon reconstruction performance of the ATLAS detector using 2011 and 2012 LHC proton-proton collision data. Eur. Phys. J. C **74**, 3130 (2014). doi:10.1140/epjc/s10052-014-3130-x. arXiv:1407.3935 [hep-ex]
68. ATLAS Collaboration, Electron and photon energy calibration with the ATLAS detector using LHC Run 1 data. Eur. Phys. J. C **74**, 3071 (2014). doi:10.1140/epjc/s10052-014-3071-4. arXiv:1407.5063 [hep-ex]
69. ATLAS Collaboration, Performance of the ATLAS electron and photon trigger in pp collisions at $\sqrt{s} = 7$ TeV in 2011. ATLAS-CONF-2012-048 (2012). https://cds.cern.ch/record/1450089
70. ATLAS Collaboration, Performance of the ATLAS muon trigger in pp collisions at $\sqrt{s} = 8$ TeV. Eur. Phys. J. C **75**, 120 (2015). doi:10.1140/epjc/s10052-015-3325-9. arXiv:1408.3179 [hep-ex]
71. ATLAS Collaboration, Reconstruction of primary vertices at the ATLAS experiment in run 1 proton-proton collisions at the LHC. Eur. Phys. J. C **77**, 332 (2017). doi:10.1140/epjc/s10052-017-4887-5. arXiv:1611.10235 [physics.ins-det]
72. ATLAS Collaboration, Luminosity determination in pp collisions at $\sqrt{s}$= 8 TeV using the ATLAS detector at the LHC. Eur. Phys. J. C **76**, 653 (2016). doi:10.1140/epjc/s10052-016-4466-1. arXiv:1608.03953 [hep-ex]
73. I.W. Stewart, F.J. Tackmann, Theory uncertainties for Higgs and other searches using jet bins. Phys. Rev. D **85**, 034011 (2012). doi:10.1103/PhysRevD.85.034011. arXiv:1107.2117 [hep-ph]
74. G. Cowan, K. Cranmer, E. Gross, O. Vitells, Asymptotic formulae for likelihood-based tests of new physics. Eur. Phys. J. C 71, 1554 (2011). doi:10.1140/epjc/s10052-011-1554-0. arXiv:1007.1727 [physics.data-an]. Erratum. Eur. Phys. J. C **73**, 2501 (2013). doi:10.1140/epjc/s10052-013-2501-z
75. F. Caola, K. Melnikov, R. Röntsch, L. Tancredi, QCD corrections to W^+W^- production through gluon fusion. Phys. Lett. B **754**, 275 (2015). doi:10.1016/j.physletb.2016.01.046. arXiv:1511.08617 [hep-ph]
76. G. Gounaris et al., Triple gauge boson couplings (1996). arXiv:hep-ph/9601233
77. K. Hagiwara, S. Ishihara, R. Szalapski, D. Zeppenfeld, Low-energy effects of new interactions in the electroweak boson sector. Phys. Rev. D **48**, 2182 (1993). doi:10.1103/PhysRevD.48.2182
78. C. Degrande et al., Effective field theory: a modern approach to anomalous couplings. Ann. Phys. **335**, 21 (2013). doi:10.1016/j.aop.2013.04.016. arXiv:1205.4231 [hep-ph]
79. G.J. Feldman, R.D. Cousins, Unified approach to the classical statistical analysis of small signals. Phys. Rev. D **57**, 3873 (1998). doi:10.1103/PhysRevD.57.3873. arXiv:physics/9711021 [physics.data-an]
80. H. Aihara et al., Anomalous gauge boson interactions (1995). arXiv:hep-ph/9503425
81. ATLAS Collaboration, ATLAS Computing Acknowledgements 2016–2017. ATL-GEN-PUB-2016-002 (2016). https://cds.cern.ch/record/2202407

ATLAS Collaboration

M. Aaboud[137d], G. Aad[88], B. Abbott[115], O. Abdinov[12,*], B. Abeloos[119], S. H. Abidi[161], O. S. AbouZeid[139], N. L. Abraham[151], H. Abramowicz[155], H. Abreu[154], R. Abreu[118], Y. Abulaiti[148a,148b], B. S. Acharya[167a,167b,a], S. Adachi[157], L. Adamczyk[41a], J. Adelman[110], M. Adersberger[102], T. Adye[133], A. A. Affolder[139], T. Agatonovic-Jovin[14], C. Agheorghiesei[28c], J. A. Aguilar-Saavedra[128a,128f], S. P. Ahlen[24], F. Ahmadov[68,b], G. Aielli[135a,135b], S. Akatsuka[71], H. Akerstedt[148a,148b], T. P. A. Åkesson[84], E. Akilli[52], A. V. Akimov[98], G. L. Alberghi[22a,22b], J. Albert[172], P. Albicocco[50], M. J. Alconada Verzini[74], S. C. Alderweireldt[108], M. Aleksa[32], I. N. Aleksandrov[68], C. Alexa[28b], G. Alexander[155], T. Alexopoulos[10], M. Alhroob[115], B. Ali[130], M. Aliev[76a,76b], G. Alimonti[94a], J. Alison[33], S. P. Alkire[38], B. M. M. Allbrooke[151], B. W. Allen[118], P. P. Allport[19], A. Aloisio[106a,106b], A. Alonso[39], F. Alonso[74], C. Alpigiani[140], A. A. Alshehri[56], M. I. Alstaty[88], B. Alvarez Gonzalez[32], D. Álvarez Piqueras[170], M. G. Alviggi[106a,106b], B. T. Amadio[16], Y. Amaral Coutinho[26a], C. Amelung[25], D. Amidei[92], S. P. Amor Dos Santos[128a,128c], A. Amorim[128a,128b], S. Amoroso[32], G. Amundsen[25], C. Anastopoulos[141], L. S. Ancu[52], N. Andari[19], T. Andeen[11], C. F. Anders[60b], J. K. Anders[77], K. J. Anderson[33], A. Andreazza[94a,94b], V. Andrei[60a], S. Angelidakis[9], I. Angelozzi[109], A. Angerami[38], A. V. Anisenkov[111,c], N. Anjos[13], A. Annovi[126a,126b], C. Antel[60a], M. Antonelli[50], A. Antonov[100,*], D. J. Antrim[166], F. Anulli[134a], M. Aoki[69], L. Aperio Bella[32], G. Arabidze[93], Y. Arai[69], J. P. Araque[128a], V. Araujo Ferraz[26a], A. T. H. Arce[48], R. E. Ardell[80], F. A. Arduh[74], J-F. Arguin[97], S. Argyropoulos[66], M. Arik[20a], A. J. Armbruster[32], L. J. Armitage[79], O. Arnaez[161], H. Arnold[51], M. Arratia[30], O. Arslan[23], A. Artamonov[99], G. Artoni[122], S. Artz[86], S. Asai[157], N. Asbah[45], A. Ashkenazi[155], L. Asquith[151], K. Assamagan[27], R. Astalos[146a], M. Atkinson[169], N. B. Atlay[143], K. Augsten[130], G. Avolio[32], B. Axen[16], M. K. Ayoub[119], G. Azuelos[97,d], A. E. Baas[60a], M. J. Baca[19], H. Bachacou[138], K. Bachas[76a,76b], M. Backes[122], M. Backhaus[32], P. Bagnaia[134a,134b], M. Bahmani[42], H. Bahrasemani[144], J. T. Baines[133], M. Bajic[39], O. K. Baker[179], E. M. Baldin[111,c], P. Balek[175], F. Balli[138], W. K. Balunas[124], E. Banas[42], A. Bandyopadhyay[23], Sw. Banerjee[176,e], A. A. E. Bannoura[178], L. Barak[32], E. L. Barberio[91], D. Barberis[53a,53b], M. Barbero[88], T. Barillari[103], M-S Barisits[32], J. T. Barkeloo[118], T. Barklow[145], N. Barlow[30], S. L. Barnes[36c], B. M. Barnett[133], R. M. Barnett[16],

Z. Barnovska-Blenessy[36a], A. Baroncelli[136a], G. Barone[25], A. J. Barr[122], L. Barranco Navarro[170], F. Barreiro[85], J. Barreiro Guimarães da Costa[35a], R. Bartoldus[145], A. E. Barton[75], P. Bartos[146a], A. Basalaev[125], A. Bassalat[119,f], R. L. Bates[56], S. J. Batista[161], J. R. Batley[30], M. Battaglia[139], M. Bauce[134a,134b], F. Bauer[138], H. S. Bawa[145,g], J. B. Beacham[113], M. D. Beattie[75], T. Beau[83], P. H. Beauchemin[165], P. Bechtle[23], H. P. Beck[18,h], H. C. Beck[57], K. Becker[122], M. Becker[86], M. Beckingham[173], C. Becot[112], A. J. Beddall[20d], A. Beddall[20b], V. A. Bednyakov[68], M. Bedognetti[109], C. P. Bee[150], T. A. Beermann[32], M. Begalli[26a], M. Begel[27], J. K. Behr[45], A. S. Bell[81], G. Bella[155], L. Bellagamba[22a], A. Bellerive[31], M. Bellomo[154], K. Belotskiy[100], O. Beltramello[32], N. L. Belyaev[100], O. Benary[155,*], D. Benchekroun[137a], M. Bender[102], K. Bendtz[148a,148b], N. Benekos[10], Y. Benhammou[155], E. Benhar Noccioli[179], J. Benitez[66], D. P. Benjamin[48], M. Benoit[52], J. R. Bensinger[25], S. Bentvelsen[109], L. Beresford[122], M. Beretta[50], D. Berge[109], E. Bergeaas Kuutmann[168], N. Berger[5], J. Beringer[16], S. Berlendis[58], N. R. Bernard[89], G. Bernardi[83], C. Bernius[145], F. U. Bernlochner[23], T. Berry[80], P. Berta[131], C. Bertella[35a], G. Bertoli[148a,148b], F. Bertolucci[126a,126b], I. A. Bertram[75], C. Bertsche[45], D. Bertsche[115], G. J. Besjes[39], O. Bessidskaia Bylund[148a,148b], M. Bessner[45], N. Besson[138], C. Betancourt[51], A. Bethani[87], S. Bethke[103], A. J. Bevan[79], J. Beyer[103], R. M. Bianchi[127], O. Biebel[102], D. Biedermann[17], R. Bielski[87], K. Bierwagen[86], N. V. Biesuz[126a,126b], M. Biglietti[136a], T. R. V. Billoud[97], H. Bilokon[50], M. Bindi[57], A. Bingul[20b], C. Bini[134a,134b], S. Biondi[22a,22b], T. Bisanz[57], C. Bittrich[47], D. M. Bjergaard[48], C. W. Black[152], J. E. Black[145], K. M. Black[24], R. E. Blair[6], T. Blazek[146a], I. Bloch[45], C. Blocker[25], A. Blue[56], W. Blum[86,*], U. Blumenschein[79], S. Blunier[34a], G. J. Bobbink[109], V. S. Bobrovnikov[111,c], S. S. Bocchetta[84], A. Bocci[48], C. Bock[102], M. Boehler[51], D. Boerner[178], D. Bogavac[102], A. G. Bogdanchikov[111], C. Bohm[148a], V. Boisvert[80], P. Bokan[168,i], T. Bold[41a], A. S. Boldyrev[101], A. E. Bolz[60b], M. Bomben[83], M. Bona[79], M. Boonekamp[138], A. Borisov[132], G. Borissov[75], J. Bortfeldt[32], D. Bortoletto[122], V. Bortolotto[62a,62b,62c], D. Boscherini[22a], M. Bosman[13], J. D. Bossio Sola[29], J. Boudreau[127], J. Bouffard[2], E. V. Bouhova-Thacker[75], D. Boumediene[37], C. Bourdarios[119], S. K. Boutle[56], A. Boveia[113], J. Boyd[32], I. R. Boyko[68], J. Bracinik[19], A. Brandt[8], G. Brandt[57], O. Brandt[60a], U. Bratzler[158], B. Brau[89], J. E. Brau[118], W. D. Breaden Madden[56], K. Brendlinger[45], A. J. Brennan[91], L. Brenner[109], R. Brenner[168], S. Bressler[175], D. L. Briglin[19], T. M. Bristow[49], D. Britton[56], D. Britzger[45], F. M. Brochu[30], I. Brock[23], R. Brock[93], G. Brooijmans[38], T. Brooks[80], W. K. Brooks[34b], J. Brosamer[16], E. Brost[110], J. H Broughton[19], P. A. Bruckman de Renstrom[42], D. Bruncko[146b], A. Bruni[22a], G. Bruni[22a], L. S. Bruni[109], BH Brunt[30], M. Bruschi[22a], N. Bruscino[23], P. Bryant[33], L. Bryngemark[45], T. Buanes[15], Q. Buat[144], P. Buchholz[143], A. G. Buckley[56], I. A. Budagov[68], F. Buehrer[51], M. K. Bugge[121], O. Bulekov[100], D. Bullock[8], T. J. Burch[110], S. Burdin[77], C. D. Burgard[51], A. M. Burger[5], B. Burghgrave[110], K. Burka[42], S. Burke[133], I. Burmeister[46], J. T. P. Burr[122], E. Busato[37], D. Büscher[51], V. Büscher[86], P. Bussey[56], J. M. Butler[24], C. M. Buttar[56], J. M. Butterworth[81], P. Butti[32], W. Buttinger[27], A. Buzatu[35c], A. R. Buzykaev[111,c], S. Cabrera Urbán[170], D. Caforio[130], V. M. Cairo[40a,40b], O. Cakir[4a], N. Calace[52], P. Calafiura[16], A. Calandri[88], G. Calderini[83], P. Calfayan[64], G. Callea[40a,40b], L. P. Caloba[26a], S. Calvente Lopez[85], D. Calvet[37], S. Calvet[37], T. P. Calvet[88], M. Calvetti[126a,126b], R. Camacho Toro[33], S. Camarda[32], P. Camarri[135a,135b], D. Cameron[121], R. Caminal Armadans[169], C. Camincher[58], S. Campana[32], M. Campanelli[81], A. Camplani[94a,94b], A. Campoverde[143], V. Canale[106a,106b], M. Cano Bret[36c], J. Cantero[116], T. Cao[155], M. D. M. Capeans Garrido[32], I. Caprini[28b], M. Caprini[28b], M. Capua[40a,40b], R. M. Carbone[38], R. Cardarelli[135a], F. Cardillo[51], I. Carli[131], T. Carli[32], G. Carlino[106a], B. T. Carlson[127], L. Carminati[94a,94b], R. M. D. Carney[148a,148b], S. Caron[108], E. Carquin[34b], S. Carrá[94a,94b], G. D. Carrillo-Montoya[32], J. Carvalho[128a,128c], D. Casadei[19], M. P. Casado[13,j], M. Casolino[13], D. W. Casper[166], R. Castelijn[109], V. Castillo Gimenez[170], N. F. Castro[128a,k], A. Catinaccio[32], J. R. Catmore[121], A. Cattai[32], J. Caudron[23], V. Cavaliere[169], E. Cavallaro[13], D. Cavalli[94a], M. Cavalli-Sforza[13], V. Cavasinni[126a,126b], E. Celebi[20c], F. Ceradini[136a,136b], L. Cerda Alberich[170], A. S. Cerqueira[26b], A. Cerri[151], L. Cerrito[135a,135b], F. Cerutti[16], A. Cervelli[18], S. A. Cetin[20d], A. Chafaq[137a], D. Chakraborty[110], S. K. Chan[59], W. S. Chan[109], Y. L. Chan[62a], P. Chang[169], J. D. Chapman[30], D. G. Charlton[19], C. C. Chau[31], C. A. Chavez Barajas[151], S. Che[113], S. Cheatham[167a,167c], A. Chegwidden[93], S. Chekanov[6], S. V. Chekulaev[163a], G. A. Chelkov[68,l], M. A. Chelstowska[32], C. Chen[67], H. Chen[27], J. Chen[36a], S. Chen[35b], S. Chen[157], X. Chen[35c,m], Y. Chen[70], H. C. Cheng[92], H. J. Cheng[35a], A. Cheplakov[68], E. Cheremushkina[132], R. Cherkaoui El Moursli[137e], E. Cheu[7], K. Cheung[63], L. Chevalier[138], V. Chiarella[50], G. Chiarelli[126a,126b], G. Chiodini[76a], A. S. Chisholm[32], A. Chitan[28b], Y. H. Chiu[172], M. V. Chizhov[68], K. Choi[64], A. R. Chomont[37], S. Chouridou[156], Y. S. Chow[62a], V. Christodoulou[81], M. C. Chu[62a], J. Chudoba[129], A. J. Chuinard[90], J. J. Chwastowski[42], L. Chytka[117], A. K. Ciftci[4a], D. Cinca[46], V. Cindro[78], I. A. Cioara[23], C. Ciocca[22a,22b], A. Ciocio[16], F. Cirotto[106a,106b], Z. H. Citron[175], M. Citterio[94a], M. Ciubancan[28b], A. Clark[52], B. L. Clark[59], M. R. Clark[38], P. J. Clark[49], R. N. Clarke[16], C. Clement[148a,148b], Y. Coadou[88], M. Cobal[167a,167c], A. Coccaro[52], J. Cochran[67], L. Colasurdo[108], B. Cole[38], A. P. Colijn[109], J. Collot[58], T. Colombo[166], P. Conde Muiño[128a,128b], E. Coniavitis[51], S. H. Connell[147b], I. A. Connelly[87], S. Constantinescu[28b], G. Conti[32], F. Conventi[106a,n], M. Cooke[16], A. M. Cooper-Sarkar[122], F. Cormier[171], K. J. R. Cormier[161], M. Corradi[134a,134b],

F. Corriveau[90,o], A. Cortes-Gonzalez[32], G. Cortiana[103], G. Costa[94a], M. J. Costa[170], D. Costanzo[141], G. Cottin[30], G. Cowan[80], B. E. Cox[87], K. Cranmer[112], S. J. Crawley[56], R. A. Creager[124], G. Cree[31], S. Crépé-Renaudin[58], F. Crescioli[83], W. A. Cribbs[148a,148b], M. Cristinziani[23], V. Croft[108], G. Crosetti[40a,40b], A. Cueto[85], T. Cuhadar Donszelmann[141], A. R. Cukierman[145], J. Cummings[179], M. Curatolo[50], J. Cúth[86], S. Czekierda[42], P. Czodrowski[32], G. D'amen[22a,22b], S. D'Auria[56], L. D'eramo[83], M. D'Onofrio[77], M. J. Da Cunha Sargedas De Sousa[128a,128b], C. Da Via[87], W. Dabrowski[41a], T. Dado[146a], T. Dai[92], O. Dale[15], F. Dallaire[97], C. Dallapiccola[89], M. Dam[39], J. R. Dandoy[124], M. F. Daneri[29], N. P. Dang[176], A. C. Daniells[19], N. S. Dann[87], M. Danninger[171], M. Dano Hoffmann[138], V. Dao[150], G. Darbo[53a], S. Darmora[8], J. Dassoulas[3], A. Dattagupta[118], T. Daubney[45], W. Davey[23], C. David[45], T. Davidek[131], D. R. Davis[48], P. Davison[81], E. Dawe[91], I. Dawson[141], K. De[8], R. de Asmundis[106a], A. De Benedetti[115], S. De Castro[22a,22b], S. De Cecco[83], N. De Groot[108], P. de Jong[109], H. De la Torre[93], F. De Lorenzi[67], A. De Maria[57], D. De Pedis[134a], A. De Salvo[134a], U. De Sanctis[135a,135b], A. De Santo[151], K. De Vasconcelos Corga[88], J. B. De Vivie De Regie[119], W. J. Dearnaley[75], R. Debbe[27], C. Debenedetti[139], D. V. Dedovich[68], N. Dehghanian[3], I. Deigaard[109], M. Del Gaudio[40a,40b], J. Del Peso[85], D. Delgove[119], F. Deliot[138], C. M. Delitzsch[7], A. Dell'Acqua[32], L. Dell'Asta[24], M. Dell'Orso[126a,126b], M. Della Pietra[106a,106b], D. della Volpe[52], M. Delmastro[5], C. Delporte[119], P. A. Delsart[58], D. A. DeMarco[161], S. Demers[179], M. Demichev[68], A. Demilly[83], S. P. Denisov[132], D. Denysiuk[138], D. Derendarz[42], J. E. Derkaoui[137d], F. Derue[83], P. Dervan[77], K. Desch[23], C. Deterre[45], K. Dette[46], M. R. Devesa[29], P. O. Deviveiros[32], A. Dewhurst[133], S. Dhaliwal[25], F. A. Di Bello[52], A. Di Ciaccio[135a,135b], L. Di Ciaccio[5], W. K. Di Clemente[124], C. Di Donato[106a,106b], A. Di Girolamo[32], B. Di Girolamo[32], B. Di Micco[136a,136b], R. Di Nardo[32], K. F. Di Petrillo[59], A. Di Simone[51], R. Di Sipio[161], D. Di Valentino[31], C. Diaconu[88], M. Diamond[161], F. A. Dias[39], M. A. Diaz[34a], E. B. Diehl[92], J. Dietrich[17], S. Díez Cornell[45], A. Dimitrievska[14], J. Dingfelder[23], P. Dita[28b], S. Dita[28b], F. Dittus[32], F. Djama[88], T. Djobava[54b], J. I. Djuvsland[60a], M. A. B. do Vale[26c], D. Dobos[32], M. Dobre[28b], C. Doglioni[84], J. Dolejsi[131], Z. Dolezal[131], M. Donadelli[26d], S. Donati[126a,126b], P. Dondero[123a,123b], J. Donini[37], J. Dopke[133], A. Doria[106a], M. T. Dova[74], A. T. Doyle[56], E. Drechsler[57], M. Dris[10], Y. Du[36b], J. Duarte-Campderros[155], A. Dubreuil[52], E. Duchovni[175], G. Duckeck[102], A. Ducourthial[83], O. A. Ducu[97,p], D. Duda[109], A. Dudarev[32], A. Chr. Dudder[86], E. M. Duffield[16], L. Duflot[119], M. Dührssen[32], M. Dumancic[175], A. E. Dumitriu[28b], A. K. Duncan[56], M. Dunford[60a], H. Duran Yildiz[4a], M. Düren[55], A. Durglishvili[54b], D. Duschinger[47], B. Dutta[45], D. Duvnjak[1], M. Dyndal[45], B. S. Dziedzic[42], C. Eckardt[45], K. M. Ecker[103], R. C. Edgar[92], T. Eifert[32], G. Eigen[15], K. Einsweiler[16], T. Ekelof[168], M. El Kacimi[137c], R. El Kosseifi[88], V. Ellajosyula[88], M. Ellert[168], S. Elles[5], F. Ellinghaus[178], A. A. Elliot[172], N. Ellis[32], J. Elmsheuser[27], M. Elsing[32], D. Emeliyanov[133], Y. Enari[157], O. C. Endner[86], J. S. Ennis[173], J. Erdmann[46], A. Ereditato[18], M. Ernst[27], S. Errede[169], M. Escalier[119], C. Escobar[170], B. Esposito[50], O. Estrada Pastor[170], A. I. Etienvre[138], E. Etzion[155], H. Evans[64], A. Ezhilov[125], M. Ezzi[137e], F. Fabbri[22a,22b], L. Fabbri[22a,22b], V. Fabiani[108], G. Facini[81], R. M. Fakhrutdinov[132], S. Falciano[134a], R. J. Falla[81], J. Faltova[32], Y. Fang[35a], M. Fanti[94a,94b], A. Farbin[8], A. Farilla[136a], C. Farina[127], E. M. Farina[123a,123b], T. Farooque[93], S. Farrell[16], S. M. Farrington[173], P. Farthouat[32], F. Fassi[137e], P. Fassnacht[32], D. Fassouliotis[9], M. Faucci Giannelli[80], A. Favareto[53a,53b], W. J. Fawcett[122], L. Fayard[119], O. L. Fedin[125,q], W. Fedorko[171], S. Feigl[121], L. Feligioni[88], C. Feng[36b], E. J. Feng[32], H. Feng[92], M. J. Fenton[56], A. B. Fenyuk[132], L. Feremenga[8], P. Fernandez Martinez[170], S. Fernandez Perez[13], J. Ferrando[45], A. Ferrari[168], P. Ferrari[109], R. Ferrari[123a], D. E. Ferreira de Lima[60b], A. Ferrer[170], D. Ferrere[52], C. Ferretti[92], F. Fiedler[86], A. Filipčič[78], M. Filipuzzi[45], F. Filthaut[108], M. Fincke-Keeler[172], K. D. Finelli[152], M. C. N. Fiolhais[128a,128c,r], L. Fiorini[170], A. Fischer[2], C. Fischer[13], J. Fischer[178], W. C. Fisher[93], N. Flaschel[45], I. Fleck[143], P. Fleischmann[92], R. R. M. Fletcher[124], T. Flick[178], B. M. Flierl[102], L. R. Flores Castillo[62a], M. J. Flowerdew[103], G. T. Forcolin[87], A. Formica[138], F. A. Förster[13], A. Forti[87], A. G. Foster[19], D. Fournier[119], H. Fox[75], S. Fracchia[141], P. Francavilla[83], M. Franchini[22a,22b], S. Franchino[60a], D. Francis[32], L. Franconi[121], M. Franklin[59], M. Frate[166], M. Fraternali[123a,123b], D. Freeborn[81], S. M. Fressard-Batraneanu[32], B. Freund[97], D. Froidevaux[32], J. A. Frost[122], C. Fukunaga[158], T. Fusayasu[104], J. Fuster[170], C. Gabaldon[58], O. Gabizon[154], A. Gabrielli[22a,22b], A. Gabrielli[16], G. P. Gach[41a], S. Gadatsch[32], S. Gadomski[80], G. Gagliardi[53a,53b], L. G. Gagnon[97], C. Galea[108], B. Galhardo[128a,128c], E. J. Gallas[122], B. J. Gallop[133], P. Gallus[130], G. Galster[39], K. K. Gan[113], S. Ganguly[37], Y. Gao[77], Y. S. Gao[145,g], F. M. Garay Walls[49], C. García[170], J. E. García Navarro[170], J. A. García Pascual[35a], M. Garcia-Sciveres[16], R. W. Gardner[33], N. Garelli[145], V. Garonne[121], A. Gascon Bravo[45], K. Gasnikova[45], C. Gatti[50], A. Gaudiello[53a,53b], G. Gaudio[123a], I. L. Gavrilenko[98], C. Gay[171], G. Gaycken[23], E. N. Gazis[10], C. N. P. Gee[133], J. Geisen[57], M. Geisen[86], M. P. Geisler[60a], K. Gellerstedt[148a,148b], C. Gemme[53a], M. H. Genest[58], C. Geng[92], S. Gentile[134a,134b], C. Gentsos[156], S. George[80], D. Gerbaudo[13], A. Gershon[155], G. Geßner[46], S. Ghasemi[143], M. Ghneimat[23], B. Giacobbe[22a], S. Giagu[134a,134b], N. Giangiacomi[22a,22b], P. Giannetti[126a,126b], S. M. Gibson[80], M. Gignac[171], M. Gilchriese[16], D. Gillberg[31], G. Gilles[178], D. M. Gingrich[3,d], N. Giokaris[9,*], M. P. Giordani[167a,167c], F. M. Giorgi[22a], P. F. Giraud[138], P. Giromini[59], G. Giugliarelli[167a,167c], D. Giugni[94a], F. Giuli[122], C. Giuliani[103], M. Giulini[60b], B. K. Gjelsten[121], S. Gkaitatzis[156], I. Gkialas[9,s], E. L. Gkougkousis[139], P. Gkountoumis[10],

L. K. Gladilin[101], C. Glasman[85], J. Glatzer[13], P. C. F. Glaysher[45], A. Glazov[45], M. Goblirsch-Kolb[25], J. Godlewski[42], S. Goldfarb[91], T. Golling[52], D. Golubkov[132], A. Gomes[128a,128b,128d], R. Gonçalo[128a], R. Goncalves Gama[26a], J. Goncalves Pinto Firmino Da Costa[138], G. Gonella[51], L. Gonella[19], A. Gongadze[68], S. González de la Hoz[170], S. Gonzalez-Sevilla[52], L. Goossens[32], P. A. Gorbounov[99], H. A. Gordon[27], I. Gorelov[107], B. Gorini[32], E. Gorini[76a,76b], A. Gorišek[78], A. T. Goshaw[48], C. Gössling[46], M. I. Gostkin[68], C. A. Gottardo[23], C. R. Goudet[119], D. Goujdami[137c], A. G. Goussiou[140], N. Govender[147b,t], E. Gozani[154], L. Graber[57], I. Grabowska-Bold[41a], P. O. J. Gradin[168], J. Gramling[166], E. Gramstad[121], S. Grancagnolo[17], V. Gratchev[125], P. M. Gravila[28f], C. Gray[56], H. M. Gray[16], Z. D. Greenwood[82,u], C. Grefe[23], K. Gregersen[81], I. M. Gregor[45], P. Grenier[145], K. Grevtsov[5], J. Griffiths[8], A. A. Grillo[139], K. Grimm[75], S. Grinstein[13,v], Ph. Gris[37], J.-F. Grivaz[119], S. Groh[86], E. Gross[175], J. Grosse-Knetter[57], G. C. Grossi[82], Z. J. Grout[81], A. Grummer[107], L. Guan[92], W. Guan[176], J. Guenther[65], F. Guescini[163a], D. Guest[166], O. Gueta[155], B. Gui[113], E. Guido[53a,53b], T. Guillemin[5], S. Guindon[2], U. Gul[56], C. Gumpert[32], J. Guo[36c], W. Guo[92], Y. Guo[36a], R. Gupta[43], S. Gupta[122], G. Gustavino[115], P. Gutierrez[115], N. G. Gutierrez Ortiz[81], C. Gutschow[81], C. Guyot[138], M. P. Guzik[41a], C. Gwenlan[122], C. B. Gwilliam[77], A. Haas[112], C. Haber[16], H. K. Hadavand[8], N. Haddad[137e], A. Hadef[88], S. Hageböck[23], M. Hagihara[164], H. Hakobyan[180,*], M. Haleem[45], J. Haley[116], G. Halladjian[93], G. D. Hallewell[88], K. Hamacher[178], P. Hamal[117], K. Hamano[172], A. Hamilton[147a], G. N. Hamity[141], P. G. Hamnett[45], L. Han[36a], S. Han[35a], K. Hanagaki[69,w], K. Hanawa[157], M. Hance[139], B. Haney[124], P. Hanke[60a], J. B. Hansen[39], J. D. Hansen[39], M. C. Hansen[23], P. H. Hansen[39], K. Hara[164], A. S. Hard[176], T. Harenberg[178], F. Hariri[119], S. Harkusha[95], R. D. Harrington[49], P. F. Harrison[173], N. M. Hartmann[102], M. Hasegawa[70], Y. Hasegawa[142], A. Hasib[49], S. Hassani[138], S. Haug[18], R. Hauser[93], L. Hauswald[47], L. B. Havener[38], M. Havranek[130], C. M. Hawkes[19], R. J. Hawkings[32], D. Hayakawa[159], D. Hayden[93], C. P. Hays[122], J. M. Hays[79], H. S. Hayward[77], S. J. Haywood[133], S. J. Head[19], T. Heck[86], V. Hedberg[84], L. Heelan[8], S. Heer[23], K. K. Heidegger[51], S. Heim[45], T. Heim[16], B. Heinemann[45,x], J. J. Heinrich[102], L. Heinrich[112], C. Heinz[55], J. Hejbal[129], L. Helary[32], A. Held[171], S. Hellman[148a,148b], C. Helsens[32], R. C. W. Henderson[75], Y. Heng[176], S. Henkelmann[171], A. M. Henriques Correia[32], S. Henrot-Versille[119], G. H. Herbert[17], H. Herde[25], V. Herget[177], Y. Hernández Jiménez[147c], H. Herr[86], G. Herten[51], R. Hertenberger[102], L. Hervas[32], T. C. Herwig[124], G. G. Hesketh[81], N. P. Hessey[163a], J. W. Hetherly[43], S. Higashino[69], E. Higón-Rodriguez[170], K. Hildebrand[33], E. Hill[172], J. C. Hill[30], K. H. Hiller[45], S. J. Hillier[19], M. Hils[47], I. Hinchliffe[16], M. Hirose[51], D. Hirschbuehl[178], B. Hiti[78], O. Hladik[129], X. Hoad[49], J. Hobbs[150], N. Hod[163a], M. C. Hodgkinson[141], P. Hodgson[141], A. Hoecker[32], M. R. Hoeferkamp[107], F. Hoenig[102], D. Hohn[23], T. R. Holmes[33], M. Homann[46], S. Honda[164], T. Honda[69], T. M. Hong[127], B. H. Hooberman[169], W. H. Hopkins[118], Y. Horii[105], A. J. Horton[144], J-Y. Hostachy[58], S. Hou[153], A. Hoummada[137a], J. Howarth[87], J. Hoya[74], M. Hrabovsky[117], J. Hrdinka[32], I. Hristova[17], J. Hrivnac[119], T. Hryn'ova[5], A. Hrynevich[96], P. J. Hsu[63], S.-C. Hsu[140], Q. Hu[36a], S. Hu[36c], Y. Huang[35a], Z. Hubacek[130], F. Hubaut[88], F. Huegging[23], T. B. Huffman[122], E. W. Hughes[38], G. Hughes[75], M. Huhtinen[32], P. Huo[150], N. Huseynov[68,b], J. Huston[93], J. Huth[59], G. Iacobucci[52], G. Iakovidis[27], I. Ibragimov[143], L. Iconomidou-Fayard[119], Z. Idrissi[137e], P. Iengo[32], O. Igonkina[109,y], T. Iizawa[174], Y. Ikegami[69], M. Ikeno[69], Y. Ilchenko[11,z], D. Iliadis[156], N. Ilic[145], G. Introzzi[123a,123b], P. Ioannou[9,*], M. Iodice[136a], K. Iordanidou[38], V. Ippolito[59], M. F. Isacson[168], N. Ishijima[120], M. Ishino[157], M. Ishitsuka[159], C. Issever[122], S. Istin[20a], F. Ito[164], J. M. Iturbe Ponce[62a], R. Iuppa[162a,162b], H. Iwasaki[69], J. M. Izen[44], V. Izzo[106a], S. Jabbar[3], P. Jackson[1], R. M. Jacobs[23], V. Jain[2], K. B. Jakobi[86], K. Jakobs[51], S. Jakobsen[65], T. Jakoubek[129], D. O. Jamin[116], D. K. Jana[82], R. Jansky[52], J. Janssen[23], M. Janus[57], P. A. Janus[41a], G. Jarlskog[84], N. Javadov[68,b], T. Javůrek[51], M. Javurkova[51], F. Jeanneau[138], L. Jeanty[16], J. Jejelava[54a,aa], A. Jelinskas[173], P. Jenni[51,ab], C. Jeske[173], S. Jézéquel[5], H. Ji[176], J. Jia[150], H. Jiang[67], Y. Jiang[36a], Z. Jiang[145], S. Jiggins[81], J. Jimenez Pena[170], S. Jin[35a], A. Jinaru[28b], O. Jinnouchi[159], H. Jivan[147c], P. Johansson[141], K. A. Johns[7], C. A. Johnson[64], W. J. Johnson[140], K. Jon-And[148a,148b], R. W. L. Jones[75], S. D. Jones[151], S. Jones[7], T. J. Jones[77], J. Jongmanns[60a], P. M. Jorge[128a,128b], J. Jovicevic[163a], X. Ju[176], A. Juste Rozas[13,v], M. K. Köhler[175], A. Kaczmarska[42], M. Kado[119], H. Kagan[113], M. Kagan[145], S. J. Kahn[88], T. Kaji[174], E. Kajomovitz[48], C. W. Kalderon[84], A. Kaluza[86], S. Kama[43], A. Kamenshchikov[132], N. Kanaya[157], L. Kanjir[78], V. A. Kantserov[100], J. Kanzaki[69], B. Kaplan[112], L. S. Kaplan[176], D. Kar[147c], K. Karakostas[10], N. Karastathis[10], M. J. Kareem[57], E. Karentzos[10], S. N. Karpov[68], Z. M. Karpova[68], K. Karthik[112], V. Kartvelishvili[75], A. N. Karyukhin[132], K. Kasahara[164], L. Kashif[176], R. D. Kass[113], A. Kastanas[149], Y. Kataoka[157], C. Kato[157], A. Katre[52], J. Katzy[45], K. Kawade[70], K. Kawagoe[73], T. Kawamoto[157], G. Kawamura[57], E. F. Kay[77], V. F. Kazanin[111,c], R. Keeler[172], R. Kehoe[43], J. S. Keller[31], E. Kellermann[84], J. J. Kempster[80], J Kendrick[19], H. Keoshkerian[161], O. Kepka[129], B. P. Kerševan[78], S. Kersten[178], R. A. Keyes[90], M. Khader[169], F. Khalil-zada[12], A. Khanov[116], A. G. Kharlamov[111,c], T. Kharlamova[111,c], A. Khodinov[160], T. J. Khoo[52], V. Khovanskiy[99,*], E. Khramov[68], J. Khubua[54b,ac], S. Kido[70], C. R. Kilby[80], H. Y. Kim[8], S. H. Kim[164], Y. K. Kim[33], N. Kimura[156], O. M. Kind[17], B. T. King[77], D. Kirchmeier[47], J. Kirk[133], A. E. Kiryunin[103], T. Kishimoto[157], D. Kisielewska[41a], V. Kitali[45], K. Kiuchi[164], O. Kivernyk[5], E. Kladiva[146b], T. Klapdor-Kleingrothaus[51], M. H. Klein[92], M. Klein[77], U. Klein[77],

K. Kleinknecht[86], P. Klimek[110], A. Klimentov[27], R. Klingenberg[46], T. Klingl[23], T. Klioutchnikova[32], E.-E. Kluge[60a], P. Kluit[109], S. Kluth[103], E. Kneringer[65], E. B. F. G. Knoops[88], A. Knue[103], A. Kobayashi[157], D. Kobayashi[159], T. Kobayashi[157], M. Kobel[47], M. Kocian[145], P. Kodys[131], T. Koffas[31], E. Koffeman[109], N. M. Köhler[103], T. Koi[145], M. Kolb[60b], I. Koletsou[5], A. A. Komar[98,*], Y. Komori[157], T. Kondo[69], N. Kondrashova[36c], K. Köneke[51], A. C. König[108], T. Kono[69,ad], R. Konoplich[112,ae], N. Konstantinidis[81], R. Kopeliansky[64], S. Koperny[41a], A. K. Kopp[51], K. Korcyl[42], K. Kordas[156], A. Korn[81], A. A. Korol[111,c], I. Korolkov[13], E. V. Korolkova[141], O. Kortner[103], S. Kortner[103], T. Kosek[131], V. V. Kostyukhin[23], A. Kotwal[48], A. Koulouris[10], A. Kourkoumeli-Charalampidi[123a,123b], C. Kourkoumelis[9], E. Kourlitis[141], V. Kouskoura[27], A. B. Kowalewska[42], R. Kowalewski[172], T. Z. Kowalski[41a], C. Kozakai[157], W. Kozanecki[138], A. S. Kozhin[132], V. A. Kramarenko[101], G. Kramberger[78], D. Krasnopevtsev[100], M. W. Krasny[83], A. Krasznahorkay[32], D. Krauss[103], J. A. Kremer[41a], J. Kretzschmar[77], K. Kreutzfeldt[55], P. Krieger[161], K. Krizka[33], K. Kroeninger[46], H. Kroha[103], J. Kroll[129], J. Kroll[124], J. Kroseberg[23], J. Krstic[14], U. Kruchonak[68], H. Krüger[23], N. Krumnack[67], M. C. Kruse[48], T. Kubota[91], H. Kucuk[81], S. Kuday[4b], J. T. Kuechler[178], S. Kuehn[32], A. Kugel[60a], F. Kuger[177], T. Kuhl[45], V. Kukhtin[68], R. Kukla[88], Y. Kulchitsky[95], S. Kuleshov[34b], Y. P. Kulinich[169], M. Kuna[134a,134b], T. Kunigo[71], A. Kupco[129], T. Kupfer[46], O. Kuprash[155], H. Kurashige[70], L. L. Kurchaninov[163a], Y. A. Kurochkin[95], M. G. Kurth[35a], V. Kus[129], E. S. Kuwertz[172], M. Kuze[159], J. Kvita[117], T. Kwan[172], D. Kyriazopoulos[141], A. La Rosa[103], J. L. La Rosa Navarro[26d], L. La Rotonda[40a,40b], F. La Ruffa[40a,40b], C. Lacasta[170], F. Lacava[134a,134b], J. Lacey[45], H. Lacker[17], D. Lacour[83], E. Ladygin[68], R. Lafaye[5], B. Laforge[83], T. Lagouri[179], S. Lai[57], S. Lammers[64], W. Lampl[7], E. Lançon[27], U. Landgraf[51], M. P. J. Landon[79], M. C. Lanfermann[52], V. S. Lang[60a], J. C. Lange[13], R. J. Langenberg[32], A. J. Lankford[166], F. Lanni[27], K. Lantzsch[23], A. Lanza[123a], A. Lapertosa[53a,53b], S. Laplace[83], J. F. Laporte[138], T. Lari[94a], F. Lasagni Manghi[22a,22b], M. Lassnig[32], P. Laurelli[50], W. Lavrijsen[16], A. T. Law[139], P. Laycock[77], T. Lazovich[59], M. Lazzaroni[94a,94b], B. Le[91], O. Le Dortz[83], E. Le Guirriec[88], E. P. Le Quilleuc[138], M. LeBlanc[172], T. LeCompte[6], F. Ledroit-Guillon[58], C. A. Lee[27], G. R. Lee[133,af], S. C. Lee[153], L. Lee[59], B. Lefebvre[90], G. Lefebvre[83], M. Lefebvre[172], F. Legger[102], C. Leggett[16], G. Lehmann Miotto[32], X. Lei[7], W. A. Leight[45], M. A. L. Leite[26d], R. Leitner[131], D. Lellouch[175], B. Lemmer[57], K. J. C. Leney[81], T. Lenz[23], B. Lenzi[32], R. Leone[7], S. Leone[126a,126b], C. Leonidopoulos[49], G. Lerner[151], C. Leroy[97], A. A. J. Lesage[138], C. G. Lester[30], M. Levchenko[125], J. Levêque[5], D. Levin[92], L. J. Levinson[175], M. Levy[19], D. Lewis[79], B. Li[36a,ag], C.-Q. Li[36a], H. Li[150], L. Li[36c], Q. Li[35a], S. Li[48], X. Li[36c], Y. Li[143], Z. Liang[35a], B. Liberti[135a], A. Liblong[161], K. Lie[62c], J. Liebal[23], W. Liebig[15], A. Limosani[152], S. C. Lin[182], T. H. Lin[86], R. A. Linck[64], B. E. Lindquist[150], A. E. Lionti[52], E. Lipeles[124], A. Lipniacka[15], M. Lisovyi[60b], T. M. Liss[169,ah], A. Lister[171], A. M. Litke[139], B. Liu[153,ai], H. Liu[92], H. Liu[27], J. K. K. Liu[122], J. Liu[36b], J. B. Liu[36a], K. Liu[88], L. Liu[169], M. Liu[36a], Y. L. Liu[36a], Y. Liu[36a], M. Livan[123a,123b], A. Lleres[58], J. Llorente Merino[35a], S. L. Lloyd[79], C. Y. Lo[62b], F. Lo Sterzo[153], E. M. Lobodzinska[45], P. Loch[7], F. K. Loebinger[87], A. Loesle[51], K. M. Loew[25], A. Loginov[179,*], T. Lohse[17], K. Lohwasser[141], M. Lokajicek[129], B. A. Long[24], J. D. Long[169], R. E. Long[75], L. Longo[76a,76b], K. A. Looper[113], J. A. Lopez[34b], D. Lopez Mateos[59], I. Lopez Paz[13], A. Lopez Solis[83], J. Lorenz[102], N. Lorenzo Martinez[5], M. Losada[21], P. J. Lösel[102], X. Lou[35a], A. Lounis[119], J. Love[6], P. A. Love[75], H. Lu[62a], N. Lu[92], Y. J. Lu[63], H. J. Lubatti[140], C. Luci[134a,134b], A. Lucotte[58], C. Luedtke[51], F. Luehring[64], W. Lukas[65], L. Luminari[134a], O. Lundberg[148a,148b], B. Lund-Jensen[149], M. S. Lutz[89], P. M. Luzi[83], D. Lynn[27], R. Lysak[129], E. Lytken[84], F. Lyu[35a], V. Lyubushkin[68], H. Ma[27], L. L. Ma[36b], Y. Ma[36b], G. Maccarrone[50], A. Macchiolo[103], C. M. Macdonald[141], B. Maček[78], J. Machado Miguens[124,128b], D. Madaffari[170], R. Madar[37], W. F. Mader[47], A. Madsen[45], J. Maeda[70], S. Maeland[15], T. Maeno[27], A. S. Maevskiy[101], V. Magerl[51], J. Mahlstedt[109], C. Maiani[119], C. Maidantchik[26a], A. A. Maier[103], T. Maier[102], A. Maio[128a,128b,128d], O. Majersky[146a], S. Majewski[118], Y. Makida[69], N. Makovec[119], B. Malaescu[83], Pa. Malecki[42], V. P. Maleev[125], F. Malek[58], U. Mallik[66], D. Malon[6], C. Malone[30], S. Maltezos[10], S. Malyukov[32], J. Mamuzic[170], G. Mancini[50], I. Mandić[78], J. Maneira[128a,128b], L. Manhaes de Andrade Filho[26b], J. Manjarres Ramos[47], K. H. Mankinen[84], A. Mann[102], A. Manousos[32], B. Mansoulie[138], J. D. Mansour[35a], R. Mantifel[90], M. Mantoani[57], S. Manzoni[94a,94b], L. Mapelli[32], G. Marceca[29], L. March[52], L. Marchese[122], G. Marchiori[83], M. Marcisovsky[129], M. Marjanovic[37], D. E. Marley[92], F. Marroquim[26a], S. P. Marsden[87], Z. Marshall[16], M. U. F Martensson[168], S. Marti-Garcia[170], C. B. Martin[113], T. A. Martin[173], V. J. Martin[49], B. Martin dit Latourınst15, M. Martinez[13,v], V. I. Martinez Outschoorn[169], S. Martin-Haugh[133], V. S. Martoiu[28b], A. C. Martyniuk[81], A. Marzin[32], L. Masetti[86], T. Mashimo[157], R. Mashinistov[98], J. Masik[87], A. L. Maslennikov[111,c], L. Massa[135a,135b], P. Mastrandrea[5], A. Mastroberardino[40a,40b], T. Masubuchi[157], P. Mättig[178], J. Maurer[28b], S. J. Maxfield[77], D. A. Maximov[111,c], R. Mazini[153], I. Maznas[156], S. M. Mazza[94a,94b], N. C. Mc Fadden[107], G. Mc Goldrick[161], S. P. Mc Kee[92], A. McCarn[92], R. L. McCarthy[150], T. G. McCarthy[103], L. I. McClymont[81], E. F. McDonald[91], J. A. Mcfayden[81], G. Mchedlidze[57], S. J. McMahon[133], P. C. McNamara[91], R. A. McPherson[172,o], S. Meehan[140], T. J. Megy[51], S. Mehlhase[102], A. Mehta[77], T. Meideck[58], K. Meier[60a], B. Meirose[44], D. Melini[170,aj], B. R. Mellado Garcia[147c], J. D. Mellenthin[57], M. Melo[146a], F. Meloni[18], A. Melzer[23], S. B. Menary[87], L. Meng[77], X. T. Meng[92], A. Mengarelli[22a,22b], S. Menke[103], E. Meoni[40a,40b], S. Mergelmeyer[17], P. Mermod[52],

L. Merola[106a,106b], C. Meroni[94a], F. S. Merritt[33], A. Messina[134a,134b], J. Metcalfe[6], A. S. Mete[166], C. Meyer[124], J-P. Meyer[138], J. Meyer[109], H. Meyer Zu Theenhausen[60a], F. Miano[151], R. P. Middleton[133], S. Miglioranzi[53a,53b], L. Mijović[49], G. Mikenberg[175], M. Mikestikova[129], M. Mikuž[78], M. Milesi[91], A. Milic[161], D. W. Miller[33], C. Mills[49], A. Milov[175], D. A. Milstead[148a,148b], A. A. Minaenko[132], Y. Minami[157], I. A. Minashvili[68], A. I. Mincer[112], B. Mindur[41a], M. Mineev[68], Y. Minegishi[157], Y. Ming[176], L. M. Mir[13], K. P. Mistry[124], T. Mitani[174], J. Mitrevski[102], V. A. Mitsou[170], A. Miucci[18], P. S. Miyagawa[141], A. Mizukami[69], J. U. Mjörnmark[84], T. Mkrtchyan[180], M. Mlynarikova[131], T. Moa[148a,148b], K. Mochizuki[97], P. Mogg[51], S. Mohapatra[38], S. Molander[148a,148b], R. Moles-Valls[23], R. Monden[71], M. C. Mondragon[93], K. Mönig[45], J. Monk[39], E. Monnier[88], A. Montalbano[150], J. Montejo Berlingen[32], F. Monticelli[74], S. Monzani[94a,94b], R. W. Moore[3], N. Morange[119], D. Moreno[21], M. Moreno Llácer[32], P. Morettini[53a], S. Morgenstern[32], D. Mori[144], T. Mori[157], M. Morii[59], M. Morinaga[157], V. Morisbak[121], A. K. Morley[32], G. Mornacchi[32], J. D. Morris[79], L. Morvaj[150], P. Moschovakos[10], M. Mosidze[54b], H. J. Moss[141], J. Moss[145,ak], K. Motohashi[159], R. Mount[145], E. Mountricha[27], E. J. W. Moyse[89], S. Muanza[88], F. Mueller[103], J. Mueller[127], R. S. P. Mueller[102], D. Muenstermann[75], P. Mullen[56], G. A. Mullier[18], F. J. Munoz Sanchez[87], W. J. Murray[173,133], H. Musheghyan[32], M. Muškinja[78], A. G. Myagkov[132,al], M. Myska[130], B. P. Nachman[16], O. Nackenhorst[52], K. Nagai[122], R. Nagai[69,ad], K. Nagano[69], Y. Nagasaka[61], K. Nagata[164], M. Nagel[51], E. Nagy[88], A. M. Nairz[32], Y. Nakahama[105], K. Nakamura[69], T. Nakamura[157], I. Nakano[114], R. F. Naranjo Garcia[45], R. Narayan[11], D. I. Narrias Villar[60a], I. Naryshkin[125], T. Naumann[45], G. Navarro[21], R. Nayyar[7], H. A. Neal[92], P. Yu. Nechaeva[98], T. J. Neep[138], A. Negri[123a,123b], M. Negrini[22a], S. Nektarijevic[108], C. Nellist[119], A. Nelson[166], M. E. Nelson[122], S. Nemecek[129], P. Nemethy[112], M. Nessi[32,am], M. S. Neubauer[169], M. Neumann[178], P. R. Newman[19], T. Y. Ng[62c], T. Nguyen Manh[97], R. B. Nickerson[122], R. Nicolaidou[138], J. Nielsen[139], V. Nikolaenko[132,al], I. Nikolic-Audit[83], K. Nikolopoulos[19], J. K. Nilsen[121], P. Nilsson[27], Y. Ninomiya[157], A. Nisati[134a], N. Nishu[35c], R. Nisius[103], I. Nitsche[46], T. Nitta[174], T. Nobe[157], Y. Noguchi[71], M. Nomachi[120], I. Nomidis[31], M. A. Nomura[27], T. Nooney[79], M. Nordberg[32], N. Norjoharuddeen[122], O. Novgorodova[47], M. Nozaki[69], L. Nozka[117], K. Ntekas[166], E. Nurse[81], F. Nuti[91], K. O'connor[25], D. C. O'Neil[144], A. A. O'Rourke[45], V. O'Shea[56], F. G. Oakham[31,d], H. Oberlack[103], T. Obermann[23], J. Ocariz[83], A. Ochi[70], I. Ochoa[38], J. P. Ochoa-Ricoux[34a], S. Oda[73], S. Odaka[69], A. Oh[87], S. H. Oh[48], C. C. Ohm[16], H. Ohman[168], H. Oide[53a,53b], H. Okawa[164], Y. Okumura[157], T. Okuyama[69], A. Olariu[28b], L. F. Oleiro Seabra[128a], S. A. Olivares Pino[34a], D. Oliveira Damazio[27], A. Olszewski[42], J. Olszowska[42], A. Onofre[128a,128e], K. Onogi[105], P. U. E. Onyisi[11,z], H. Oppen[121], M. J. Oreglia[33], Y. Oren[155], D. Orestano[136a,136b], N. Orlando[62b], R. S. Orr[161], B. Osculati[53a,53b,*], R. Ospanov[36a], G. Otero y Garzon[29], H. Otono[73], M. Ouchrif[137d], F. Ould-Saada[121], A. Ouraou[138], K. P. Oussoren[109], Q. Ouyang[35a], M. Owen[56], R. E. Owen[19], V. E. Ozcan[20a], N. Ozturk[8], K. Pachal[144], A. Pacheco Pages[13], L. Pacheco Rodriguez[138], C. Padilla Aranda[13], S. Pagan Griso[16], M. Paganini[179], F. Paige[27], G. Palacino[64], S. Palazzo[40a,40b], S. Palestini[32], M. Palka[41b], D. Pallin[37], E. St. Panagiotopoulou[10], I. Panagoulias[10], C. E. Pandini[126a,126b], J. G. Panduro Vazquez[80], P. Pani[32], S. Panitkin[27], D. Pantea[28b], L. Paolozzi[52], Th. D. Papadopoulou[10], K. Papageorgiou[9,s], A. Paramonov[6], D. Paredes Hernandez[179], A. J. Parker[75], M. A. Parker[30], K. A. Parker[45], F. Parodi[53a,53b], J. A. Parsons[38], U. Parzefall[51], V. R. Pascuzzi[161], J. M. Pasner[139], E. Pasqualucci[134a], S. Passaggio[53a], Fr. Pastore[80], S. Pataraia[86], J. R. Pater[87], T. Pauly[32], B. Pearson[103], S. Pedraza Lopez[170], R. Pedro[128a,128b], S. V. Peleganchuk[111,c], O. Penc[129], C. Peng[35a], H. Peng[36a], J. Penwell[64], B. S. Peralva[26b], M. M. Perego[138], D. V. Perepelitsa[27], F. Peri[17], L. Perini[94a,94b], H. Pernegger[32], S. Perrella[106a,106b], R. Peschke[45], V. D. Peshekhonov[68,*], K. Peters[45], R. F. Y. Peters[87], B. A. Petersen[32], T. C. Petersen[39], E. Petit[58], A. Petridis[1], C. Petridou[156], P. Petroff[119], E. Petrolo[134a], M. Petrov[122], F. Petrucci[136a,136b], N. E. Pettersson[89], A. Peyaud[138], R. Pezoa[34b], F. H. Phillips[93], P. W. Phillips[133], G. Piacquadio[150], E. Pianori[173], A. Picazio[89], E. Piccaro[79], M. A. Pickering[122], R. Piegaia[29], J. E. Pilcher[33], A. D. Pilkington[87], A. W. J. Pin[87], M. Pinamonti[135a,135b], J. L. Pinfold[3], H. Pirumov[45], M. Pitt[175], L. Plazak[146a], M.-A. Pleier[27], V. Pleskot[86], E. Plotnikova[68], D. Pluth[67], P. Podberezko[111], R. Poettgen[84], R. Poggi[123a,123b], L. Poggioli[119], D. Pohl[23], G. Polesello[123a], A. Poley[45], A. Policicchio[40a,40b], R. Polifka[32], A. Polini[22a], C. S. Pollard[56], V. Polychronakos[27], K. Pommès[32], D. Ponomarenko[100], L. Pontecorvo[134a], G. A. Popeneciu[28d], S. Pospisil[130], K. Potamianos[16], I. N. Potrap[68], C. J. Potter[30], T. Poulsen[84], J. Poveda[32], M. E. Pozo Astigarraga[32], P. Pralavorio[88], A. Pranko[16], S. Prell[67], D. Price[87], M. Primavera[76a], S. Prince[90], N. Proklova[100], K. Prokofiev[62c], F. Prokoshin[34b], S. Protopopescu[27], J. Proudfoot[6], M. Przybycien[41a], A. Puri[169], P. Puzo[119], J. Qian[92], G. Qin[56], Y. Qin[87], A. Quadt[57], M. Queitsch-Maitland[45], D. Quilty[56], S. Raddum[121], V. Radeka[27], V. Radescu[122], S. K. Radhakrishnan[150], P. Radloff[118], P. Rados[91], F. Ragusa[94a,94b], G. Rahal[181], J. A. Raine[87], S. Rajagopalan[27], C. Rangel-Smith[168], T. Rashid[119], S. Raspopov[5], M. G. Ratti[94a,94b], D. M. Rauch[45], F. Rauscher[102], S. Rave[86], I. Ravinovich[175], J. H. Rawling[87], M. Raymond[32], A. L. Read[121], N. P. Readioff[58], M. Reale[76a,76b], D. M. Rebuzzi[123a,123b], A. Redelbach[177], G. Redlinger[27], R. Reece[139], R. G. Reed[147c], K. Reeves[44], L. Rehnisch[17], J. Reichert[124], A. Reiss[86], C. Rembser[32], H. Ren[35a], M. Rescigno[134a], S. Resconi[94a], E. D. Resseguie[124], S. Rettie[171], E. Reynolds[19], O. L. Rezanova[111,c], P. Reznicek[131], R. Rezvani[97], R. Richter[103], S. Richter[81], E. Richter-Was[41b],

O. Ricken[23], M. Ridel[83], P. Rieck[103], C. J. Riegel[178], J. Rieger[57], O. Rifki[115], M. Rijssenbeek[150], A. Rimoldi[123a,123b], M. Rimoldi[18], L. Rinaldi[22a], G. Ripellino[149], B. Ristić[32], E. Ritsch[32], I. Riu[13], F. Rizatdinova[116], E. Rizvi[79], C. Rizzi[13], R. T. Roberts[87], S. H. Robertson[90,o], A. Robichaud-Veronneau[90], D. Robinson[30], J. E. M. Robinson[45], A. Robson[56], E. Rocco[86], C. Roda[126a,126b], Y. Rodina[88,an], S. Rodriguez Bosca[170], A. Rodriguez Perez[13], D. Rodriguez Rodriguez[170], S. Roe[32], C. S. Rogan[59], O. Røhne[121], J. Roloff[59], A. Romaniouk[100], M. Romano[22a,22b], S. M. Romano Saez[37], E. Romero Adam[170], N. Rompotis[77], M. Ronzani[51], L. Roos[83], S. Rosati[134a], K. Rosbach[51], P. Rose[139], N.-A. Rosien[57], E. Rossi[106a,106b], L. P. Rossi[53a], J. H. N. Rosten[30], R. Rosten[140], M. Rotaru[28b], J. Rothberg[140], D. Rousseau[119], A. Rozanov[88], Y. Rozen[154], X. Ruan[147c], F. Rubbo[145], F. Rühr[51], A. Ruiz-Martinez[31], Z. Rurikova[51], N. A. Rusakovich[68], H. L. Russell[90], J. P. Rutherfoord[7], N. Ruthmann[32], Y. F. Ryabov[125], M. Rybar[169], G. Rybkin[119], S. Ryu[6], A. Ryzhov[132], G. F. Rzehorz[57], A. F. Saavedra[152], G. Sabato[109], S. Sacerdoti[29], H.F-W. Sadrozinski[139], R. Sadykov[68], F. Safai Tehrani[134a], P. Saha[110], M. Sahinsoy[60a], M. Saimpert[45], M. Saito[157], T. Saito[157], H. Sakamoto[157], Y. Sakurai[174], G. Salamanna[136a,136b], J. E. Salazar Loyola[34b], D. Salek[109], P. H. Sales De Bruin[168], D. Salihagic[103], A. Salnikov[145], J. Salt[170], D. Salvatore[40a,40b], F. Salvatore[151], A. Salvucci[62a,62b,62c], A. Salzburger[32], D. Sammel[51], D. Sampsonidis[156], D. Sampsonidou[156], J. Sánchez[170], V. Sanchez Martinez[170], A. Sanchez Pineda[167a,167c], H. Sandaker[121], R. L. Sandbach[79], C. O. Sander[45], M. Sandhoff[178], C. Sandoval[21], D. P. C. Sankey[133], M. Sannino[53a,53b], Y. Sano[105], A. Sansoni[50], C. Santoni[37], H. Santos[128a], I. Santoyo Castillo[151], A. Sapronov[68], J. G. Saraiva[128a,128d], B. Sarrazin[23], O. Sasaki[69], K. Sato[164], E. Sauvan[5], G. Savage[80], P. Savard[161,d], N. Savic[103], C. Sawyer[133], L. Sawyer[82,u], J. Saxon[33], C. Sbarra[22a], A. Sbrizzi[22a,22b], T. Scanlon[81], D. A. Scannicchio[166], M. Scarcella[152], J. Schaarschmidt[140], P. Schacht[103], B. M. Schachtner[102], D. Schaefer[32], L. Schaefer[124], R. Schaefer[45], J. Schaeffer[86], S. Schaepe[23], S. Schaetzel[60b], U. Schäfer[86], A. C. Schaffer[119], D. Schaile[102], R. D. Schamberger[150], V. A. Schegelsky[125], D. Scheirich[131], M. Schernau[166], C. Schiavi[53a,53b], S. Schier[139], L. K. Schildgen[23], C. Schillo[51], M. Schioppa[40a,40b], S. Schlenker[32], K. R. Schmidt-Sommerfeld[103], K. Schmieden[32], C. Schmitt[86], S. Schmitt[45], S. Schmitz[86], U. Schnoor[51], L. Schoeffel[138], A. Schoening[60b], B. D. Schoenrock[93], E. Schopf[23], M. Schott[86], J. F. P. Schouwenberg[108], J. Schovancova[32], S. Schramm[52], N. Schuh[86], A. Schulte[86], M. J. Schultens[23], H.-C. Schultz-Coulon[60a], H. Schulz[17], M. Schumacher[51], B. A. Schumm[139], Ph. Schune[138], A. Schwartzman[145], T. A. Schwarz[92], H. Schweiger[87], Ph. Schwemling[138], R. Schwienhorst[93], J. Schwindling[138], A. Sciandra[23], G. Sciolla[25], M. Scornajenghi[40a,40b], F. Scuri[126a,126b], F. Scutti[91], J. Searcy[92], P. Seema[23], S. C. Seidel[107], A. Seiden[139], J. M. Seixas[26a], G. Sekhniaidze[106a], K. Sekhon[92], S. J. Sekula[43], N. Semprini-Cesari[22a,22b], S. Senkin[37], C. Serfon[121], L. Serin[119], L. Serkin[167a,167b], M. Sessa[136a,136b], R. Seuster[172], H. Severini[115], T. Sfiligoj[78], F. Sforza[32], A. Sfyrla[52], E. Shabalina[57], N. W. Shaikh[148a,148b], L. Y. Shan[35a], R. Shang[169], J. T. Shank[24], M. Shapiro[16], P. B. Shatalov[99], K. Shaw[167a,167b], S. M. Shaw[87], A. Shcherbakova[148a,148b], C. Y. Shehu[151], Y. Shen[115], N. Sherafati[31], P. Sherwood[81], L. Shi[153,ao], S. Shimizu[70], C. O. Shimmin[179], M. Shimojima[104], I. P. J. Shipsey[122], S. Shirabe[73], M. Shiyakova[68,ap], J. Shlomi[175], A. Shmeleva[98], D. Shoaleh Saadi[97], M. J. Shochet[33], S. Shojaii[94a], D. R. Shope[115], S. Shrestha[113], E. Shulga[100], M. A. Shupe[7], P. Sicho[129], A. M. Sickles[169], P. E. Sidebo[149], E. Sideras Haddad[147c], O. Sidiropoulou[177], A. Sidoti[22a,22b], F. Siegert[47], Dj. Sijacki[14], J. Silva[128a,128d], S. B. Silverstein[148a], V. Simak[130], Lj. Simic[14], S. Simion[119], E. Simioni[86], B. Simmons[81], M. Simon[86], P. Sinervo[161], N. B. Sinev[118], M. Sioli[22a,22b], G. Siragusa[177], I. Siral[92], S. Yu. Sivoklokov[101], J. Sjölin[148a,148b], M. B. Skinner[75], P. Skubic[115], M. Slater[19], T. Slavicek[130], M. Slawinska[42], K. Sliwa[165], R. Slovak[131], V. Smakhtin[175], B. H. Smart[5], J. Smiesko[146a], N. Smirnov[100], S. Yu. Smirnov[100], Y. Smirnov[100], L. N. Smirnova[101,aq], O. Smirnova[84], J. W. Smith[57], M. N. K. Smith[38], R. W. Smith[38], M. Smizanska[75], K. Smolek[130], A. A. Snesarev[98], I. M. Snyder[118], S. Snyder[27], R. Sobie[172,o], F. Socher[47], A. Soffer[155], A. Søgaard[49], D. A. Soh[153], G. Sokhrannyi[78], C. A. Solans Sanchez[32], M. Solar[130], E. Yu. Soldatov[100], U. Soldevila[170], A. A. Solodkov[132], A. Soloshenko[68], O. V. Solovyanov[132], V. Solovyev[125], P. Sommer[51], H. Son[165], A. Sopczak[130], D. Sosa[60b], C. L. Sotiropoulou[126a,126b], R. Soualah[167a,167c], A. M. Soukharev[111,c], D. South[45], B. C. Sowden[80], S. Spagnolo[76a,76b], M. Spalla[126a,126b], M. Spangenberg[173], F. Spanò[80], D. Sperlich[17], F. Spettel[103], T. M. Spieker[60a], R. Spighi[22a], G. Spigo[32], L. A. Spiller[91], M. Spousta[131], R. D. St. Denis[56,*], A. Stabile[94a], R. Stamen[60a], S. Stamm[17], E. Stanecka[42], R. W. Stanek[6], C. Stanescu[136a], M. M. Stanitzki[45], B. S. Stapf[109], S. Stapnes[121], E. A. Starchenko[132], G. H. Stark[33], J. Stark[58], S. H Stark[39], P. Staroba[129], P. Starovoitov[60a], S. Stärz[32], R. Staszewski[42], P. Steinberg[27], B. Stelzer[144], H. J. Stelzer[32], O. Stelzer-Chilton[163a], H. Stenzel[55], G. A. Stewart[56], M. C. Stockton[118], M. Stoebe[90], G. Stoicea[28b], P. Stolte[57], S. Stonjek[103], A. R. Stradling[8], A. Straessner[47], M. E. Stramaglia[18], J. Strandberg[149], S. Strandberg[148a,148b], M. Strauss[115], P. Strizenec[146b], R. Ströhmer[177], D. M. Strom[118], R. Stroynowski[43], A. Strubig[49], S. A. Stucci[27], B. Stugu[15], N. A. Styles[45], D. Su[145], J. Su[127], S. Suchek[60a], Y. Sugaya[120], M. Suk[130], V. V. Sulin[98], DMS Sultan[162a,162b], S. Sultansoy[4c], T. Sumida[71], S. Sun[59], X. Sun[3], K. Suruliz[151], C. J. E. Suster[152], M. R. Sutton[151], S. Suzuki[69], M. Svatos[129], M. Swiatlowski[33], S. P. Swift[2], I. Sykora[146a], T. Sykora[131], D. Ta[51], K. Tackmann[45], J. Taenzer[155], A. Taffard[166], R. Tafirout[163a], E. Tahirovic[79], N. Taiblum[155], H. Takai[27], R. Takashima[72], E. H. Takasugi[103], T. Takeshita[142], Y. Takubo[69], M. Talby[88], A. A. Talyshev[111,c], J. Tanaka[157],

M. Tanaka[159], R. Tanaka[119], S. Tanaka[69], R. Tanioka[70], B. B. Tannenwald[113], S. Tapia Araya[34b], S. Tapprogge[86], S. Tarem[154], G. F. Tartarelli[94a], P. Tas[131], M. Tasevsky[129], T. Tashiro[71], E. Tassi[40a,40b], A. Tavares Delgado[128a,128b], Y. Tayalati[137e], A. C. Taylor[107], G. N. Taylor[91], P. T. E. Taylor[91], W. Taylor[163b], P. Teixeira-Dias[80], D. Temple[144], H. Ten Kate[32], P. K. Teng[153], J. J. Teoh[120], F. Tepel[178], S. Terada[69], K. Terashi[157], J. Terron[85], S. Terzo[13], M. Testa[50], R. J. Teuscher[161,o], T. Theveneaux-Pelzer[88], F. Thiele[39], J. P. Thomas[19], J. Thomas-Wilsker[80], P. D. Thompson[19], A. S. Thompson[56], L. A. Thomsen[179], E. Thomson[124], M. J. Tibbetts[16], R. E. Ticse Torres[88], V. O. Tikhomirov[98,ar], Yu. A. Tikhonov[111,c], S. Timoshenko[100], P. Tipton[179], S. Tisserant[88], K. Todome[159], S. Todorova-Nova[5], S. Todt[47], J. Tojo[73], S. Tokár[146a], K. Tokushuku[69], E. Tolley[59], L. Tomlinson[87], M. Tomoto[105], L. Tompkins[145,as], K. Toms[107], B. Tong[59], P. Tornambe[51], E. Torrence[118], H. Torres[144], E. Torró Pastor[140], J. Toth[88,at], F. Touchard[88], D. R. Tovey[141], C. J. Treado[112], T. Trefzger[177], F. Tresoldi[151], A. Tricoli[27], I. M. Trigger[163a], S. Trincaz-Duvoid[83], M. F. Tripiana[13], W. Trischuk[161], B. Trocmé[58], A. Trofymov[45], C. Troncon[94a], M. Trottier-McDonald[16], M. Trovatelli[172], L. Truong[147b], M. Trzebinski[42], A. Trzupek[42], K. W. Tsang[62a], J.C-L. Tseng[122], P. V. Tsiareshka[95], G. Tsipolitis[10], N. Tsirintanis[9], S. Tsiskaridze[13], V. Tsiskaridze[51], E. G. Tskhadadze[54a], K. M. Tsui[62a], I. I. Tsukerman[99], V. Tsulaia[16], S. Tsuno[69], D. Tsybychev[150], Y. Tu[62b], A. Tudorache[28b], V. Tudorache[28b], T. T. Tulbure[28a], A. N. Tuna[59], S. A. Tupputi[22a,22b], S. Turchikhin[68], D. Turgeman[175], I. Turk Cakir[4b,au], R. Turra[94a], P. M. Tuts[38], G. Ucchielli[22a,22b], I. Ueda[69], M. Ughetto[148a,148b], F. Ukegawa[164], G. Unal[32], A. Undrus[27], G. Unel[166], F. C. Ungaro[91], Y. Unno[69], C. Unverdorben[102], J. Urban[146b], P. Urquijo[91], P. Urrejola[86], G. Usai[8], J. Usui[69], L. Vacavant[88], V. Vacek[130], B. Vachon[90], K. O. H. Vadla[121], A. Vaidya[81], C. Valderanis[102], E. Valdes Santurio[148a,148b], M. Valente[52], S. Valentinetti[22a,22b], A. Valero[170], L. Valéry[13], S. Valkar[131], A. Vallier[5], J. A. Valls Ferrer[170], W. Van Den Wollenberg[109], H. van der Graaf[109], P. van Gemmeren[6], J. Van Nieuwkoop[144], I. van Vulpen[109], M. C. van Woerden[109], M. Vanadia[135a,135b], W. Vandelli[32], A. Vaniachine[160], P. Vankov[109], G. Vardanyan[180], R. Vari[134a], E. W. Varnes[7], C. Varni[53a,53b], T. Varol[43], D. Varouchas[119], A. Vartapetian[8], K. E. Varvell[152], J. G. Vasquez[179], G. A. Vasquez[34b], F. Vazeille[37], T. Vazquez Schroeder[90], J. Veatch[57], V. Veeraraghavan[7], L. M. Veloce[161], F. Veloso[128a,128c], S. Veneziano[134a], A. Ventura[76a,76b], M. Venturi[172], N. Venturi[32], A. Venturini[25], V. Vercesi[123a], M. Verducci[136a,136b], W. Verkerke[109], A. T. Vermeulen[109], J. C. Vermeulen[109], M. C. Vetterli[144,d], N. Viaux Maira[34b], O. Viazlo[84], I. Vichou[169,*], T. Vickey[141], O. E. Vickey Boeriu[141], G. H. A. Viehhauser[122], S. Viel[16], L. Vigani[122], M. Villa[22a,22b], M. Villaplana Perez[94a,94b], E. Vilucchi[50], M. G. Vincter[31], V. B. Vinogradov[68], A. Vishwakarma[45], C. Vittori[22a,22b], I. Vivarelli[151], S. Vlachos[10], M. Vogel[178], P. Vokac[130], G. Volpi[126a,126b], H. von der Schmitt[103], E. von Toerne[23], V. Vorobel[131], K. Vorobev[100], M. Vos[170], R. Voss[32], J. H. Vossebeld[77], N. Vranjes[14], M. Vranjes Milosavljevic[14], V. Vrba[130], M. Vreeswijk[109], R. Vuillermet[32], I. Vukotic[33], P. Wagner[23], W. Wagner[178], J. Wagner-Kuhr[102], H. Wahlberg[74], S. Wahrmund[47], J. Wakabayashi[105], J. Walder[75], R. Walker[102], W. Walkowiak[143], V. Wallangen[148a,148b], C. Wang[35b], C. Wang[36b,av], F. Wang[176], H. Wang[16], H. Wang[3], J. Wang[45], J. Wang[152], Q. Wang[115], R. Wang[6], S. M. Wang[153], T. Wang[38], W. Wang[153,aw], W. Wang[36a], Z. Wang[36c], C. Wanotayaroj[118], A. Warburton[90], C. P. Ward[30], D. R. Wardrope[81], A. Washbrook[49], P. M. Watkins[19], A. T. Watson[19], M. F. Watson[19], G. Watts[140], S. Watts[87], B. M. Waugh[81], A. F. Webb[11], S. Webb[86], M. S. Weber[18], S. W. Weber[177], S. A. Weber[31], J. S. Webster[6], A. R. Weidberg[122], B. Weinert[64], J. Weingarten[57], M. Weirich[86], C. Weiser[51], H. Weits[109], P. S. Wells[32], T. Wenaus[27], T. Wengler[32], S. Wenig[32], N. Wermes[23], M. D. Werner[67], P. Werner[32], M. Wessels[60a], T. D. Weston[18], K. Whalen[118], N. L. Whallon[140], A. M. Wharton[75], A. S. White[92], A. White[8], M. J. White[1], R. White[34b], D. Whiteson[166], B. W. Whitmore[75], F. J. Wickens[133], W. Wiedenmann[176], M. Wielers[133], C. Wiglesworth[39], L. A. M. Wiik-Fuchs[51], A. Wildauer[103], F. Wilk[87], H. G. Wilkens[32], H. H. Williams[124], S. Williams[109], C. Willis[93], S. Willocq[89], J. A. Wilson[19], I. Wingerter-Seez[5], E. Winkels[151], F. Winklmeier[118], O. J. Winston[151], B. T. Winter[23], M. Wittgen[145], M. Wobisch[82,u], T. M. H. Wolf[109], R. Wolff[88], M. W. Wolter[42], H. Wolters[128a,128c], V. W. S. Wong[171], S. D. Worm[19], B. K. Wosiek[42], J. Wotschack[32], K. W. Wozniak[42], M. Wu[33], S. L. Wu[176], X. Wu[52], Y. Wu[92], T. R. Wyatt[87], B. M. Wynne[49], S. Xella[39], Z. Xi[92], L. Xia[35c], D. Xu[35a], L. Xu[27], T. Xu[138], B. Yabsley[152], S. Yacoob[147a], D. Yamaguchi[159], Y. Yamaguchi[120], A. Yamamoto[69], S. Yamamoto[157], T. Yamanaka[157], M. Yamatani[157], K. Yamauchi[105], Y. Yamazaki[70], Z. Yan[24], H. Yang[36c], H. Yang[16], Y. Yang[153], Z. Yang[15], W-M. Yao[16], Y. C. Yap[83], Y. Yasu[69], E. Yatsenko[5], K. H. Yau Wong[23], J. Ye[43], S. Ye[27], I. Yeletskikh[68], E. Yigitbasi[24], E. Yildirim[86], K. Yorita[174], K. Yoshihara[124], C. Young[145], C. J. S. Young[32], J. Yu[8], J. Yu[67], S. P. Y. Yuen[23], I. Yusuff[30,ax], B. Zabinski[42], G. Zacharis[10], R. Zaidan[13], A. M. Zaitsev[132,al], N. Zakharchuk[45], J. Zalieckas[15], A. Zaman[150], S. Zambito[59], D. Zanzi[91], C. Zeitnitz[178], G. Zemaityte[122], A. Zemla[41a], J. C. Zeng[169], Q. Zeng[145], O. Zenin[132], T. Ženiš[146a], D. Zerwas[119], D. Zhang[92], F. Zhang[176], G. Zhang[36a,ay], H. Zhang[35b], J. Zhang[6], L. Zhang[51], L. Zhang[36a], M. Zhang[169], P. Zhang[35b], R. Zhang[23], R. Zhang[36a,av], X. Zhang[36b], Y. Zhang[35a], Z. Zhang[119], X. Zhao[43], Y. Zhao[36b,az], Z. Zhao[36a], A. Zhemchugov[68], B. Zhou[92], C. Zhou[176], L. Zhou[43], M. Zhou[35a], M. Zhou[150], N. Zhou[35c], C. G. Zhu[36b], H. Zhu[35a], J. Zhu[92], Y. Zhu[36a], X. Zhuang[35a], K. Zhukov[98], A. Zibell[177], D. Zieminska[64],

N. I. Zimine[68], C. Zimmermann[86], S. Zimmermann[51], Z. Zinonos[103], M. Zinser[86], M. Ziolkowski[143], L. Živković[14], G. Zobernig[176], A. Zoccoli[22a,22b], R. Zou[33], M. zur Nedden[17], L. Zwalinski[32]

[1] Department of Physics, University of Adelaide, Adelaide, Australia
[2] Physics Department, SUNY Albany, Albany, NY, USA
[3] Department of Physics, University of Alberta, Edmonton, AB, Canada
[4] [(a)]Department of Physics, Ankara University, Ankara, Turkey; [(b)]Istanbul Aydin University, Istanbul, Turkey; [(c)]Division of Physics, TOBB University of Economics and Technology, Ankara, Turkey
[5] LAPP, CNRS/IN2P3 and Université Savoie Mont Blanc, Annecy-le-Vieux, France
[6] High Energy Physics Division, Argonne National Laboratory, Argonne, IL, USA
[7] Department of Physics, University of Arizona, Tucson, AZ, USA
[8] Department of Physics, The University of Texas at Arlington, Arlington, TX, USA
[9] Physics Department, National and Kapodistrian University of Athens, Athens, Greece
[10] Physics Department, National Technical University of Athens, Zografou, Greece
[11] Department of Physics, The University of Texas at Austin, Austin, TX, USA
[12] Institute of Physics, Azerbaijan Academy of Sciences, Baku, Azerbaijan
[13] Institut de Física d'Altes Energies (IFAE), The Barcelona Institute of Science and Technology, Barcelona, Spain
[14] Institute of Physics, University of Belgrade, Belgrade, Serbia
[15] Department for Physics and Technology, University of Bergen, Bergen, Norway
[16] Physics Division, Lawrence Berkeley National Laboratory and University of California, Berkeley, CA, USA
[17] Department of Physics, Humboldt University, Berlin, Germany
[18] Albert Einstein Center for Fundamental Physics and Laboratory for High Energy Physics, University of Bern, Bern, Switzerland
[19] School of Physics and Astronomy, University of Birmingham, Birmingham, UK
[20] [(a)]Department of Physics, Bogazici University, Istanbul, Turkey; [(b)]Department of Physics Engineering, Gaziantep University, Gaziantep, Turkey; [(c)]Faculty of Engineering and Natural Sciences, Istanbul Bilgi University, Istanbul, Turkey; [(d)]Faculty of Engineering and Natural Sciences, Bahcesehir University, Istanbul, Turkey
[21] Centro de Investigaciones, Universidad Antonio Narino, Bogotá, Colombia
[22] [(a)]INFN Sezione di Bologna, Bologna, Italy; [(b)]Dipartimento di Fisica e Astronomia, Università di Bologna, Bologna, Italy
[23] Physikalisches Institut, University of Bonn, Bonn, Germany
[24] Department of Physics, Boston University, Boston, MA, USA
[25] Department of Physics, Brandeis University, Waltham, MA, USA
[26] [(a)]Universidade Federal do Rio De Janeiro COPPE/EE/IF, Rio de Janeiro, Brazil; [(b)]Electrical Circuits Department, Federal University of Juiz de Fora (UFJF), Juiz de Fora, Brazil; [(c)]Federal University of Sao Joao del Rei (UFSJ), Sao Joao del Rei, Brazil; [(d)]Instituto de Fisica, Universidade de Sao Paulo, Sao Paulo, Brazil
[27] Physics Department, Brookhaven National Laboratory, Upton, NY, USA
[28] [(a)]Transilvania University of Brasov, Brasov, Romania; [(b)]Horia Hulubei National Institute of Physics and Nuclear Engineering, Bucharest, Romania; [(c)]Department of Physics, Alexandru Ioan Cuza University of Iasi, Iasi, Romania; [(d)]Physics Department, National Institute for Research and Development of Isotopic and Molecular Technologies, Cluj Napoca, Romania; [(e)]University Politehnica Bucharest, Bucharest, Romania; [(f)]West University in Timisoara, Timisoara, Romania
[29] Departamento de Física, Universidad de Buenos Aires, Buenos Aires, Argentina
[30] Cavendish Laboratory, University of Cambridge, Cambridge, UK
[31] Department of Physics, Carleton University, Ottawa, ON, Canada
[32] CERN, Geneva, Switzerland
[33] Enrico Fermi Institute, University of Chicago, Chicago, IL, USA
[34] [(a)]Departamento de Física, Pontificia Universidad Católica de Chile, Santiago, Chile; [(b)]Departamento de Física, Universidad Técnica Federico Santa María, Valparaiso, Chile
[35] [(a)]Institute of High Energy Physics, Chinese Academy of Sciences, Beijing, China; [(b)]Department of Physics, Nanjing University, Nanjing, Jiangsu, China; [(c)]Physics Department, Tsinghua University, Beijing 100084, China
[36] [(a)]Department of Modern Physics and State Key Laboratory of Particle Detection and Electronics, University of Science and Technology of China, Hefei, Anhui, China; [(b)]School of Physics, Shandong University, Shandong,

China; [c]Department of Physics and Astronomy, Key Laboratory for Particle Physics, Astrophysics and Cosmology, Ministry of Education, Shanghai Key Laboratory for Particle Physics and Cosmology, Shanghai Jiao Tong University (also at PKU-CHEP), Shanghai, China
[37] Université Clermont Auvergne, CNRS/IN2P3, LPC, Clermont-Ferrand, France
[38] Nevis Laboratory, Columbia University, Irvington, NY, USA
[39] Niels Bohr Institute, University of Copenhagen, Copenhagen, Denmark
[40] [a]INFN Gruppo Collegato di Cosenza, Laboratori Nazionali di Frascati, Frascati, Italy; [b]Dipartimento di Fisica, Università della Calabria, Rende, Italy
[41] [a]Faculty of Physics and Applied Computer Science, AGH University of Science and Technology, Kraków, Poland; [b]Marian Smoluchowski Institute of Physics, Jagiellonian University, Kraków, Poland
[42] Institute of Nuclear Physics, Polish Academy of Sciences, Kraków, Poland
[43] Physics Department, Southern Methodist University, Dallas, TX, USA
[44] Physics Department, University of Texas at Dallas, Richardson, TX, USA
[45] DESY, Hamburg and Zeuthen, Germany
[46] Lehrstuhl für Experimentelle Physik IV, Technische Universität Dortmund, Dortmund, Germany
[47] Institut für Kern- und Teilchenphysik, Technische Universität Dresden, Dresden, Germany
[48] Department of Physics, Duke University, Durham, NC, USA
[49] SUPA-School of Physics and Astronomy, University of Edinburgh, Edinburgh, UK
[50] INFN e Laboratori Nazionali di Frascati, Frascati, Italy
[51] Fakultät für Mathematik und Physik, Albert-Ludwigs-Universität, Freiburg, Germany
[52] Departement de Physique Nucleaire et Corpusculaire, Université de Genève, Geneva, Switzerland
[53] [a]INFN Sezione di Genova, Genoa, Italy; [b]Dipartimento di Fisica, Università di Genova, Genoa, Italy
[54] [a]E. Andronikashvili Institute of Physics, Iv. Javakhishvili Tbilisi State University, Tbilisi, Georgia; [b]High Energy Physics Institute, Tbilisi State University, Tbilisi, Georgia
[55] II Physikalisches Institut, Justus-Liebig-Universität Giessen, Giessen, Germany
[56] SUPA-School of Physics and Astronomy, University of Glasgow, Glasgow, UK
[57] II Physikalisches Institut, Georg-August-Universität, Göttingen, Germany
[58] Laboratoire de Physique Subatomique et de Cosmologie, Université Grenoble-Alpes, CNRS/IN2P3, Grenoble, France
[59] Laboratory for Particle Physics and Cosmology, Harvard University, Cambridge, MA, USA
[60] [a]Kirchhoff-Institut für Physik, Ruprecht-Karls-Universität Heidelberg, Heidelberg, Germany; [b]Physikalisches Institut, Ruprecht-Karls-Universität Heidelberg, Heidelberg, Germany
[61] Faculty of Applied Information Science, Hiroshima Institute of Technology, Hiroshima, Japan
[62] [a]Department of Physics, The Chinese University of Hong Kong, Shatin, N.T., Hong Kong; [b]Department of Physics, The University of Hong Kong, Hong Kong, China; [c]Department of Physics and Institute for Advanced Study, The Hong Kong University of Science and Technology, Clear Water Bay, Kowloon, Hong Kong, China
[63] Department of Physics, National Tsing Hua University, Taiwan, Taiwan
[64] Department of Physics, Indiana University, Bloomington, IN, USA
[65] Institut für Astro- und Teilchenphysik, Leopold-Franzens-Universität, Innsbruck, Austria
[66] University of Iowa, Iowa City, IA, USA
[67] Department of Physics and Astronomy, Iowa State University, Ames, IA, USA
[68] Joint Institute for Nuclear Research, JINR Dubna, Dubna, Russia
[69] KEK, High Energy Accelerator Research Organization, Tsukuba, Japan
[70] Graduate School of Science, Kobe University, Kobe, Japan
[71] Faculty of Science, Kyoto University, Kyoto, Japan
[72] Kyoto University of Education, Kyoto, Japan
[73] Research Center for Advanced Particle Physics and Department of Physics, Kyushu University, Fukuoka, Japan
[74] Instituto de Física La Plata, Universidad Nacional de La Plata and CONICET, La Plata, Argentina
[75] Physics Department, Lancaster University, Lancaster, UK
[76] [a]INFN Sezione di Lecce, Lecce, Italy; [b]Dipartimento di Matematica e Fisica, Università del Salento, Lecce, Italy
[77] Oliver Lodge Laboratory, University of Liverpool, Liverpool, UK

[78] Department of Experimental Particle Physics, Jožef Stefan Institute and Department of Physics, University of Ljubljana, Ljubljana, Slovenia
[79] School of Physics and Astronomy, Queen Mary University of London, London, UK
[80] Department of Physics, Royal Holloway University of London, Surrey, UK
[81] Department of Physics and Astronomy, University College London, London, UK
[82] Louisiana Tech University, Ruston, LA, USA
[83] Laboratoire de Physique Nucléaire et de Hautes Energies, UPMC and Université Paris-Diderot and CNRS/IN2P3, Paris, France
[84] Fysiska institutionen, Lunds universitet, Lund, Sweden
[85] Departamento de Fisica Teorica C-15, Universidad Autonoma de Madrid, Madrid, Spain
[86] Institut für Physik, Universität Mainz, Mainz, Germany
[87] School of Physics and Astronomy, University of Manchester, Manchester, UK
[88] CPPM, Aix-Marseille Université and CNRS/IN2P3, Marseille, France
[89] Department of Physics, University of Massachusetts, Amherst, MA, USA
[90] Department of Physics, McGill University, Montreal, QC, Canada
[91] School of Physics, University of Melbourne, Victoria, Australia
[92] Department of Physics, The University of Michigan, Ann Arbor, MI, USA
[93] Department of Physics and Astronomy, Michigan State University, East Lansing, MI, USA
[94] [(a)]INFN Sezione di Milano, Milan, Italy; [(b)]Dipartimento di Fisica, Università di Milano, Milan, Italy
[95] B.I. Stepanov Institute of Physics, National Academy of Sciences of Belarus, Minsk, Republic of Belarus
[96] Research Institute for Nuclear Problems of Byelorussian State University, Minsk, Republic of Belarus
[97] Group of Particle Physics, University of Montreal, Montreal, QC, Canada
[98] P.N. Lebedev Physical Institute of the Russian Academy of Sciences, Moscow, Russia
[99] Institute for Theoretical and Experimental Physics (ITEP), Moscow, Russia
[100] National Research Nuclear University MEPhI, Moscow, Russia
[101] D.V. Skobeltsyn Institute of Nuclear Physics, M.V. Lomonosov Moscow State University, Moscow, Russia
[102] Fakultät für Physik, Ludwig-Maximilians-Universität München, Munich, Germany
[103] Max-Planck-Institut für Physik (Werner-Heisenberg-Institut), Munich, Germany
[104] Nagasaki Institute of Applied Science, Nagasaki, Japan
[105] Graduate School of Science and Kobayashi-Maskawa Institute, Nagoya University, Nagoya, Japan
[106] [(a)]INFN Sezione di Napoli, Naples, Italy; [(b)]Dipartimento di Fisica, Università di Napoli, Naples, Italy
[107] Department of Physics and Astronomy, University of New Mexico, Albuquerque, NM, USA
[108] Institute for Mathematics, Astrophysics and Particle Physics, Radboud University Nijmegen/Nikhef, Nijmegen, The Netherlands
[109] Nikhef National Institute for Subatomic Physics and University of Amsterdam, Amsterdam, The Netherlands
[110] Department of Physics, Northern Illinois University, DeKalb, IL, USA
[111] Budker Institute of Nuclear Physics, SB RAS, Novosibirsk, Russia
[112] Department of Physics, New York University, New York, NY, USA
[113] Ohio State University, Columbus, OH, USA
[114] Faculty of Science, Okayama University, Okayama, Japan
[115] Homer L. Dodge Department of Physics and Astronomy, University of Oklahoma, Norman, OK, USA
[116] Department of Physics, Oklahoma State University, Stillwater, OK, USA
[117] Palacký University, RCPTM, Olomouc, Czech Republic
[118] Center for High Energy Physics, University of Oregon, Eugene, OR, USA
[119] LAL, Univ. Paris-Sud, CNRS/IN2P3, Université Paris-Saclay, Orsay, France
[120] Graduate School of Science, Osaka University, Osaka, Japan
[121] Department of Physics, University of Oslo, Oslo, Norway
[122] Department of Physics, Oxford University, Oxford, UK
[123] [(a)]INFN Sezione di Pavia, Pavia, Italy; [(b)]Dipartimento di Fisica, Università di Pavia, Pavia, Italy
[124] Department of Physics, University of Pennsylvania, Philadelphia, PA, USA
[125] National Research Centre "Kurchatov Institute" B.P. Konstantinov Petersburg Nuclear Physics Institute, St. Petersburg, Russia
[126] [(a)]INFN Sezione di Pisa, Pisa, Italy; [(b)]Dipartimento di Fisica E. Fermi, Università di Pisa, Pisa, Italy

[127] Department of Physics and Astronomy, University of Pittsburgh, Pittsburgh, PA, USA
[128] [(a)]Laboratório de Instrumentação e Física Experimental de Partículas-LIP, Lisbon, Portugal; [(b)]Faculdade de Ciências, Universidade de Lisboa, Lisbon, Portugal; [(c)]Department of Physics, University of Coimbra, Coimbra, Portugal; [(d)]Centro de Física Nuclear da Universidade de Lisboa, Lisbon, Portugal; [(e)]Departamento de Fisica, Universidade do Minho, Braga, Portugal; [(f)]Departamento de Fisica Teorica y del Cosmos, Universidad de Granada, Granada, Spain; [(g)]Dep Fisica and CEFITEC of Faculdade de Ciencias e Tecnologia, Universidade Nova de Lisboa, Caparica, Portugal
[129] Institute of Physics, Academy of Sciences of the Czech Republic, Prague, Czech Republic
[130] Czech Technical University in Prague, Prague, Czech Republic
[131] Faculty of Mathematics and Physics, Charles University, Prague, Czech Republic
[132] State Research Center Institute for High Energy Physics (Protvino), NRC KI, Protvino, Russia
[133] Particle Physics Department, Rutherford Appleton Laboratory, Didcot, UK
[134] [(a)]INFN Sezione di Roma, Rome, Italy; [(b)]Dipartimento di Fisica, Sapienza Università di Roma, Rome, Italy
[135] [(a)]INFN Sezione di Roma Tor Vergata, Rome, Italy; [(b)]Dipartimento di Fisica, Università di Roma Tor Vergata, Rome, Italy
[136] [(a)]INFN Sezione di Roma Tre, Rome, Italy; [(b)]Dipartimento di Matematica e Fisica, Università Roma Tre, Rome, Italy
[137] [(a)]Faculté des Sciences Ain Chock, Réseau Universitaire de Physique des Hautes Energies-Université Hassan II, Casablanca, Morocco; [(b)]Centre National de l'Energie des Sciences Techniques Nucleaires, Rabat, Morocco; [(c)]Faculté des Sciences Semlalia, Université Cadi Ayyad, LPHEA-Marrakech, Marrakech, Morocco; [(d)]Faculté des Sciences, Université Mohamed Premier and LPTPM, Oujda, Morocco; [(e)]Faculté des Sciences, Université Mohammed V, Rabat, Morocco
[138] DSM/IRFU (Institut de Recherches sur les Lois Fondamentales de l'Univers), CEA Saclay (Commissariat à l'Energie Atomique et aux Energies Alternatives), Gif-sur-Yvette, France
[139] Santa Cruz Institute for Particle Physics, University of California Santa Cruz, Santa Cruz, CA, USA
[140] Department of Physics, University of Washington, Seattle, WA, USA
[141] Department of Physics and Astronomy, University of Sheffield, Sheffield, UK
[142] Department of Physics, Shinshu University, Nagano, Japan
[143] Department Physik, Universität Siegen, Siegen, Germany
[144] Department of Physics, Simon Fraser University, Burnaby, BC, Canada
[145] SLAC National Accelerator Laboratory, Stanford, CA, USA
[146] [(a)]Faculty of Mathematics, Physics and Informatics, Comenius University, Bratislava, Slovak Republic; [(b)]Department of Subnuclear Physics, Institute of Experimental Physics of the Slovak Academy of Sciences, Kosice, Slovak Republic
[147] [(a)]Department of Physics, University of Cape Town, Cape Town, South Africa; [(b)]Department of Physics, University of Johannesburg, Johannesburg, South Africa; [(c)]School of Physics, University of the Witwatersrand, Johannesburg, South Africa
[148] [(a)]Department of Physics, Stockholm University, Stockholm, Sweden; [(b)]The Oskar Klein Centre, Stockholm, Sweden
[149] Physics Department, Royal Institute of Technology, Stockholm, Sweden
[150] Departments of Physics and Astronomy and Chemistry, Stony Brook University, Stony Brook, NY, USA
[151] Department of Physics and Astronomy, University of Sussex, Brighton, UK
[152] School of Physics, University of Sydney, Sydney, Australia
[153] Institute of Physics, Academia Sinica, Taipei, Taiwan
[154] Department of Physics, Technion: Israel Institute of Technology, Haifa, Israel
[155] Raymond and Beverly Sackler School of Physics and Astronomy, Tel Aviv University, Tel Aviv, Israel
[156] Department of Physics, Aristotle University of Thessaloniki, Thessaloniki, Greece
[157] International Center for Elementary Particle Physics and Department of Physics, The University of Tokyo, Tokyo, Japan
[158] Graduate School of Science and Technology, Tokyo Metropolitan University, Tokyo, Japan
[159] Department of Physics, Tokyo Institute of Technology, Tokyo, Japan
[160] Tomsk State University, Tomsk, Russia
[161] Department of Physics, University of Toronto, Toronto, ON, Canada
[162] [(a)]INFN-TIFPA, Trento, Italy; [(b)]University of Trento, Trento, Italy
[163] [(a)]TRIUMF, Vancouver, BC, Canada; [(b)]Department of Physics and Astronomy, York University, Toronto, ON, Canada
[164] Faculty of Pure and Applied Sciences, and Center for Integrated Research in Fundamental Science and Engineering, University of Tsukuba, Tsukuba, Japan

[165] Department of Physics and Astronomy, Tufts University, Medford, MA, USA
[166] Department of Physics and Astronomy, University of California Irvine, Irvine, CA, USA
[167] [(a)]INFN Gruppo Collegato di Udine, Sezione di Trieste, Udine, Italy; [(b)]ICTP, Trieste, Italy; [(c)]Dipartimento di Chimica, Fisica e Ambiente, Università di Udine, Udine, Italy
[168] Department of Physics and Astronomy, University of Uppsala, Uppsala, Sweden
[169] Department of Physics, University of Illinois, Urbana, IL, USA
[170] Instituto de Fisica Corpuscular (IFIC), Centro Mixto Universidad de Valencia-CSIC, Valencia, Spain
[171] Department of Physics, University of British Columbia, Vancouver, BC, Canada
[172] Department of Physics and Astronomy, University of Victoria, Victoria, BC, Canada
[173] Department of Physics, University of Warwick, Coventry, UK
[174] Waseda University, Tokyo, Japan
[175] Department of Particle Physics, The Weizmann Institute of Science, Rehovot, Israel
[176] Department of Physics, University of Wisconsin, Madison, WI, USA
[177] Fakultät für Physik und Astronomie, Julius-Maximilians-Universität, Würzburg, Germany
[178] Fakultät für Mathematik und Naturwissenschaften, Fachgruppe Physik, Bergische Universität Wuppertal, Wuppertal, Germany
[179] Department of Physics, Yale University, New Haven, CT, USA
[180] Yerevan Physics Institute, Yerevan, Armenia
[181] Centre de Calcul de l'Institut National de Physique Nucléaire et de Physique des Particules (IN2P3), Villeurbanne, France
[182] Academia Sinica Grid Computing, Institute of Physics, Academia Sinica, Taipei, Taiwan

[a] Also at Department of Physics, King's College London, London, United Kingdom
[b] Also at Institute of Physics, Azerbaijan Academy of Sciences, Baku, Azerbaijan
[c] Also at Novosibirsk State University, Novosibirsk, Russia
[d] Also at TRIUMF, Vancouver BC, Canada
[e] Also at Department of Physics and Astronomy, University of Louisville, Louisville, KY, United States of America
[f] Also at Physics Department, An-Najah National University, Nablus, Palestine
[g] Also at Department of Physics, California State University, Fresno CA, United States of America
[h] Also at Department of Physics, University of Fribourg, Fribourg, Switzerland
[i] Also at II Physikalisches Institut, Georg-August-Universität, Göttingen, Germany
[j] Also at Departament de Fisica de la Universitat Autonoma de Barcelona, Barcelona, Spain
[k] Also at Departamento de Fisica e Astronomia, Faculdade de Ciencias, Universidade do Porto, Portugal
[l] Also at Tomsk State University, Tomsk, and Moscow Institute of Physics and Technology State University, Dolgoprudny, Russia
[m] Also at The Collaborative Innovation Center of Quantum Matter (CICQM), Beijing, China
[n] Also at Universita di Napoli Parthenope, Napoli, Italy
[o] Also at Institute of Particle Physics (IPP), Canada
[p] Also at Horia Hulubei National Institute of Physics and Nuclear Engineering, Bucharest, Romania
[q] Also at Department of Physics, St. Petersburg State Polytechnical University, St. Petersburg, Russia
[r] Also at Borough of Manhattan Community College, City University of New York, New York City, United States of America
[s] Also at Department of Financial and Management Engineering, University of the Aegean, Chios, Greece
[t] Also at Centre for High Performance Computing, CSIR Campus, Rosebank, Cape Town, South Africa
[u] Also at Louisiana Tech University, Ruston LA, United States of America
[v] Also at Institucio Catalana de Recerca i Estudis Avancats, ICREA, Barcelona, Spain
[w] Also at Graduate School of Science, Osaka University, Osaka, Japan
[x] Also at Fakultät für Mathematik und Physik, Albert-Ludwigs-Universität, Freiburg, Germany
[y] Also at Institute for Mathematics, Astrophysics and Particle Physics, Radboud University Nijmegen/Nikhef, Nijmegen, Netherlands
[z] Also at Department of Physics, The University of Texas at Austin, Austin TX, United States of America
[aa] Also at Institute of Theoretical Physics, Ilia State University, Tbilisi, Georgia
[ab] Also at CERN, Geneva, Switzerland

[ac] Also at Georgian Technical University (GTU),Tbilisi, Georgia
[ad] Also at Ochadai Academic Production, Ochanomizu University, Tokyo, Japan
[ae] Also at Manhattan College, New York NY, United States of America
[af] Also at Departamento de Física, Pontificia Universidad Católica de Chile, Santiago, Chile
[ag] Also at Department of Physics, The University of Michigan, Ann Arbor MI, United States of America
[ah] Also at The City College of New York, New York NY, United States of America
[ai] Also at School of Physics, Shandong University, Shandong, China
[aj] Also at Departamento de Fisica Teorica y del Cosmos, Universidad de Granada, Granada, Portugal
[ak] Also at Department of Physics, California State University, Sacramento CA, United States of America
[al] Also at Moscow Institute of Physics and Technology State University, Dolgoprudny, Russia
[am] Also at Departement de Physique Nucleaire et Corpusculaire, Université de Genève, Geneva, Switzerland
[an] Also at Institut de Física d'Altes Energies (IFAE), The Barcelona Institute of Science and Technology, Barcelona, Spain
[ao] Also at School of Physics, Sun Yat-sen University, Guangzhou, China
[ap] Also at Institute for Nuclear Research and Nuclear Energy (INRNE) of the Bulgarian Academy of Sciences, Sofia, Bulgaria
[aq] Also at Faculty of Physics, M.V.Lomonosov Moscow State University, Moscow, Russia
[ar] Also at National Research Nuclear University MEPhI, Moscow, Russia
[as] Also at Department of Physics, Stanford University, Stanford CA, United States of America
[at] Also at Institute for Particle and Nuclear Physics, Wigner Research Centre for Physics, Budapest, Hungary
[au] Also at Giresun University, Faculty of Engineering, Turkey
[av] Also at CPPM, Aix-Marseille Université and CNRS/IN2P3, Marseille, France
[aw] Also at Department of Physics, Nanjing University, Jiangsu, China
[ax] Also at University of Malaya, Department of Physics, Kuala Lumpur, Malaysia
[ay] Also at Institute of Physics, Academia Sinica, Taipei, Taiwan
[az] Also at LAL, Univ. Paris-Sud, CNRS/IN2P3, Université Paris-Saclay, Orsay, France
*Deceased